A STUDY OF THE SUBCOOLED LIQUID FLASH, BOILING CYCLE; A NOVEL HEAT CYCLE AND ITS APPLICATION IN A RECIPROCATING PISTON ENGINE FOR AUTOMOTIVE WASTE HEAT RECOVERY

By

Dhaminda Nadeesha Hewavitarane

B. Sci., The University of The South Pacific, 1998
M. Eng., The University of Kitakyushu, 2012

THESIS

Submitted in partial fulfilment of the requirements for the degree of Doctor of Philosophy in Engineering in the Graduate School of Environmental Engineering of The University of Kitakyushu, 2016

Kitakyushu City, Japan

Dedication

I dedicate this thesis to God the Father Almighty, who has, is and will always be my source of sustenance and pillar of strength.
To my parents Charmaine and Vimal, my wife Chiho, my brother in Christ Don, and the rest of my family for their understanding and support.
I love you all very much.

Fear thou not; for I am with thee: be not dismayed; for I am thy God: I will strengthen thee; yea, I will help thee; yea, I will uphold thee with the right hand of my righteousness.

Isaiah 41:10

Acknowledgements

The inspiration for this research originally came from the work of Mr Jeremy Holmes and his internet website http://flashsteam.com/. It was Mr Holmes and his concept of the “Flash Steam Engine” that introduced me to the phenomenon of “Flashing” and how it can be used to power an engine. The credit for making any of this research possible goes to Prof Sadami Yoshiyama, who through his acceptance of me into his research lab started me along this path of academic research. Him giving me the freedom to pursue my research as I wanted to, while guiding me as a researcher, has resulted in this thesis and has opened up an exciting future in the current research theme. His vast experience and extensive knowledge have made invaluable contributions to the concepts within this work. On a more personal note, his friendship and understanding has made the difficult and trying times bearable and has kept me focused. I would also like to acknowledge the contributions made by former students of the Yoshiyama lab who have been involved in this research project; Mr Li Shin, Mr Hisashi Wadahama and Mr Kohei Maruyama who were involved in the designing and building of the experimental engines and other apparatus, and Mr Ryouta Kamichika, Mr Kousuke Nakamura and Mr Kazuma Shingu for assisting with the long and arduous experiments. A special debt of gratitude is owed to the staff, both past and present, of The Machining and Manufacturing Centre of The University of Kitakyushu namely Mr Noriaki Uramune, Mr Takayuki Taguchi, Mr Masaaki Horie, Mr Jyunji Ueda, Mr Hiroyuki Otsubo and Mr Susumu Matsukuma, for their invaluable advice and assistance in getting components manufactured with special attention and importance within the shortest possible time. I’d also like to acknowledge the contributions made by Prof Koichi Inoue and Prof Yoshiaki Miyazato who have furthered my knowledge in fields of heat transfer and fluid dynamics respectively that are integral to this research, Prof Masaaki Izumi for providing much needed instruments for experiments and continued support and encouragement and Prof Katsutoshi Yamamoto for reviewing this thesis. The exhaust heat exchanger used in these experiments was provided by Yamaichi Co, Ltd and has been of tremendous importance to this research and has gone a long way in helping develop the concept of the waste heat recovery system of this thesis. For this I am indebted to them for their contribution. Acknowledgment is also made of Mr Yuji Kido, for his advice and assistance with manufacturing the engine bench and sourcing components, and the staff of The Bosch Diesel service centre in Tobata-ku, Kitakyushu City for supplying parts and knowhow for the diesel injectors used. Special acknowledgement is also made of the financial support provided the JSPS KAKENHI Grant (Grant Number 15K06690) which is supporting this research from 2015 through to 2017

Abstract

This report is concerned with a novel heat cycle termed the Subcooled Liquid Flash, Boiling cycle (SLFB) and its applicability to waste heat recovery from automotive internal combustion engines.
The internal combustion engine is set to continue to dominate the transportation sector as the means of power generation. This is due to its reliability, higher power to weight ratio than battery powered electrical vehicles, ready availability of liquid fuels and relative low cost. However, the IC engine is relatively inefficient in its conversion of combustion energy to mechanical work and up to 60% of combustion energy is wasted. The recovery of this waste heat is an obvious and effective means of improving the IC engine's overall efficiency.
The SLFB cycle belongs to the family of Power Flash Cycles of which the Trilateral cycle (TLC) also known as the Trilateral Flash cycle, is relatively well known and widely researched. The SLFB cycle is however different to the hitherto well-known TLC in that it makes use of the un-flashed portion of the working fluid by inducing convective boiling on this through a second heat transfer process. The vapour thus generated expands in a near adiabatic expander. In addition, there is improved efficiency with which heat transfer occurs in the heat exchanger that generates the subcooled working fluid for the cycle, as no phase change occurs within the heat exchanger reducing exergy destruction. Furthermore the phase change during Flashing is an internal heat transfer process within the working medium and no heat exchanger is required. These points make the SLFB Cycle more efficient in power production than both the Rankine Cycle (RC) and the TLC.
The proof of concept of the SLFB Cycle has shown that it is best suited for application in a positive displacement volumetric expander such as a reciprocating piston. This is due to the working fluid being in a two-phase state in the expansion stage of the cycle. The ideal piston engine for the cycle would have a long stroke and have its components; the block and piston heated to a temperature high enough to prevent heat transfer from the working fluid to these components. The subcooled liquid is to be introduced into the expander by controlled injections with an appropriate injection mechanism. In addition, the engine would ideally be operated at low speeds and with a subcooled high temperature working medium as this would ensure that the working fluid would begin its expansion process at a high temperature, improving the cycle's Carnot efficiency. The boiling unit where the atomized unflashed liquid undergoes convective boiling needs to have the largest possible surface area to maximize boiling but the smallest possible dead volume. Furthermore, the temperature of the boiling surface should be just below the Leidenfrost point of the heated surface for the working medium concerned.
A phenomenon known as the "Residual Mass Effect" was discovered and refers to the relatively low temperature liquid that doesn't undergo complete convective boiling and remains in the boiling unit when flashing occurs. It leads to efficiency losses through heat dissipation from the flash vapour to this liquid. The residual mass effect can be mitigated by maintaining the boiling surface just below the

Leidenfrost point and by designing the boiling unit so that any unvapourised liquid is flushed out with the exhaust steam.
The Injection pattern was seen to have an effect on the efficiency of the engine. Split injections of equal masses undergo more efficient convective boiling and are better able to contribute to the expansion phase. Higher temperatures of the subcooled liquid and higher engine loads reduce the efficiency of the convective boiling process but increasing the boiling surface temperature can counteract this provided the temperature of the convective boiling surface stays bellow the Leidenfrost point.
The SLFB cycle has great potential if the various systems continue to be optimized and developed. It also has applications outside the automotive sector particularly in power generation from low grade heat sources through the use of different working fluids.

Table of Contents

Chapter 1: Automotive Waste Heat Recovery

1.1 INTRODUCTION AND LITERATURE REVIEW

The world of today is faced with many issues. The more pressing issues include climate change, poverty, disease, uncontrolled population growth and a lack of resources. The lack for energy resources is a particularly important one as most of the world's conflicts can be traced back to this. As our modern society has developed around fossil fuels, the efficient and prudent use of this limited resource has become one of the most important endeavours facing modern environmental engineering. One of the main consumers of fossil fuels is the transportation system. With the ever-growing prosperity of the emerging economies such as China, Brazil and India, the demand for new cars in these nations is putting even more stress on petroleum reserves. In addition to this stress, the carbon dioxide emissions from current and future engines are another contributor to the widely debated Greenhouse Effect and Global Warming. Climate change led by global warming has led to international regulation of CO_2 emissions. The 1992 United Nations Framework Convention on Climate Change (UNFCCC) was the first international attempt at stabilizing greenhouse gas concentrations in the atmosphere. This was followed by The Kyoto Protocol in 1997; the first legally binding agreement to this effect. All parties to the Kyoto Protocol have set targets to cut and/or reduce their CO_2 outputs. At approximately 27% [1], the transportation sector is a significant source of CO_2 emissions and is a key target of the regulations.

1.1.1 Automotive Engine CO_2 Emission Targets

While zero emission vehicles are the ideal means of transportation in terms of their emissions, the implementation of the infrastructure required to make them viable is still many years off and in their current forms, both cost and resource inhibitive, and according to some literature only offer a modest hope of CO_2 reduction in their current form. The fact of the matter remains that while there are fossil fuels, we will continue to use them. According to British Petroleum (BP), at the current rate of production and the proved oil reserves reaching 1700.1 billion barrels as of the end of 2014, there is sufficient supply for a further 52.5 years. In

fact world oil reserves at the end of 2014 were 3 times their level in 1971. The world's oil reserves have steadily increased even in the face of rising consumption [2]. Our dependence on fossil fuels is set to continue in the near future. As mentioned earlier, all parties to the Kyoto Protocol have set CO_2 emission targets for automotive vehicles. Of these parties, the European Union has some of the strictest. At the end of 2013, the European Parliament and the council of the European Union set mandatory 2020 CO_2 emission targets for new passenger cars and light-commercial vehicles in the European Union. The passenger car standards are set at 95 g/km of CO_2 and the light-commercial vehicle standards are 147 g/km of CO_2. If these goals are to be met, it becomes the goal of the engineer to make the current fossil fuel based energy generation technologies for these vehicles, namely the Internal Combustion Engines (ICEs) more efficient.

1.1.2 Internal Combustion Engines: More than 370 Years and Still the First Choice

Christiaan Huygens back in 1678 first introduced the concept of the Internal Combustion Engine (ICE). Unlike its modern counterparts, this engine generated its power from the combustion of gunpowder and consisted of a vertical tube containing a piston. Gunpowder was inserted into the tube below the piston at the base and lit much like a cannon. The expanding gasses drove the piston up the tube until it reached a point near the top. Here, holes in the tube were uncovered allowing any remaining hot gasses to escape. The weight of the piston then caused it to drop, covering the holes and re-sealing the tube below the piston. The weight of the piston combined with the vacuum formed by the cooling gasses drew the piston back down the tube providing additional power.

With the invention of the Atmospheric Engine in 1712 by Thomas Newcomen and further improvement of it by James Watt, steam powered external combustion engines captured almost all the development efforts up until the early 20th century. While the stationary steam engine can be considered the key component of the Industrial Revolution, it did not make inroads into the Automobile and Aircraft sector due to the weight of boilers and condensers which made the power-to-weight ratio of a steam plant lower than that of an internal combustion engine. This saw the resurgence of the internal combustion engine in the late 19th century.

With ever growing standards of living and wealth of individuals, the demand for

personal transportation gave impetus to the development of the automobile and with it, its ideal partner the internal combustion engine. The keys to this partnership were firstly the high power to weight ratio of the ICEs and secondly and more importantly, its liquid fuel source which has a high energy to weight ratio and ease and simplicity of storage and use. The ICE continues to evolve and remains the first choice for automobile power plants.

1.1.3 Electrical Vehicles: Not a Viable Solution As Yet.

The rising cost of Petroleum based fuels for ICEs and the carbon dioxide and other undesirable emissions from these engines has led to a move into zero emission vehicles powered by Electricity. In fact the Electric Automobile itself is as old as the ICE powered automobile. A century ago, the Electric Automobile lost out to the ICE powered automobile due to two main factors; the poor power to weight ratio of electrical batteries and the relatively short mileage capable on a full charge. A hundred years later, though vastly improved, battery powered modern electrical vehicles are plagued by these same issues. Fuel cell vehicles are an exception to this issue and show promise. While all electrical vehicles including Hydrogen powered Fuel Cell Vehicles (FCV) are Zero Emission vehicles as far as their tailpipes or the lack there of go, the electricity and/or hydrogen they use are not generated from zero emission sources. According to the U.S Energy Information Administration data, 67% of the World's electricity production in 2012 was from Fossil Fuels and 95% of the Worlds Hydrogen was sourced from Fossil Fuels. According to Lindly and Haskew [3] who performed a case study of a 10% penetration of Electric Vehicles (EV), EVs appear to offer only a modest hope of reducing greenhouse gases and global environmental change in the near future. This is because electricity generating-plant emissions of CO_2 are much greater than vehicular emissions. Thus a reduction in vehicle emissions is partly counter-balanced by an increase in generating plant emissions. The infrastructural support for EVs is another issue. When compared to ICE vehicle re-fueling, the EV charging infrastructure is grossly lacking. Development of this infrastructure is vital to the proliferation of EVs but the environmental impact of these needs to be considered. According to Nansai et al [4] the development of charging infrastructure does not change the advantage of EVs compared to gasoline vehicles (GV) in terms of CO_2, NO_x, and CO emissions. In fact an EV emits more life-cycle SO_x than gasoline vehicles (GVs). These illustrate how EVs and their proliferation are faced with many

hurdles.

The underlying issue with an EV based transportation system lies with the electrical power generation system as we know it. Jochem et al [5] sums up this point very clearly; “Hence, for some countries, the EV will not necessarily help to significantly reduce CO_2 emissions of individual road transport by 2030, especially when the national power plant portfolio consists of many thermal plants and because emission of conventional vehicles will also be reduced to about 80 g CO_2/km by that time.”

1.1.4 Bio Fuels: Post Petroleum Liquid Fuels

Solar energy is a clean renewable source of energy that has the potential to solve humanity’s energy needs. The mention of the term “Solar Energy” usually conjures up the image of solar panels that generate electricity. While this is a modern artificial iteration of “Solar Energy”, the most common form is photosynthesis and this process is the source of energy for life on the planet and the main source of energy for human activity. Fossil fuels are nature’s ancient solar energy stores. While Fossil Fuels are natural, the combustion of these Fossil Fuels has upset the fine balance with which nature operates. Fossil Fuels are not part of the current carbon cycle of the planet and photosynthesis which sequesters this CO_2 cannot keep up with the rate of its production. Thus a net increase in global CO_2 levels has resulted and will continue to rise while Fossil Fuels are combusted. If however, combustible fuels were to be sourced from within the current carbon cycle the issue of rising CO_2 levels can be mitigated. Bio Fuels are fuels sourced from the planets current carbon cycle. There are differing schools of thought on the viability of bio-fuels as a future source of low carbon emission fuels. According to Graeme and Pearman [6] bio-fuels and bio-sequestration can only be a small part of a low carbon future due mainly to the inefficiency of photosynthesis in converting solar energy to usable energy and the availability of solar radiation. This may very well be the case if all of the world’s energy were to be sourced from photosynthesized bio mass, but it doesn’t completely strikeout bio-fuel use in the future. As the saying goes “One size doesn’t fit all” photosynthesized bio-fuels may not be viable in regions of low solar radiation, but in the tropical and sub-tropical zones the story is quite different. According to Baral and Guha [7], growing short rotation woody crops (SRWC) for substituting fossil fuels may become a cost-effective strategy to combat climate change. In a non-botanical bio-mass study, Ullah et al [8] have

shown the potential for algal based fuels to take the lion share of transportation fuels in the future. Other processes also exist for the sequestration of CO_2 for fuel production. According to Fortier et al [9], algal bio jet fuel can reduce the life cycle (LC) greenhouse gas (GHG) emissions by 76% when compared to conventional jet fuel. Another study by Yasin et al [10], has shown that methanogens from waste activated sludge has significant potential for converting the greenhouse gas CO_2 into the fuel methane with a 77% reduction in CO_2. Furthermore, according to Anwar et al [11], the low-cost conversion of lignocellulosic biomasses into bio-fuels has great potential due to its abundant availability and will take the focus of future bio-fuel research. According to the U.S Energy Information Administration (EIA) the last 10 years ending in 2014 has seen the energy generated from fossil fuels fall by 6.3% and increase by 53% for bio mass although bio mass accounts for 2.5% of the total energy consumed and fossil fuels account for 42.9%. [12]. What is worthy of note are the trends seen here which give support to the hypothesis that bio-fuels will remain in the picture as a post petroleum fuel.

1.1.5 The Future of the IC Engine

The first internal combustion engines had efficiencies of just about 10% but a century of development has seen its efficiency rise significantly. While the engine has undergone vast improvements in its efficiency, the most efficient road going engines today remain just under 43% and the average engine remains at approximately 35%. The most efficient, The Wartsila-Sulzer RTA96-C turbocharged two-stroke diesel engine has achieved just over 50% efficiency at optimal operation. According to Oltra and Saint Jean [13] more than 50% of automotive related firms' patent portfolios are still dedicated to ICE powered vehicles. Furthermore according to Oltra and Saint Jean, [13] and Berggren and Magnusson [14], the share of advanced diesel vehicles is expected to increase in the next 30 years. ICEs are very competitive. ICEs can be produced at a much lower cost than its competitors the EV and FCV, and liquid fuels are easily available now and according to Shafiee and Topal [15], and the BP Statistical Review of World Energy, June 2015 [2], petroleum is set to remain available for at least the next 40 years. Factoring in liquid bio-fuels and the issues facing EVs and FCVs, the dominance of the ICE is set to continue in the foreseeable future. With that being the case, the efficient use of these fuels becomes vital and the future of the ICE lies with the improvement of its thermal efficiency.

1.1.6 Waste Heat Recovery

According to Berggren and Magnusson [14], waste heat recovery (WHR) technologies are recognized as a technology with potential for achieving fuel economy goals required of future ICEs. According to Armstead and Miers [16] exhaust gas temperatures of on-road vehicles average between 500ºC and 600ºC, with maximum values of up to 1000ºC, while the coolant fluid temperatures range between 100ºC and 130ºC .Taking into account the Carnot cycle, the maximum amount of energy that ideally can be recovered ranges from 1.7 to 45kW for the exhaust which accounts for approximately 38% of total exhaust heat and from 0.9 to 4.8kW for the coolant system which is 10% of the total waste heat. Armstead also states that a WHR system that produces 1.3kW of electricity would be capable of replacing the alternator of a small passenger car and as a result improve fuel economy. This has the potential to improve the fuel consumption of hybrid vehicles by as much as 32%. Several technologies are common in waste heat recovery: (i) the Rankine cycle, (ii) the organic Rankine cycle, (iii) thermoelectric generators, (iv) turbo-compounding, (v) the Kalina cycle, and (vi) the Stirling cycle. Of these, according to Karvonen et al [17], the prominent technologies with active research in waste heat recovery from engines comprise of thermoelectric generators (TEGs), Rankine cycle (RC) based systems with steam or organic working fluids, and mechanical or electrical turbo-compounding.

1.1.6.1 Turbo Compounding

Diesel engines with mechanical turbo-compounding have been available for some years. These systems use exhaust gasses to drive a turbine on a shaft that contains both a compressor and a mechanical transmission. The compressor compresses the engine's intake charge to help reduce the engine's volumetric inefficiencies and the mechanical transmission transmits the rotational energy of the shaft to the vehicle's drivetrain. Knecht [18] argued that considerably greater reductions in engine fuel consumption could be achieved by the use of a Rankine cycle instead. And according to Armstead and Miers [16], thermoelectric generators and Rankine cycles exhibit the greatest potential for advances in cleaner energy production.

1.1.6.2 Thermoelectric generators (TEGs)

TEGs can convert waste heat directly into electricity. Such generators can be used both to convert heat into electricity and electrical power into cooling or heating power. The working principle of TEGs is based on the Seebeck effect, which converts the temperature difference between the hot source and cold source directly into electricity. The advantages of using TEG technology in waste heat recovery are its silent operation and high reliability as these systems have no moving or mechanically complex components. The primary challenge facing current TEGs is their relatively low efficiency in converting thermal energy to electricity. Zorbas et al [19] estimated that the use of TEGs could achieve a 5% reduction in the fuel consumption of a passenger car at the current technology level.

1.1.6.3 Rankine Cycle WHR systems

This is the most widely experimented upon WHR option. In the Rankine Cycle (RC), a high pressure liquid is evaporated at a constant pressure in an evaporator by a source of heat power. The high pressure vapour is then expanded to a lower pressure, and power extracted from the expansion. The expansion can be harnessed in either a turbine or a piston expander, which intern produces either mechanical power or is coupled to a generator to produce electrical power. The low pressure vapor is then condensed back into the liquid phase by a condenser, after which the pressure of the liquid is raised in a feed pump which in turn feeds the evaporator. Conventional RCs use steam as the working medium whereas the Organic Rankine Cycle (ORC) employs an organic working medium. Sprouse and Depcik [20] in their literature review discovered that the concept of using ORCs to recover waste heat from internal combustion engines had been explored in the 1970s, showing significant fuel economy improvements in the studied engine systems. According to Bombarda et al [21], Studies on systems using exhaust gas heat have shown that an approximately 10% increase in the power output of an engine system can be achieved when using ORCs to recover heat from industrial scale reciprocating engines, and smaller-scale engines are capable of achieving fuel economy improvements of around 10% if suitable working fluids are selected and advanced expander

technologies are adopted. Karvonen et al [17] in his patent landscape analysis states; “In automotive applications, RC and ORC development has focused particularly on heat recovery from long-haul truck engines, because the available amount of heat is sufficient for current expander designs and the large number of cruising hours plays an important role in profitability.” According to Sprouse and Depick [20], while the performance and technology implemented in RCs and ORCs are technologically satisfactory, lower-cost solutions are needed to make these systems economically feasible for small-scale WHR applications. Another key aspect of RC and ORC application is the choice of the working fluid. Sprouse and Depick [20] concluded that no single configuration or single working fluid can be identified as optimal for different waste heat sources at different temperature levels. They also go on to state that the available space for the WHR system for road going vehicles is limited, and working fluids having low volumetric flow rates, enabling the use of small-size heat exchangers, are desirable.

1.1.6.4 A New WHR system

It can be deduced that the ideal WHR system would be one that is compact, durable, cheap to mass produce and ultimately provide an efficiency improvement that significantly outweighs its cost. This study introduces a WHR system that operates on a novel heat cycle. Furthermore, it is capable of being produced with currently available mass produced components. Table 1 shows the proposed automotive WHR system compared with some of the current automotive systems being investigated.

Table 1. Comparison of the proposed system with some current research.

Car Maker	WHR System	Efficiency Improvement	Key Points
BMW	Twin circuit Organic Rankine Cycle	~ 15% (Fuel economy)	1. Able to extract up to 80% of waste heat. 2. Complex heat extraction system.
Toyota	Sterling	~ 2% (Engine Efficiency)	1. Simple and compact. 2. Low heat extraction efficiency from exhaust gasses.
Honda	Rankine/Electric	~ 3.8% (Fuel economy)	1. Volumetric expander has 13% efficiency. 2. Low heat extraction efficiency from exhaust gasses.
Honda	Thermo-electric	< 1 % (Fuel economy)	1. Low efficiency of thermo-electric units.
Proposed system	SLFB Cycle	~8% (Targeted engine efficiency)	1. Compact. 2. Theoretical potential for high efficiency. 3. Ability to store energy.

1.2 THE OUTLINE OF THE THESIS

This report will first introduce a novel heat cycle and the concept behind the proposed WHR system in Chapter 2. This will then be followed by experimental investigation into the proof of concept and its application to a reciprocating piston engine in Chapter 3. Chapter 4 will cover the fundamentals governing the operation and efficiency of a reciprocating engine running on the novel heat cycle. Chapter 5 will deal with optimisation of the cycle for automotive waste heat recovery based on the findings of experimentation and will also introduce some alternative means of harnessing the cycle for automotive WHR. This chapter will also lay out the path of future experimentation that will see the system realize its goal of being employed as a WHR system in mass produced vehicles. Finally Chapter 6 will deal with the conclusions drawn from the research.

REFERENCES

1. Jos G.J. Olivier, Greet Janssens-Maenhout, Marilena Muntean, Jeroen A.H.W. Peters, Trends in global CO2 emissions: 2014 Report PBL Netherlands Environmental Assessment Agency. ISBN: 978-94-91506-87-1 PBL publication number: 1490 JRC Technical Note number: JRC93171.The Hague, 2014. http://www.pbl.nl/sites/default/files/cms/publicaties/PBL_2014_Trends_in_global_CO2_emisions_2014_1490_0.pdf
2. BP, BP Statistical Review of World Energy 2015, page 7. http://www.bp.com/content/dam/bp/pdf/Energy-economics/statistical-review-2015/bp-statistical-review-of-world-energy-2015-full-report.pdf
3. Jay K. Lindly, Tim A. Haskew, Impact of electric vehicles on electric power generation and global environmental change, Advances in Environmental Research, Volume 6, Issue 3, September 2002, Pages 291-302, ISSN 1093-0191, doi:10.1016/S1093-0191(01)00060-0.
4. Keisuke Nansai, Susumu Tohno, Motoki Kono, Mikio Kasahara, Yuichi Moriguchi, Life-cycle analysis of charging infrastructure for electric vehicles, Applied Energy, Volume 70, Issue 3, November 2001, Pages 251-265, ISSN 0306-2619, doi:10.1016/S0306-2619(01)00032-0.
5. Patrick Jochem, Sonja Babrowski, Wolf Fichtner, Assessing CO_2 emissions of electric vehicles in Germany in 2030, Transportation Research Part A: Policy and Practice, Volume 78, August 2015, Pages 68-83, ISSN 0965-8564, doi:10.1016/j.tra.2015.05.007.
6. Graeme I. Pearman, Limits to the potential of bio-fuels and bio-sequestration of carbon, Energy Policy, Volume 59, August 2013, Pages 523-535, ISSN 0301-4215, doi:10.1016/j.enpol.2013.04.064.
7. Anil Baral, Gauri S. Guha, Trees for carbon sequestration or fossil fuel substitution: the issue of cost vs. carbon benefit, Biomass and Bioenergy, Volume 27, Issue 1, July 2004, Pages 41-55, ISSN 0961-9534, doi: 10.1016/j.biombioe.2003.11.004.
8. Kifayat Ullah, Mushtaq Ahmad, Sofia, Vinod Kumar Sharma, Pengmei Lu, Adam Harvey, Muhammad Zafar, Shazia Sultana, C.N. Anyanwu, Algal biomass as a global source of transport fuels: Overview and development perspectives, Progress in Natural Science: Materials International, Volume

24, Issue 4, August 2014, Pages 329-339, ISSN 1002-0071, doi:10.1016/j.pnsc.2014.06.008.
9. Marie-Odile P. Fortier, Griffin W. Roberts, Susan M. Stagg-Williams, Belinda S.M. Sturm, Life cycle assessment of bio-jet fuel from hydrothermal liquefaction of microalgae, Applied Energy, Volume 122, 1 June 2014, Pages 73-82, ISSN 0306-2619, doi:10.1016/j.apenergy.2014.01.077.
10. Nazlina Haiza Mohd Yasin, Toshinari Maeda, Anyi Hu, Chang-Ping Yu, Thomas K. Wood, CO2 sequestration by methanogens in activated sludge for methane production, Applied Energy, Volume 142, 15 March 2015, Pages 426-434, ISSN 0306-2619, doi:10.1016/j.apenergy.2014.12.069.
11. Zahid Anwar, Muhammad Gulfraz, Muhammad Irshad, Agro-industrial lignocellulosic biomass a key to unlock the future bio-energy: A brief review, Journal of Radiation Research and Applied Sciences, Volume 7, Issue 2, April 2014, Pages 163-173, ISSN 1687-8507, doi:10.1016/j.jrras.2014.02.003.
12. The U.S. Energy Information Administration (2015). Monthly Energy Review, August 2015. http://www.eia.gov/totalenergy/data/monthly/archive/00351508.pdf
13. Vanessa Oltra, Maïder Saint Jean, Variety of technological trajectories in low emission vehicles (LEVs): A patent data analysis, Journal of Cleaner Production, Volume 17, Issue 2, January 2009, Pages 201-213, ISSN 0959-6526, doi:10.1016/j.jclepro.2008.04.023.
14. Christian Berggren, Thomas Magnusson, Reducing automotive emissions—The potentials of combustion engine technologies and the power of policy, Energy Policy, Volume 41, February 2012, Pages 636-643, ISSN 0301-4215, doi:10.1016/j.enpol.2011.11.025.
15. Shahriar Shafiee, Erkan Topal, When will fossil fuel reserves be diminished?, Energy Policy, Volume 37, Issue 1, January 2009, Pages 181-189, ISSN 0301-4215, doi:10.1016/j.enpol.2008.08.016.
16. John R. Armstead and Scott A. Miers, Review of Waste Heat Recovery Mechanisms for Internal Combustion Engines, J. Thermal Sci. Eng. Appl 6(1), 014001 (Oct 21, 2013) (9 pages) doi:10.1115/1.4024882
17. Matti Karvonen, Rahul Kapoor, Antti Uusitalo, Ville Ojanen, Technology competition in the internal combustion engine waste heat recovery: a patent landscape analysis, Journal of Cleaner Production, Available online 18 June 2015, ISSN 0959-6526, doi:10.1016/j.jclepro.2015.06.031
18. Walter Knecht, Diesel engine development in view of reduced emission

standards, Energy, Volume 33, Issue 2, February 2008, Pages 264-271, ISSN 0360-5442, doi:10.1016/j.energy.2007.10.003.

19. K.T. Zorbas, E. Hatzikraniotis, and K.M. Paraskevopoulos, Power and Efficiency Calculation in Commercial TEG and Application in Wasted Heat Recovery in Automobile, The Proceedings of the 5th European Conference on Thermoelectrics, ICT2007.
20. Charles Sprouse III, Christopher Depcik, Review of organic Rankine cycles for internal combustion engine exhaust waste heat recovery, Applied Thermal Engineering, Volume 51, Issues 1–2, March 2013, Pages 711-722, ISSN 1359-4311, doi:10.1016/j.applthermaleng.2012.10.017.
21. Paola Bombarda, Costante M. Invernizzi, Claudio Pietra, Heat recovery from Diesel engines: A thermodynamic comparison between Kalina and ORC cycles, Applied Thermal Engineering, Volume 30, Issues 2–3, February 2010, Pages 212-219, ISSN 1359-4311, doi:10.1016/j.applthermaleng.2009.08.006.

Chapter 2: An Introduction to the Subcooled Liquid Flash, Boiling Cycle (SLFB)

The SLFB Cycle is a novel heat cycle. It is an augmented version of a hitherto well known cycle called the Trilateral Cycle (TLC). [1],[2],[3],[4],[5],[6],[7],[8]

2.1 THE TRILATERAL CYCLE

The ideal Trilateral Cycle may be summarized by Figure 1, which represents the temperature versus entropy diagram of this cycle.

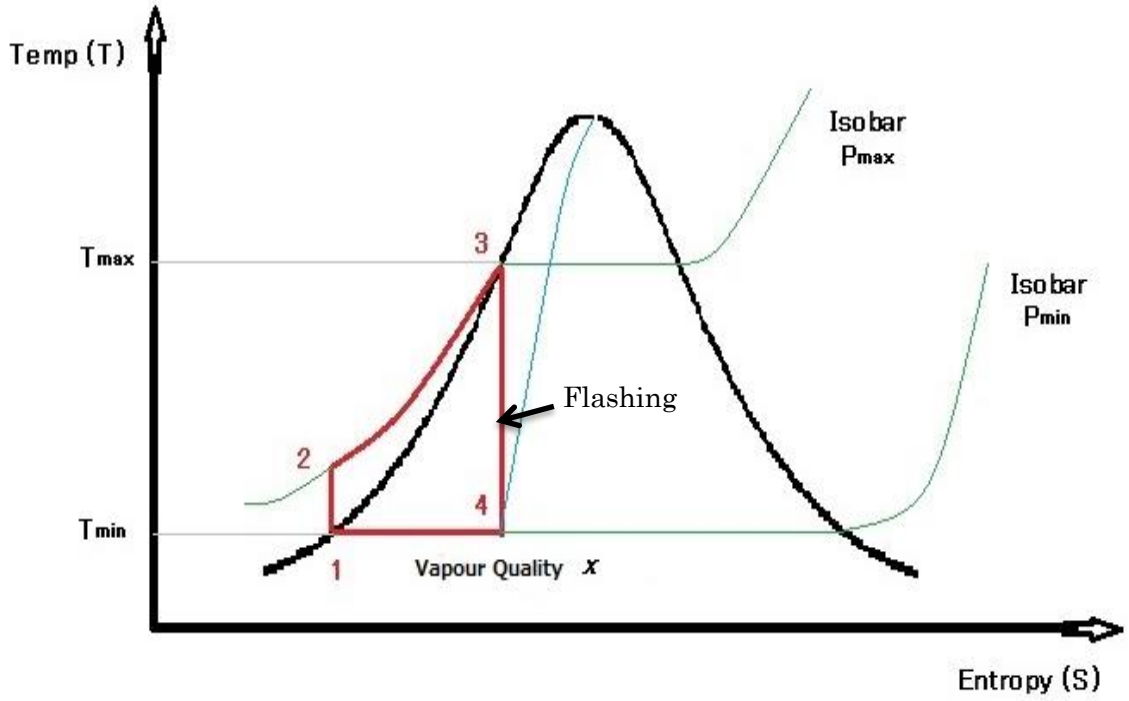

Figure 1. The TS Diagram of the TLC

1-2 is the isentropic compression of the liquid phase to a maximum pressure P_{max} by an isentropic pump. The pump compresses the liquid to a pressure high enough to maintain it in a subcooled state at T_{max}.

2-3 is the isobaric heating of the liquid phase up to the temperature T_{max}. At state 3 the liquid is in a subcooled state.

3-4 is the isentropic expansion of the vapour generated from "flashing". In this

process, wet saturated steam is generated and expands doing work. In the process, the temperature and pressure of the working fluid drops to the temperature T_{min} and pressure P_{min} with a vapour quality x.
4-1 is the condensation of the wet vapour back to state 1.
The Isentropic expansion in stage 3-4 is commonly known as “Flashing”.

2.1.1 Flashing

A high temperature liquid held in its liquid phase by a high vapour pressure is termed a subcooled liquid. When this subcooled liquid is released into a lower vapour pressure environment, the liquid phase can hold less heat and must “dump” some of this energy. This “dumping” occurs by converting a certain portion of the liquid into the gas phase and the unflashed portion of the original liquid falls to its new and lower saturation temperature. The phase change described above is an almost instantaneous process and is known as “Flashing”. The enthalpy this “Flash steam” possesses is the difference between the enthalpies of the liquid phase of the subcooled water and the liquid phase of the water at the lower vapour pressure to which it falls after flashing has taken place. The work potential of this steam comes from this heat which it possesses. The vapour content of the wet steam generated by flashing can be described by equation (1).

$$x = \frac{h_{isl} - h_{fvp}}{L_{fvp}} \tag{1}$$

x is the vapour quality (also known as the vapour content or Flash %) of the steam generated. Furthermore, the heat possessed by this vapour can be described by equation (2)

$$h_{fs} = \ h_{isl} - h_{fvp} \tag{2}$$

The example bellow illustrates the work potential of flash steam.

Subcooled water held at a temperature of 240ºC and a pressure of 5MPa has an enthalpy of 1038kJ/kg (h_{isl}). If this water were suddenly released into an

environment at a vapour pressure of 0.1MPa (atmospheric pressure), where water in its liquid phase can naturally hold a maximum of 422kJ/kg (h_{fvp}), and factoring in the latent heat of vaporisation of water (L_{fvp}) at 0.1MPa being 2281 kJ/kg, approximately 27% of the injected mass would flash into steam. The heat possessed by the vapour phase of the flash steam is 616kJ/kg and has the potential to do 616kJ/kg of expansion work.

A point worthy of note is that although the percentage of flash steam is just 27%. The energy it possesses is a much larger fraction of the original subcooled liquid. This is described by equation (3).

$$\%\ h_{isl\ \rightarrow fs} = \frac{h_{isl} - h_{fvp}}{h_{isl}} \tag{3}$$

The steam would contain approximately 59% of the original enthalpy of the subcooled water.

2.1.2 The TLC Efficiency

With reference to Figure 1, the working fluid of the TLC gains its heat from an isobaric heating process in stage 2-3. Here, heat transfer occurs from the heat carrier to the working fluid. The TLC has the advantage of the cooling down curve of the heat carrier and the heating up curve of the working fluid matching up well which means a very efficient heat transfer and resulting high system efficiency. Fischer [1] clearly demonstrates this point as do Ho et al [2] in their comparisons of TLCs and ORCs. According to Fischer [1], the exergy efficiency for power production is larger by 14% ~ 29% for TLCs than for ORCs.

Key Points of heat transfer efficiency are as follows:

1. The heat source and working fluid must be separated by a temperature difference in order for heat transfer to occur; however, heat transfer across a finite temperature difference, i.e.; constant temperature phase change, inherently causes irreversibilities.
2. Good temperature matching between the heat exchanger streams minimizes these irreversibilities

3. In a conventional heat exchanger (RC or ORC), the working fluid is first heated as a liquid, undergoes liquid to vapour phase change, and if necessary, further superheated as a vapour thereafter. Its temperature profile will first be near linear, then constant during phase change, and then near linear again, as shown in Figure. 2. Temperature mismatching causes a pinch point to form, destroys potential work or exergy, and reduces the effectiveness of the heat exchanger.

4. A method to avoid the phase change region and exergy destruction is transferring heat at pressures high enough to prevent phase change of the working fluid. This avoids the temperature mismatching encountered in the constant temperature phase change process. The improved temperature matching is shown in Figure. 3.

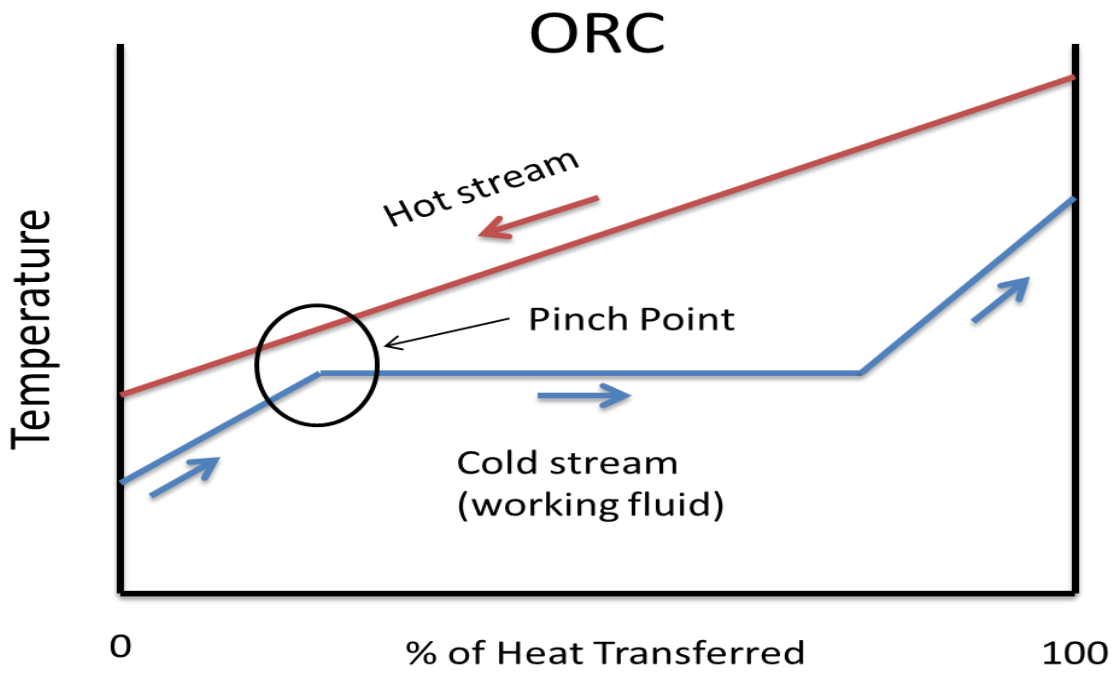

Figure 2. The variation in stream temperatures during the heat addition process for working fluids that undergo phase change.

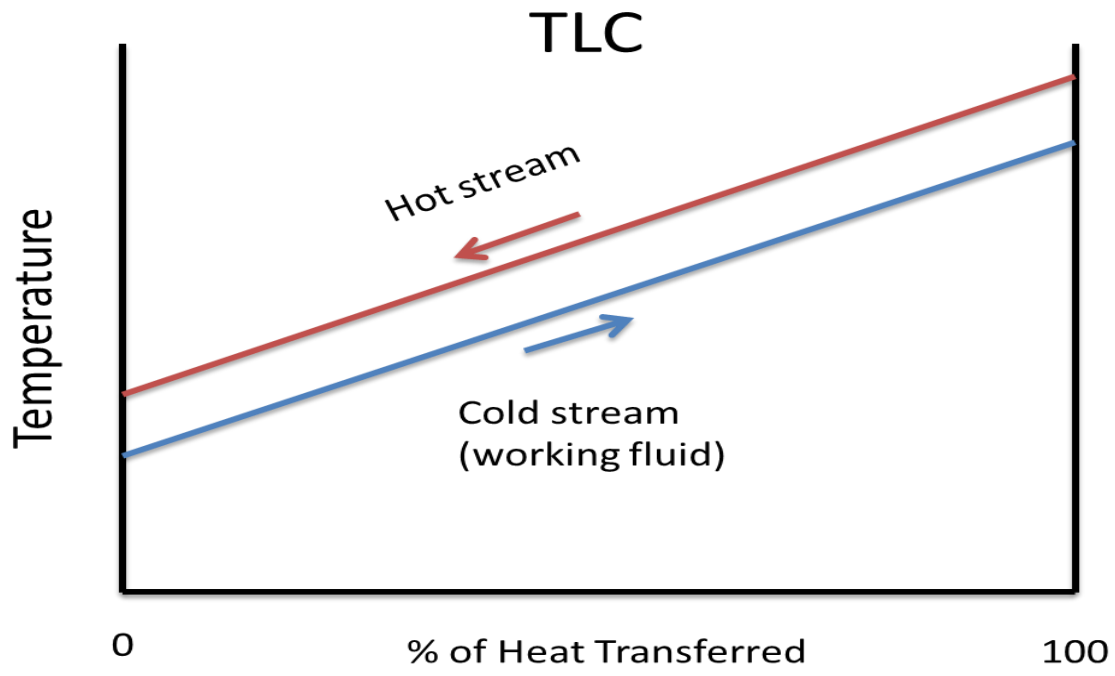

Figure 3. The variation in stream temperatures during the heat addition process for working fluids that do not undergo phase change.

For heat engines that operate on external heat sources such as the RC, ORC and TLC, the heat exchange process in the heat exchanger is a key aspect of the overall efficiency of the cycle. Thus it can be said that the TLC owes its improved efficiency for power production to the higher efficiency with which heat transfer happens between the heat carrier and the working fluid in the heat exchanger. [1], [2], [3], [4]

2.2 THE S.L.F.B CYCLE, AN AUGMENTED T.L.C

As mentioned earlier, the SLFB Cycle is an augmented version of the TLC. Figure 4 shows the temperature versus entropy representation of The SLFB Cycle.

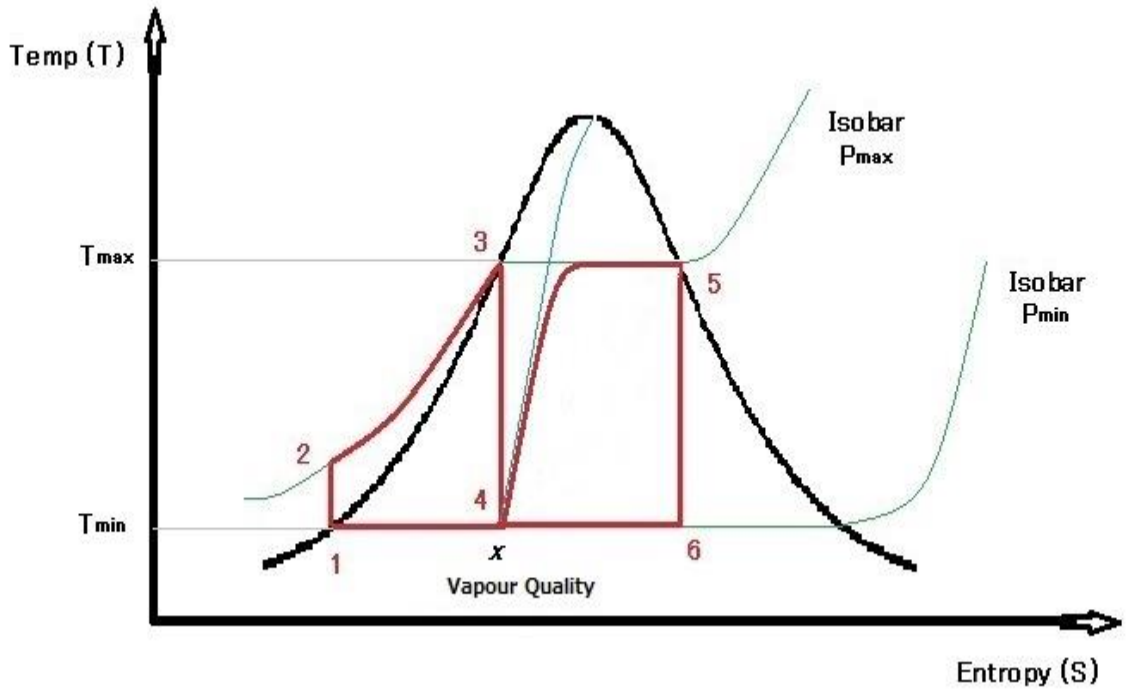

Figure 4. The SLFB Cycle.

The SLFB cycle is identical to the TLC in process stages 1-2, 2-3 and 3-4. In a conventional TLC cycle, the liquid or unflashed portion is discarded as it cannot contribute to expansion work [2]. However it possesses a significant amount of heat energy. The SLFB Cycle aims to harness this energy. Stage 4-5 is the multiphase convective boiling of this unflashed liquid portion generated in process stage 3-4. This is achieved by the impingement of this liquid onto an appropriately heated surface. The "B" in the cycle's acronym "SLFB" stands for this convective boiling process. The vapour generated from this convective

boiling is capable of reaching a maximum pressure of P_{max} determined by the wall temperature(T_{max}). Stage 5-6 is the isentropic expansion of the vapour generated and stage 6-1 is the complete condensation of the vapour back to state 1. The multiphase convective boiling supplements the work output of the cycle.

Unlike the Rankine cycle and the TLC which only has a single heat input stage in the cycle, the SLFB possesses two. The first is at the stage 1-2 where the subcooled liquid is generated, and the second at stage 4-5 where multiphase convective boiling takes place. Furthermore, the convective boiling process initiated by the spraying of finely atomised liquid droplets onto the heated surface is also very efficient [9].

I. The liquid portion is already at a significantly elevated temperature, thus relatively little energy is required in the heating up process prior to phase change.
II. The flashing of the subcooled liquid leads to fine atomisation of the unflashed liquid portion. This in turn improves its ability to transfer heat off the heated surface it impacts through increased surface coverage. [9],[10],[11],[12],[13]

Figure 5 demonstrates the expandable vapour generating process of the SLFB Cycle.

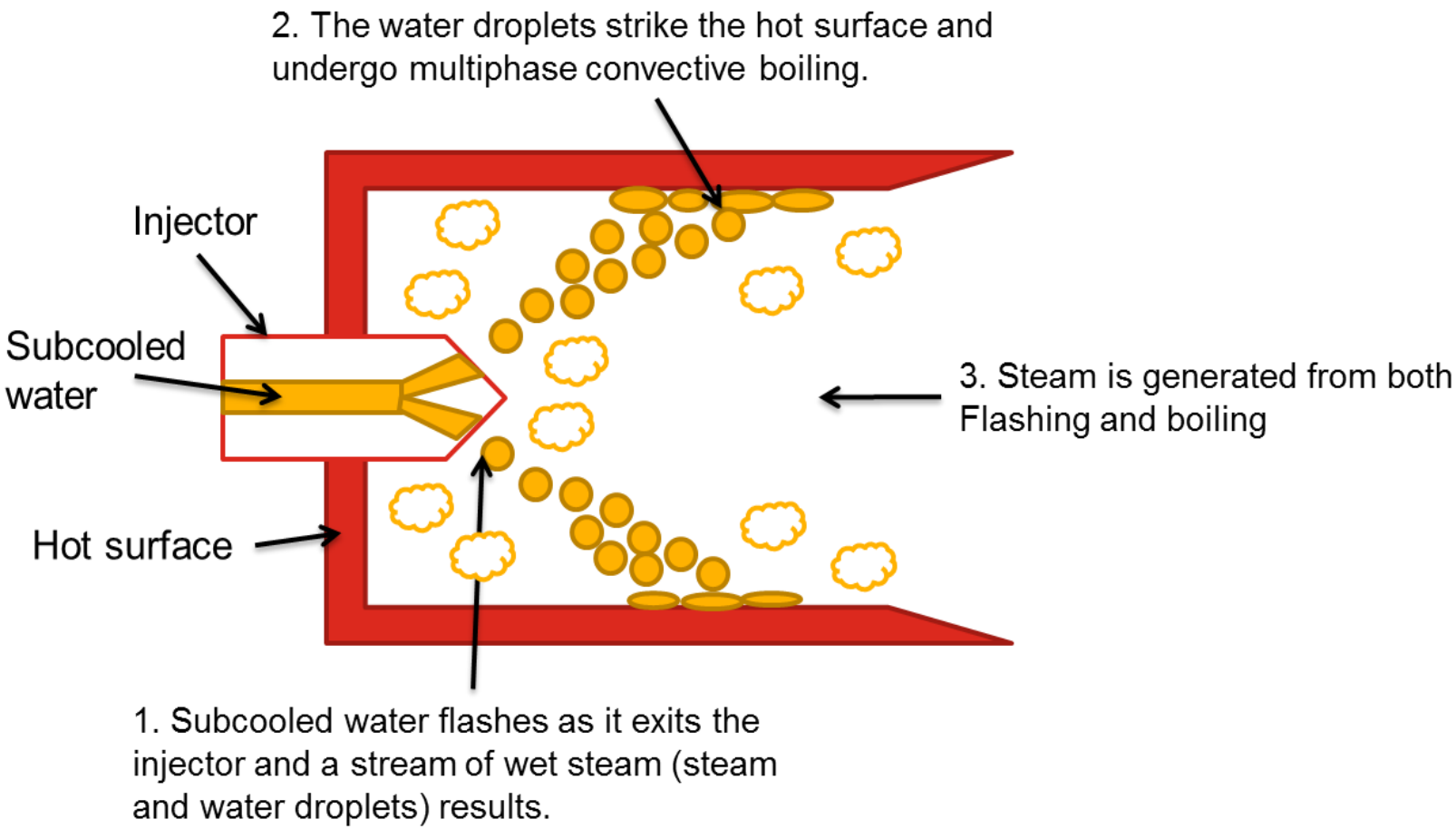

Figure 5. The Flash/Convective-Boil Mechanism

2.2.1 A Mathematical Description of Work Output of the SLFB Cycle

The theoretical net-work output of the system is governed by 4 parameters.

1.) $\boldsymbol{Q_h}$ – The heat transferred to the subcooled liquid by exhaust gasses with no phase change occurring in either of the hot or cold streams. This may be described as follows:

$$Q_h = h_{HE} \cdot A_{HE} \cdot LMTD \tag{4}$$

Where*:*

h_{HE} - heat transfer coefficient

A_{HE} - transfer area

$LMTD$ - log mean temperature difference between the hot and cold streams of the exchanger

$$LMTD = \frac{\Delta T_A - \Delta T_B}{\ln(\Delta T_A / \Delta T_B)} \tag{5}$$

Where:

ΔT_A - the temperature difference between the two streams at end A,

ΔT_B - is the temperature difference between the two streams at end B.

Ends *A* and *B* describe the points where the two fluids meet and depart respectively.

2.) $\boldsymbol{Q_{cb}}$ **–** The heat transferred in the convective boiling process. The actual boiling regime involved is dependent on many factors [12], but for the purpose of simplification, it is assumed that the impinging liquid droplets form a thin film on the heated surface before undergoing multiphase convective boiling.

$$Q_{cb} = h_{CB}(T_s - T_l).A_{cl} \quad \text{and} \quad Q_{cb} = B_s \cdot L \tag{6}$$

Where:
h_{CB} - heat transfer coefficient
T_s - temperature of heated surface
T_l - temperature of liquid
A_{cl} - surface area in contact with the liquid.
L - latent heat of vaporisation of the liquid
B_s - speed of evaporation

Thus the speed of evaporation can be described as:

$$B_s = {[h_{CB}(T_s - T_l) \cdot A_{cl}]}/{L} \tag{7}$$

This evaporation speed is the determining factor in the ability of Q_{cb} to contribute to power generation when engine speeds increase.

3.) $\boldsymbol{Q_{out}}$ **–** The heat dissipated by the condenser. The condenser is only required to return the wet steam to its liquid phase. The Q_{out} will depend on the ability of the engine unit to harness work from the generated steam. Any heat in the steam which the engine cannot convert to work will be the Q_{out}. This can thus be described as:

$$Q_{out} = (Q_h + Q_{cb}) \cdot (1 - \eta_{engine}) \tag{8}$$

Where:
η_{engine} - efficiency of the engine

4.) $\boldsymbol{W_p}$ – The pumping work loss. The pumping work will depend on the efficiency of the pump and the difference in enthalpy of the water entering it and leaving it. In the current system, the pump is only used to raise the water to a desired pressure. Due to the extremely low compressibility of the liquid phase, a relatively small increase in enthalpy of the liquid results. Thus relatively little power is needed for pumping. This can be described by as:

$$W_p = {}^{\Delta PV}/_{\eta_{pump}} \tag{9}$$

Where:

ΔP - change in pressure of the liquid

V - pumped volume

η_{pump}- efficiency of the pump

Thus all the above can be combined to give the following equation for the net-work output of a flash steam engine:

$$\begin{aligned} W_{net} &= (Q_h + Q_{cb}) - Q_{out} - W_p \\ &= \eta_{engine}(Q_h + Q_{cb}) - W_p \end{aligned}$$

Therefore:

$$W_{net} = [(U \cdot A_{HE} \cdot LMTD) + (h_{CB}(T_s - T_l) \cdot A_{cl})] - \left[{}^{\Delta PV}/_{\eta_{pump}}\right] \tag{10}$$

2.3 THE S.L.F.B AUTOMOTIVE WASTE HEAT RECOVERY SYSTEM

It has been shown that the RC and ORC are the preferred heat cycles for automotive WHR to date with over 3 decades of research history and a significant amount of current research interest and investment [14]. It has also been shown that the TLC has a higher power production efficiency than the ORC [1]. The SLFB cycle improves upon the TLC and should provide even better power production efficiencies. However, the TLC isn't without its issues. In the TLC, the working medium usually exists in a two-phase state when expansion work is extracted from it and this necessitates the use of a two-phase expander [1]. The SLFB cycle is faced with the same issue. However, such expanders do exists and the humble reciprocating piston expander is one such cost effective solution.

The waste heat output of an ICE powered vehicle varies with the driving mode [6],[7],[14]. RC and ORC based systems are capable of high power outputs when the waste heat flows from the main IC engine of the vehicle is high but don't allow on-demand power production. The SLFB based system on the other hand has the added advantage of allowing the storage of heat energy in the form of the subcooled liquid, akin to a liquid fuel, and allows on-demand use of this for power production by the expansion unit. Figure 6 shows the proposed SLFB automotive waste heat recovery system

The key aspects of an SLFB powered WHR system may be summarised as follows:

I. High power production efficiency due to the high efficiency with which heat transfer happens between the heat carrier and the working medium.
II. The existence of two heat addition processes within the cycle in the form of generating the high temperature subcooled liquid and the multiphase convective boiling of the unflashed liquid phase.
III. The ability to reduce the wetness of the working medium through the convective boiling process which helps mitigate the mechanical issues caused by two-phase working mediums on expanders.

IV. The ability to store energy from highly energetic waste heat flows and allow on-demand power generation from the system's power engine when waste heat flows are small from the main IC engine of the vehicle.
V. The ability to use cheap mass produced components such as piston expanders.

The above key aspects of an SLFB based WHR system make it an attractive option for automotive waste heat recovery.

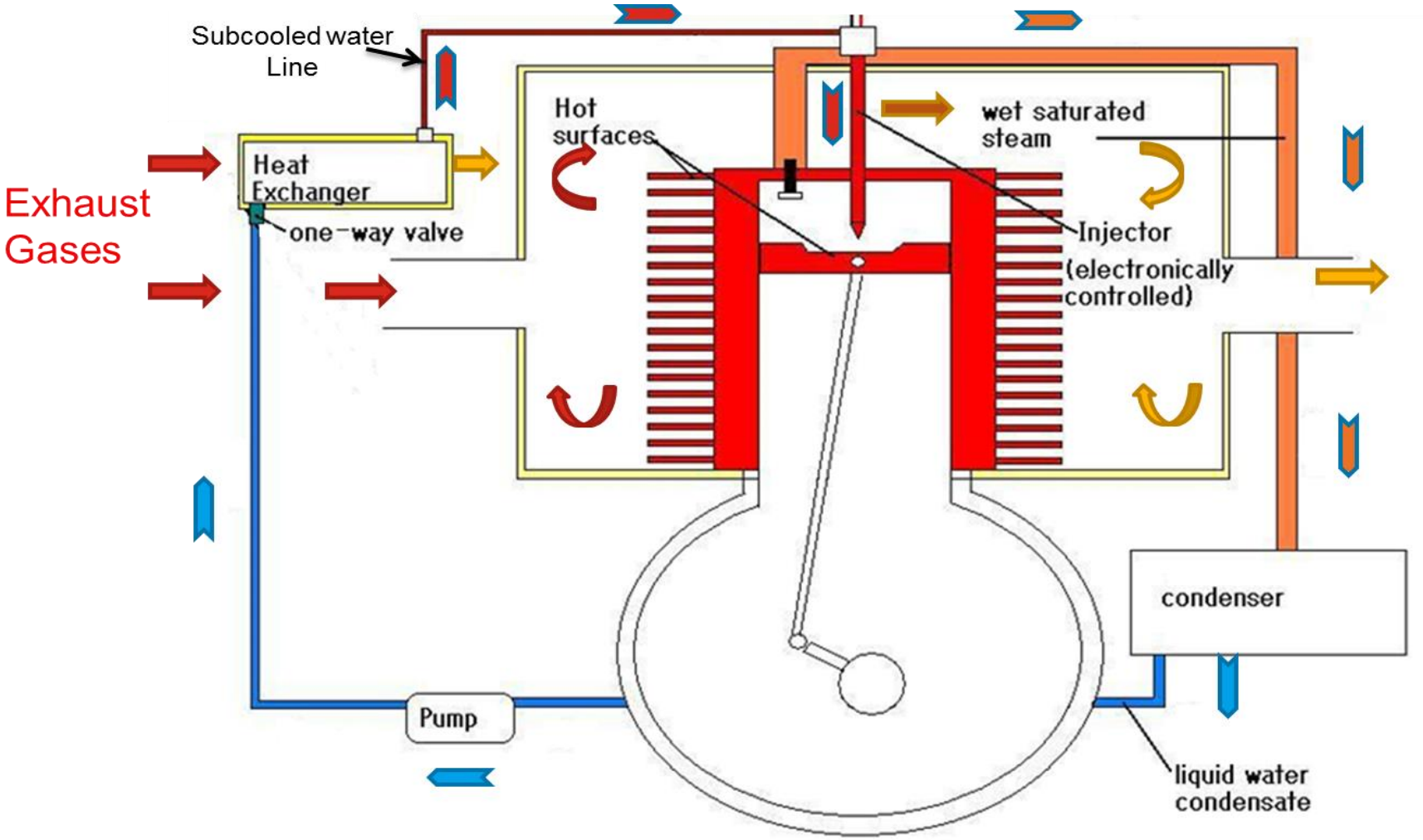

Figure 6. The proposed WHR system based on the SLFB cycle.

The SLFB Cycle automotive waste heat recovery system operation may be summarized as follows

1. Exhaust gasses of a conventional I.C engine heats water in a heat exchanger. The one-way valve and closed injector prevents any pressure from escaping and subcooled water results.

2. Exhaust gasses from the I.C engine are also directed over the head and block of the “Flash Steam Engine” unit. These exhaust gasses raise the temperature of the head, block and piston and provide further heating of the injector body to mitigate any heat losses the subcooled water may have incurred on its journey from the heat exchanger.

3. The subcooled water is injected into the cylinder in specific amounts dependant on the output desired of the engine.

4. a) Flashing of the subcooled water generates steam.
   b) The non-flashed water, now in a finely atomised state impacts the hot surfaces, forms a liquid film and undergoes multi-phase heat transfer, causing it to be converted to steam (convective boiling).

5. The expanding steam does work giving rise to the power stroke of the engine.

6. Once the piston has reached BDC, the momentum of the flywheel causes it to rise and the exhaust stroke of the engine takes place.

REFERENCES

1. Johann Fischer, Comparison of trilateral cycles and organic Rankine cycles, Energy, Volume 36, Issue 10, October 2011, Pages 6208-6219, ISSN 0360-5442, doi:10.1016/j.energy.2011.07.041.
2. Tony Ho, Samuel S. Mao, Ralph Greif, Comparison of the Organic Flash Cycle (OFC) to other advanced vapor cycles for intermediate and high temperature waste heat reclamation and solar thermal energy, Energy, Volume 42, Issue 1, June 2012, Pages 213-223, ISSN 0360-5442, doi:10.1016/j.energy.2012.03.067.
3. Ngoc Anh Lai, Johann Fischer, Efficiencies of power flash cycles, Energy, Volume 44, Issue 1, August 2012, Pages 1017-1027, ISSN 0360-5442, doi:10.1016/j.energy.2012.04.046.
4. Tony Ho, Samuel S. Mao, Ralph Greif, Increased power production through enhancements to the Organic Flash Cycle (OFC), Energy, Volume 45, Issue 1, September 2012, Pages 686-695, ISSN 0360-5442, doi:10.1016/j.energy.2012.07.023.
5. M. Yari, A.S. Mehr, V. Zare, S.M.S. Mahmoudi, M.A. Rosen, Exergoeconomic comparison of TLC (trilateral Rankine cycle), ORC (organic Rankine cycle) and Kalina cycle using a low grade heat source, Energy, Volume 83, 1 April 2015, Pages 712-722, ISSN 0360-5442, doi:10.1016/j.energy.2015.02.080.
6. Tianyou Wang, Yajun Zhang, Jie Zhang, Gequn Shu, Zhijun Peng, Analysis of recoverable exhaust energy from a light-duty gasoline engine, Applied Thermal Engineering, Volume 53, Issue 2, 2 May 2013, Pages 414-419, ISSN 1359-4311, doi:10.1016/j.applthermaleng.2012.03.025.
7. Byung Chul Choi, Young Min Kim, Thermodynamic analysis of a dual loop heat recovery system with trilateral cycle applied to exhaust gases of internal combustion engine for propulsion of the 6800 TEU container ship, Energy, Volume 58, 1 September 2013, Pages 404-416, ISSN 0360-5442, doi:10.1016/j.energy.2013.05.017.
8. H.A. Ajimotokan, I. Sher, Thermodynamic performance simulation and design optimisation of trilateral-cycle engines for waste heat recovery-to-power generation, Applied Energy, Volume 154, 15 September 2015, Pages 26-34, ISSN 0306-2619, doi:10.1016/j.apenergy.2015.04.095.

9. A. Labergue, M. Gradeck, F. Lemoine, Comparative study of the cooling of a hot temperature surface using sprays and liquid jets, International Journal of Heat and Mass Transfer, Volume 81, February 2015, Pages 889-900, ISSN 0017-9310, doi:10.1016/j.ijheatmasstransfer.2014.11.018.
10. Shou-Shing Hsieh, Sueng-Yang Luo, Ron-Yu Lee, Hao-Hsiang Liu, Spray cooling heat transfer on microstructured thin film enhanced surfaces, Experimental Thermal and Fluid Science, Volume 68, November 2015, Pages 123-134, ISSN 0894-1777, doi:10.1016/j.expthermflusci.2015.04.014.
11. Wei Zhang, Zhaoliang Wang, Heat transfer enhancement of spray cooling in straight-grooved surfaces in the non-boiling regime, Experimental Thermal and Fluid Science, Volume 69, December 2015, Pages 38-44, ISSN 0894-1777, doi:10.1016/j.expthermflusci.2015.08.001.
12. Hitoshi Fujimoto, Yosuke Oku, Tomohiro Ogihara, Hirohiko Takuda, Hydrodynamics and boiling phenomena of water droplets impinging on hot solid, International Journal of Multiphase Flow, Volume 36, Issue 8, August 2010, Pages 620-642, ISSN 0301-9322, doi:10.1016/j.ijmultiphaseflow.2010.04.004.
13. D. Chatzikyriakou, S.P. Walker, C.P. Hale, G.F. Hewitt, The measurement of heat transfer from hot surfaces to non-wetting droplets, International Journal of Heat and Mass Transfer, Volume 54, Issues 7–8, March 2011, Pages 1432-1440, ISSN 0017-9310, doi:10.1016/j.ijheatmasstransfer.2010.11.051.
14. Charles Sprouse III, Christopher Depcik, Review of organic Rankine cycles for internal combustion engine exhaust waste heat recovery, Applied Thermal Engineering, Volume 51, Issues 1–2, March 2013, Pages 711-722, ISSN 1359-4311, http://dx.doi.org/doi:10.1016/j.applthermaleng.2012.10.017.
.

DEFINITIONS, ACRONYMS, ABBREVIATIONS

ΔT_A	Temperature difference of streams at end A
ΔT_B	Temperature difference of streams at end B
h_{HE}	Heat transfer Coefficient for heat exchanger
h_{fvp}	Specific enthalpy of liquid at final vapour pressure
h_{isl}	Initial specific enthalpy of subcooled liquid
η_{engine}	Efficiency of Engine
η_{pump}	Efficiency of Pump
A_{HE}	Heat transfer area of heat exchanger
A_{cl}	Area covered by liquid
B_s	Convective boiling speed
H_{fs}	Enthalpy of flash steam
L_{fvp}	Latent heat of vaporization at final vapour pressure
P_{cyl}	In-cylinder pressure
P_{ei}	In-cylinder pressure at end of injection
P_{max}	Maximum pressure of working fluid
P_{min}	Minimum pressure of working fluid
Q_h	Heat from exhaust gasses to subcooled liquid
Q_{cb}	Heat from convective boiling
Q_{out}	Heat dissipated by condenser
T_l	Temperature of liquid striking surface
T_{max}	Maximum temperature of working fluid
T_{min}	Minimum temperature of working fluid
T_{pv}	Temperature of pressure vessel
T_s	Temperature of heated surface
W_{net}	Net-work output
h_{CB}	Heat transfer coefficient for convective boiling process
L	Latent heat of vaporization of liquid striking the heated surface
$LMTD$	Log Mean Temperature Difference
ORC	Organic Rankine Cycle
RC	Rankine Cycle
$SLFB$	Subcooled Liquid Flash Boiling Cycle
TLC	Trilateral Cycle
V	Pumped volume
x	Quality of vapour / Flash percentage / Vapour content

Chapter 3: The Development of a Subcooled Liquid Flash, Boiling (SLFB) engine for Waste Heat Recovery from Reciprocating Internal Combustion Engines

3.1 INTRODUCTION

While the reciprocating IC engine has undergone vast improvements in its efficiency, the most efficient road going engines today remain just under 45% and the average engine remains at approximately 35%. It is now generally accepted that the mass produced Otto and Diesel cycle engines will never exceed the 50% efficiency mark due to several limitations owing to practicality. In most automotive situations, it is common for 30% of combustion heat to be lost in exhaust gasses and a further 35% through heat transfer to the cylinder walls and through coolant. This energy split is shown in Figure 1. The harnessing of this waste heat is the key to improving the overall efficiency of an internal combustion engine. Automotive Waste Heat Recovery (AWHR) research has gained momentum in recent years. Unlike conventional waste heat recovery systems, one of the major hurdles faced by AWHR systems is size. The ideal AWHR system needs to be compact and efficient, and the ease of being integrated to the powertrain would be highly advantageous as well.

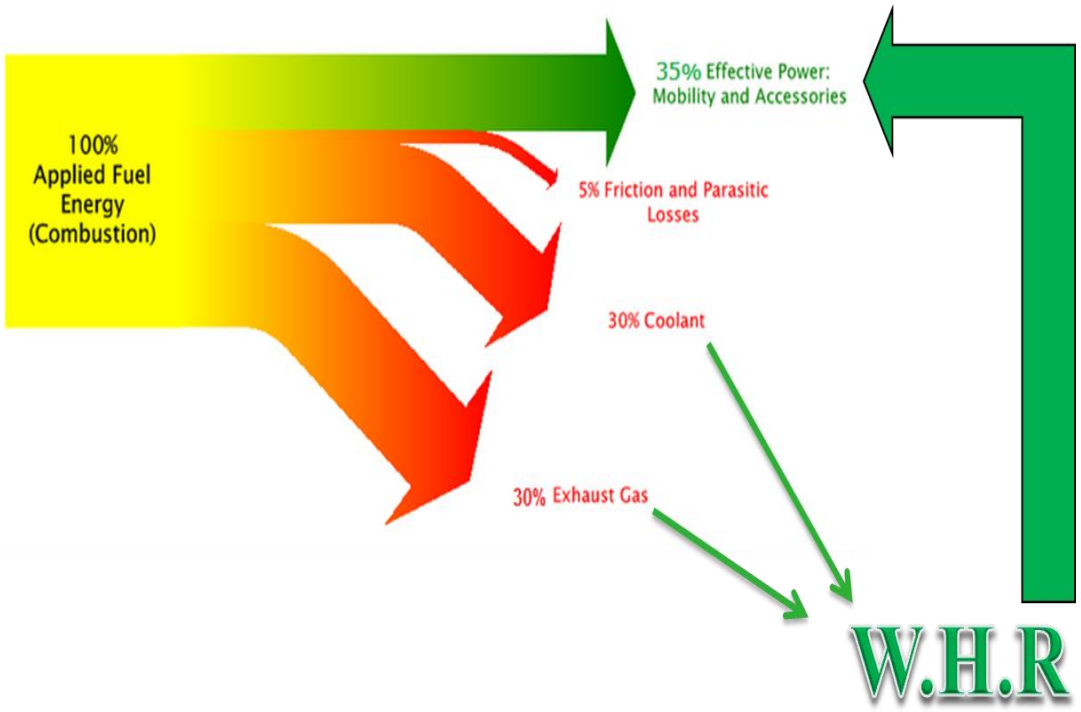

Figure 1.Typical energy split in a gasoline ICE

3.2 CURRENT SYSTEMS

While many forms of waste heat recovery exist, the most keenly researched include the Rankine cycle, Organic Rankine Cycle (and combinations of these), Thermo-electric, Turbocharging and Sterling cycles [1]. A relatively new cycle known as the Trilateral Cycle (TLC) [2],[3] is also showing promise. The commonality shared by a lot of these systems is the requirement of an intermediate storage system for the energy they produce and in most cases this is an electrical battery. As necessity dictates, an electrical power generating system is part of the package as well. The usage of batteries, while an obvious choice, brings with it the drawbacks of current electrical battery technology which include low power storage to weight ratio, relatively short life spans and high cost. While some waste heat recovery systems allow direct power delivery to the power train, it can be hypothesized that they would suffer from poor transient response due to the nature of their expansion units and not allow for "on-demand" power delivery.

3.3 THE PROPOSED SYSTEM

A WHR system that allows on-demand direct power delivery to the power train with good transient response has been envisioned by the author. The key feature of the system is its use of a working medium that is kept in its liquid phase for storing energy and then converted to its vapour phase, releasing its stored energy in the power generation unit. The cycle on which this system works has similarities to the TLC with its key benefit [2],[3],[4],[5]. Furthermore, the working medium in its liquid phase is comparable to a liquid fuel which has such inherent benefits as it relatively small volume and ease of handling [11]. Superior transient response and good efficiency is also achievable by the use of a compact positive displacement reciprocating power unit. Figure 2 illustrates the operation of the reciprocating engine powered by the SLFB Cycle.

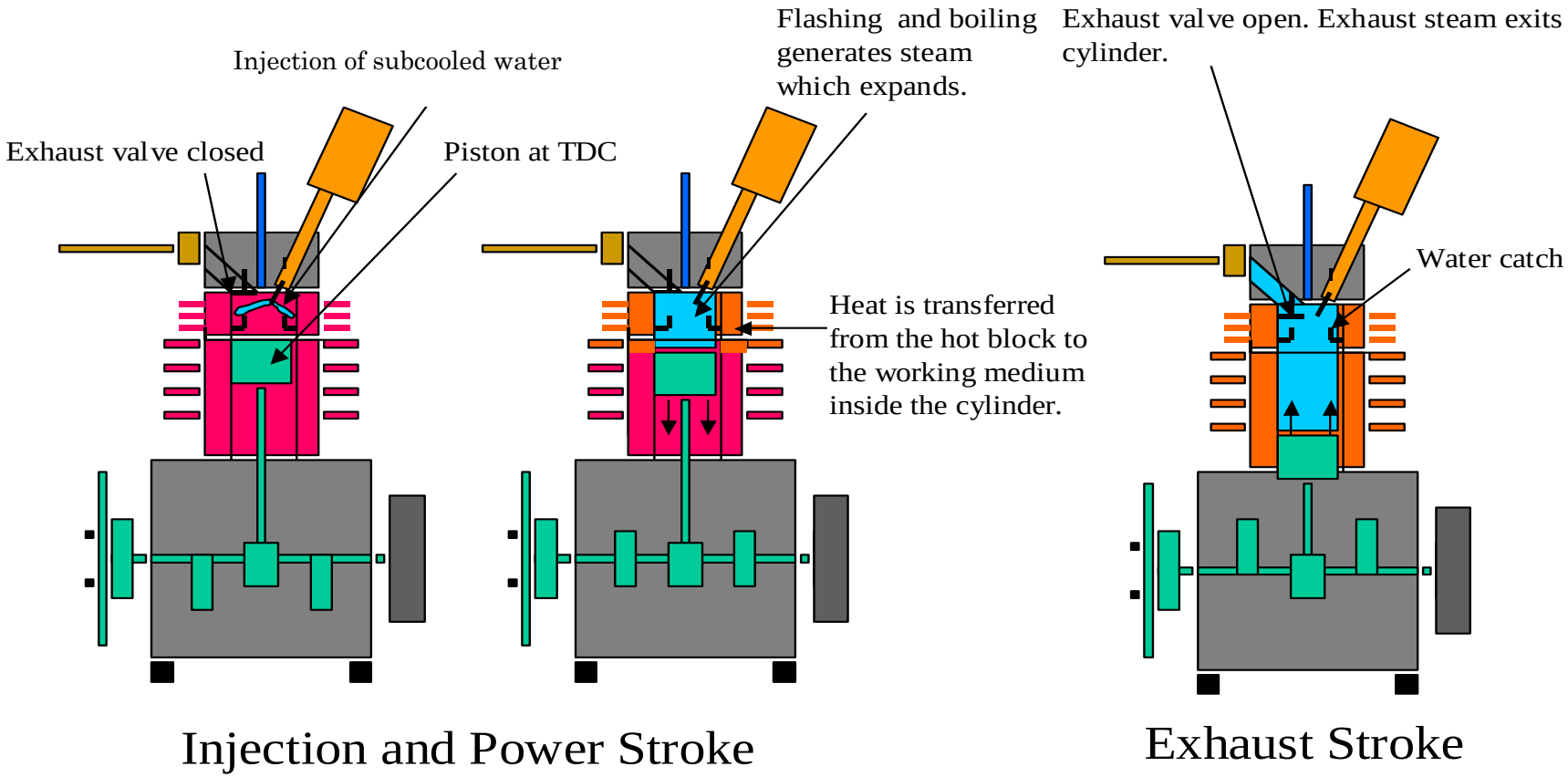

Figure 2. The Operation of a two-cycle Flash steam engine

3.3.1 The Heat Cycle Powering the Engine

The proposed system works on a heat cycle termed the Subcooled Liquid Flash, Boiling Cycle (SLFB). This cycle generates work by the harnessing of vapour expansion. The vapour is generated in two processes, namely the Flashing process and the Multiphase Convective Boiling process.

The ideal SLFB cycle can be summarized by Figure 3.

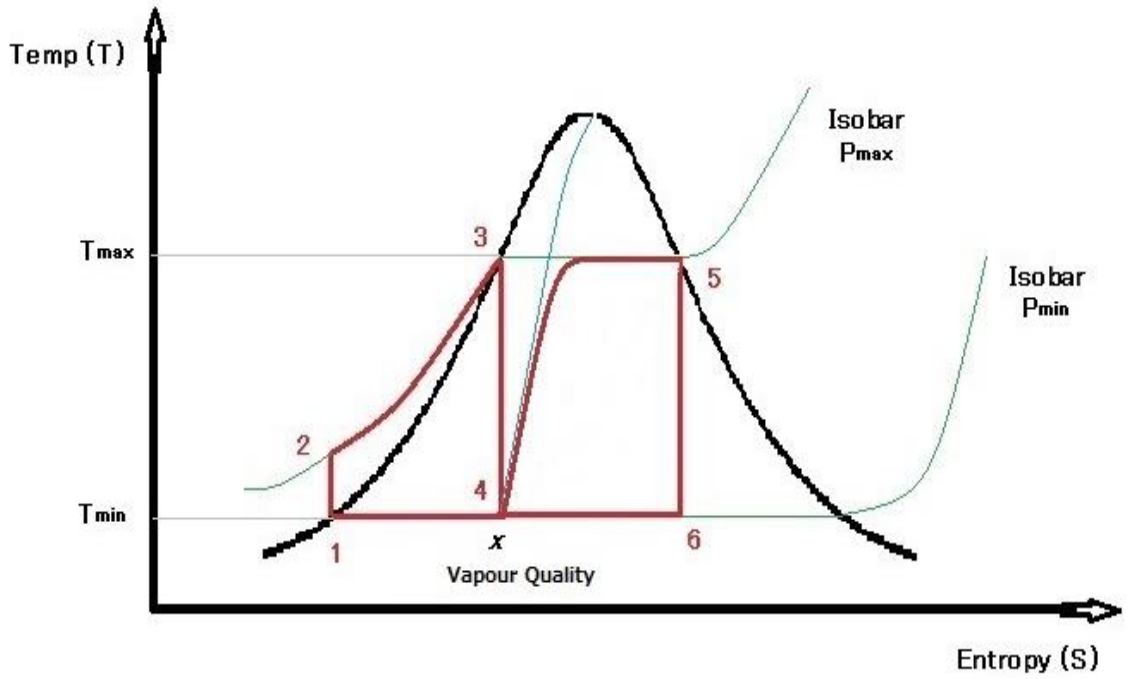

Figure 3. The TS Diagram of the ideal SLFB Cycle

The SLFB cycle is identical to the TLC [2],[3],[4],[5] in steps 1-4. 1-2 is the isentropic compression of the liquid phase to a maximum pressure P_{max} by an isentropic pump. The pump compresses the liquid to a pressure high enough to maintain it in a subcooled state at T_{max}. 2-3 is the isobaric heating of the liquid phase up to the temperature T_{max}. At state 3 the liquid is in a superheated state. 3-4 is the isentropic expansion of the vapour generated from "flashing". In this process, wet saturated steam is generated as the temperature of the working fluid drops to the temperature T_{min} and pressure P_{min} with vapour content x. Stage 4-5 is unique to the SLFB cycle and is the multiphase convective boiling of the wet portion of steam generated in process stage 3-4, from the heated walls

of a specially designed component within the expansion unit. The multiphase convective boiling supplements the work output of the cycle, and simultaneously helps reduce the wetness of the vapour generated in the process stage 3-4. This is important as it reduces the liquid phase which is undesirable for the mechanicals of the reciprocating expansion unit.

3.3.2 Unique Aspects of The SLFB System

The unique aspects of the SLFB system are as follows:

1. The working fluid (subcooled water) is delivered directly into the expansion unit using a fast response electro-mechanical injector which allows fine control of the timing and mass of working fluid injected.

2. Work is generated in the power unit from two processes; (a) The Flashing of the subcooled working medium and (b) The Multiphase Convective Boiling of the unflashed liquid portion by heat transfer from heated surfaces within the power unit.

3.4 OVERALL AIM

To investigate the nature of Flashing and Convective Boiling and its ability to generate power in a reciprocating positive displacement expansion unit.

3.5 THE EXPERIMENT OUTLINE

The experimental was carried out in 3 main stages.

Stage 1: *The construction of an injector:* The construction/modification of an electrically controlled injector capable of operating under the conditions of this experiment was the first and one of the most important goals of this experiment. This enabled the second and third stages to be carried out.

Stage 2: *The high temperature subcooled water injection experiments:* This stage was carried out to determine the potential of the Flash and Convective Boiling processes to generate work.

Stage 3: *The powering of an engine with the SLFB cycle:* This stage investigated the SLFB cycle's ability to produce power in a piston engine.

3.5.1 Stage 1: The Construction of an Injector

The injector employed in the flash engine, needs to be able to hold high temperature liquids at very high pressures. As the design and construction of an injector was beyond the scope of this research, a commercially available diesel common rail injector was used. The reasons for this was that common rail injectors operate at pressures of up to 160MPa and their all-metal construction allowed high temperature applications as well. However the original design of the injector needed some modifications for the flash experiment application. Figure 4 shows the stock common rail diesel injector used. Figures 5a and 5b illustrate the modifications made to the standard injector. The internals of the injection control system and the cooling adapter are shown disassembled in Figure 5a. Figure 5b illustrates the modifications made to allow injections at pressures lower than what the stock injector originally could.

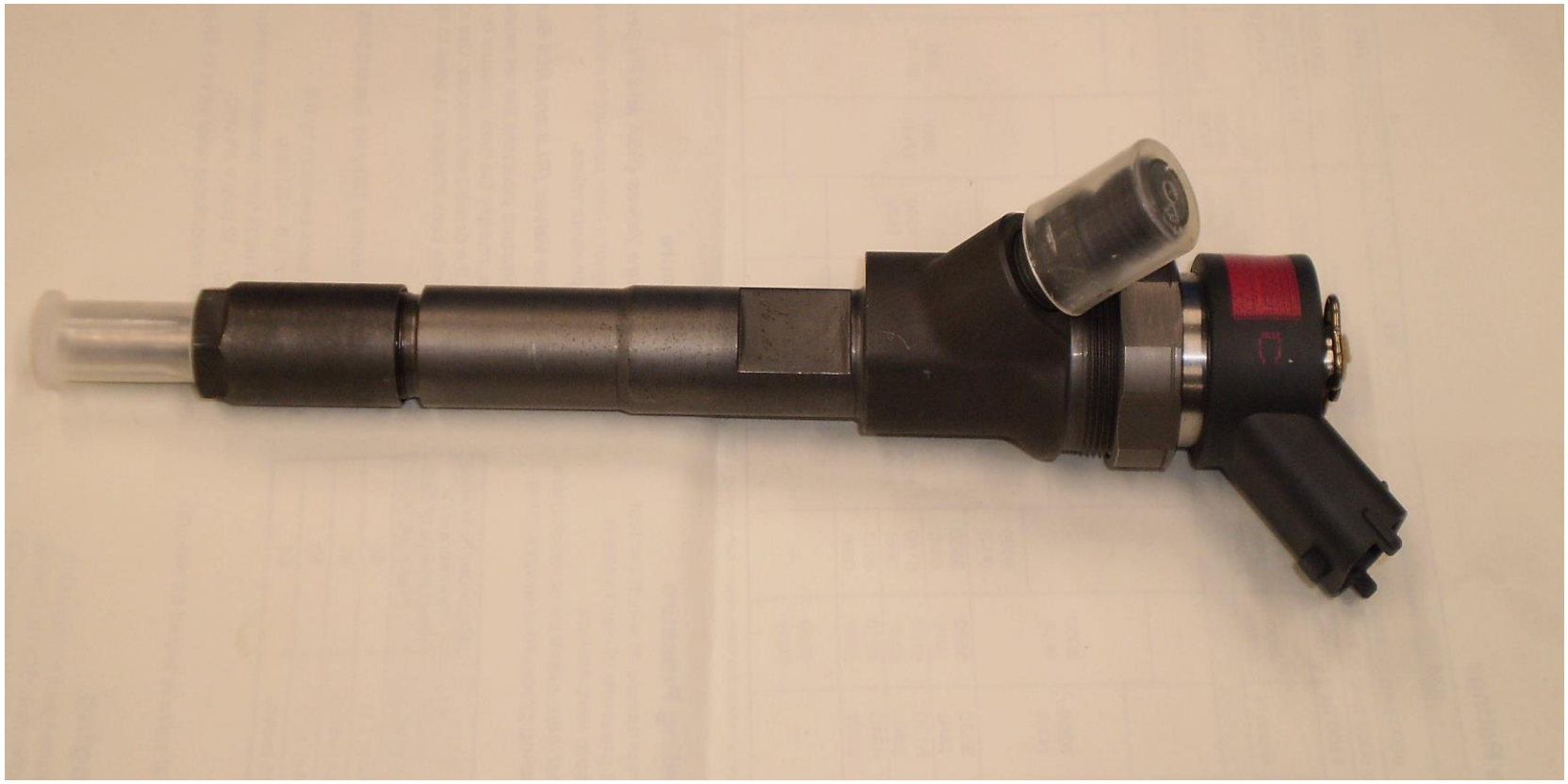

Figure 4.The Standard Injector

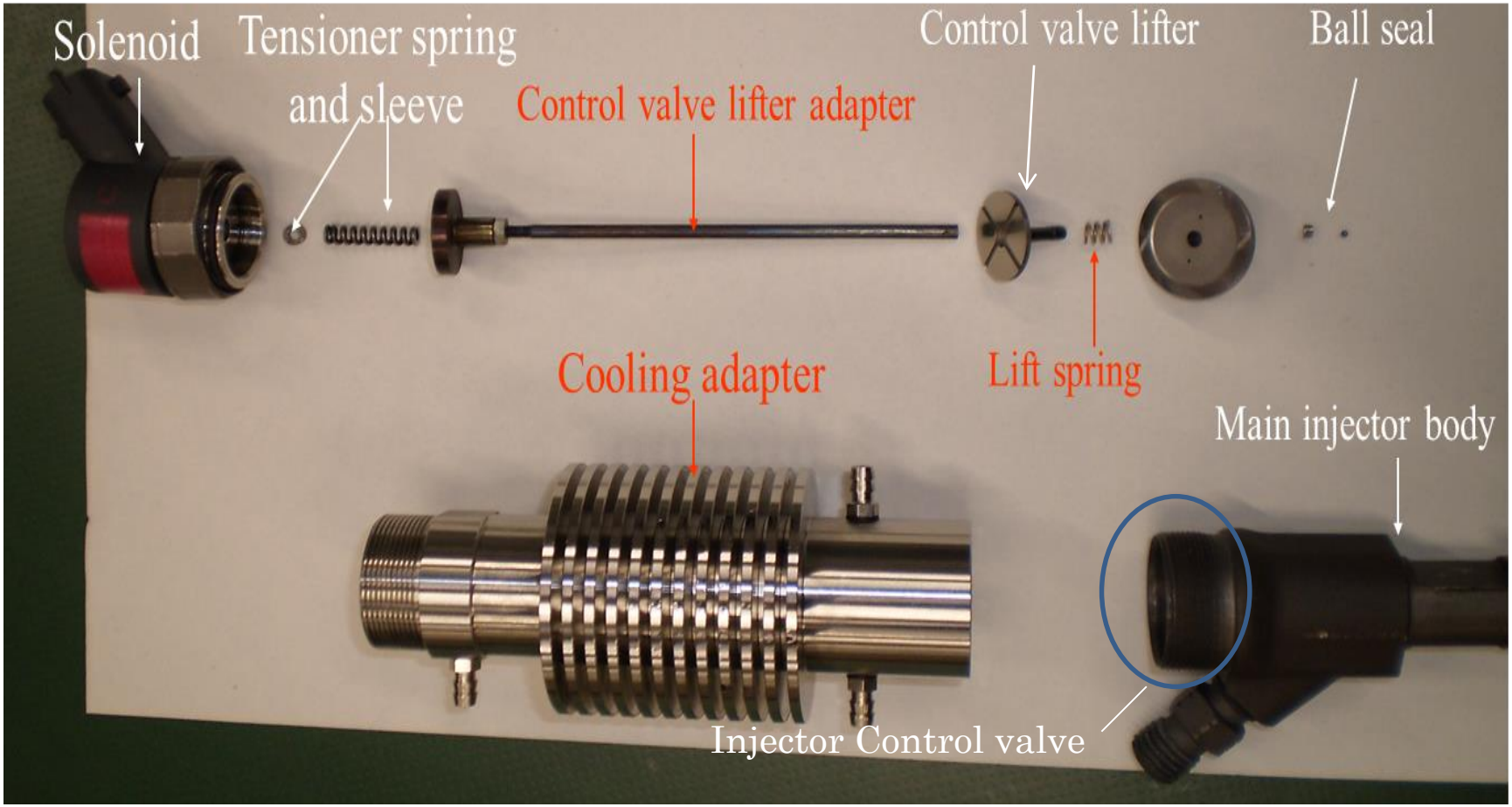

Figure 5a. Cooling adapter internal structure

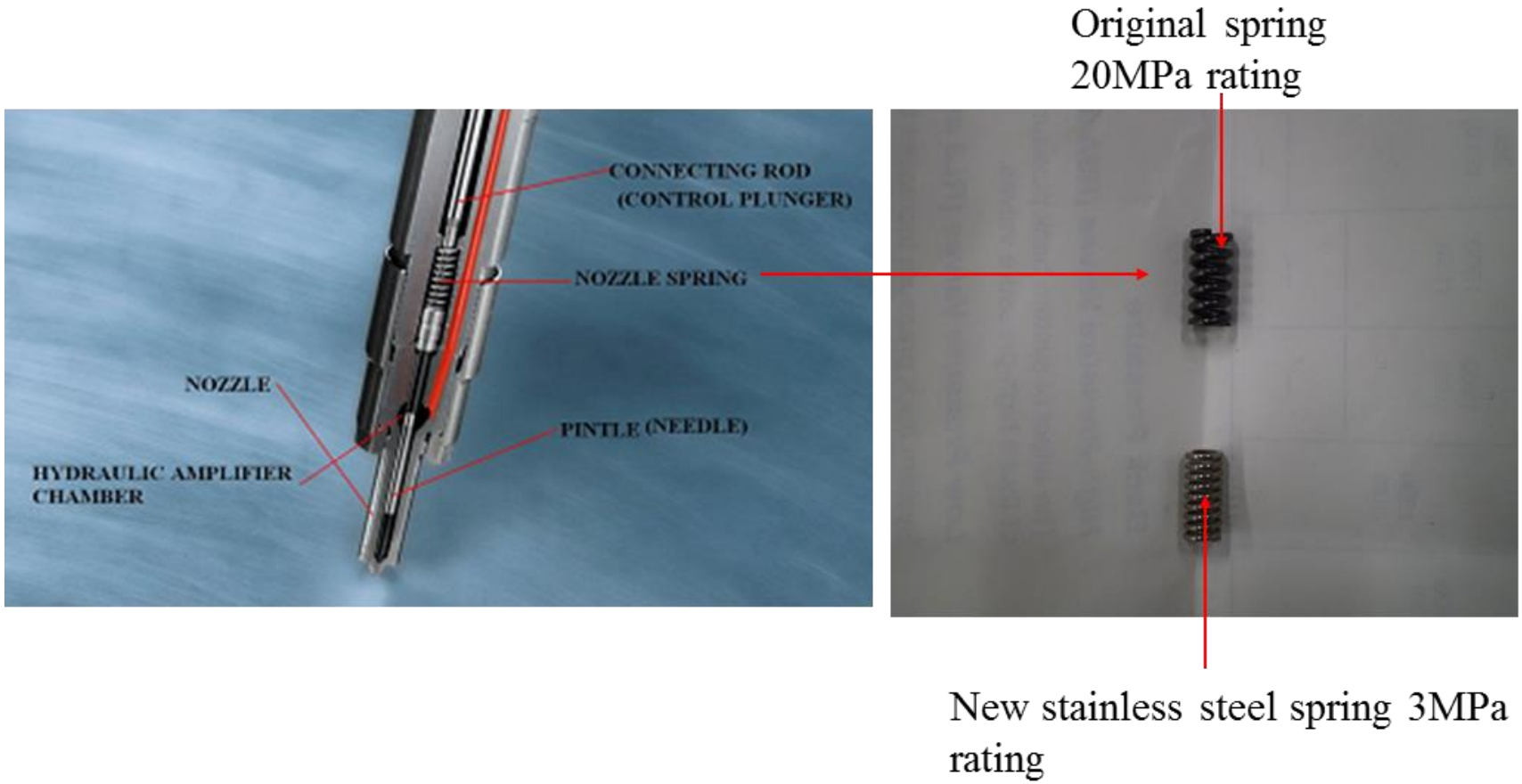

Figure 5b. The Nozzle spring modification

The injector employed (with modifications) for this experiment was a Bosch solenoid actuated common rail diesel injector that is originally used in the Toyota 1ND-TV engine. This injector contains a high speed solenoid which is sensitive to heat and requires cooling when in operation. In standard applications, this solenoid is cooled by fuel that flows through it. However, when used to inject high temperature subcooled water, this solenoid requires a separate cooling system. The Original injector was fitted with a cooling adapter to protect this heat sensitive solenoid. The adapter included a passive radiative cooling system to protect from the heat of the superheated liquid and a separate coolant circulation system to cool the solenoid while in operation.

The components starting from the solenoid down to the control valve lifter, control the “Injector Control Valve”. This control valve allows minute amounts of high-pressure liquid to leak out of the top of the injector (back leakage) which in turn allows control of the “nozzle needle lift” and injection events through a pressure difference in the hydraulic circuit within the injector body.
The “Nozzle spring” in the original injector allowed the injector to only operate at pressures above 20Mpa. As the experiment was carried out at liquid pressures of 5Mpa, this spring was replaced with one of a lower spring force that allowed operation at pressures of 3Mpa. Figure 5b shows this modification. Other modifications included the enlargement of the nozzle tip orifices’ diameter from the standard 125μm to 400μm to increase the mass flow rate. Table 1 lists these modifications, and the modified injector is pictured in Figure 6.

Table 1. The injector modifications.

	Original Injector	Modified Injector
Min operating pressure	20MPa	5MPa
Nozzle orifice diameter	125μm	400μm

3.5.2 Stage 2: The High Temperature Subcooled Water Injection Experiments

Figure 7 illustrates the experimental setup for used for investigating the SLFB process

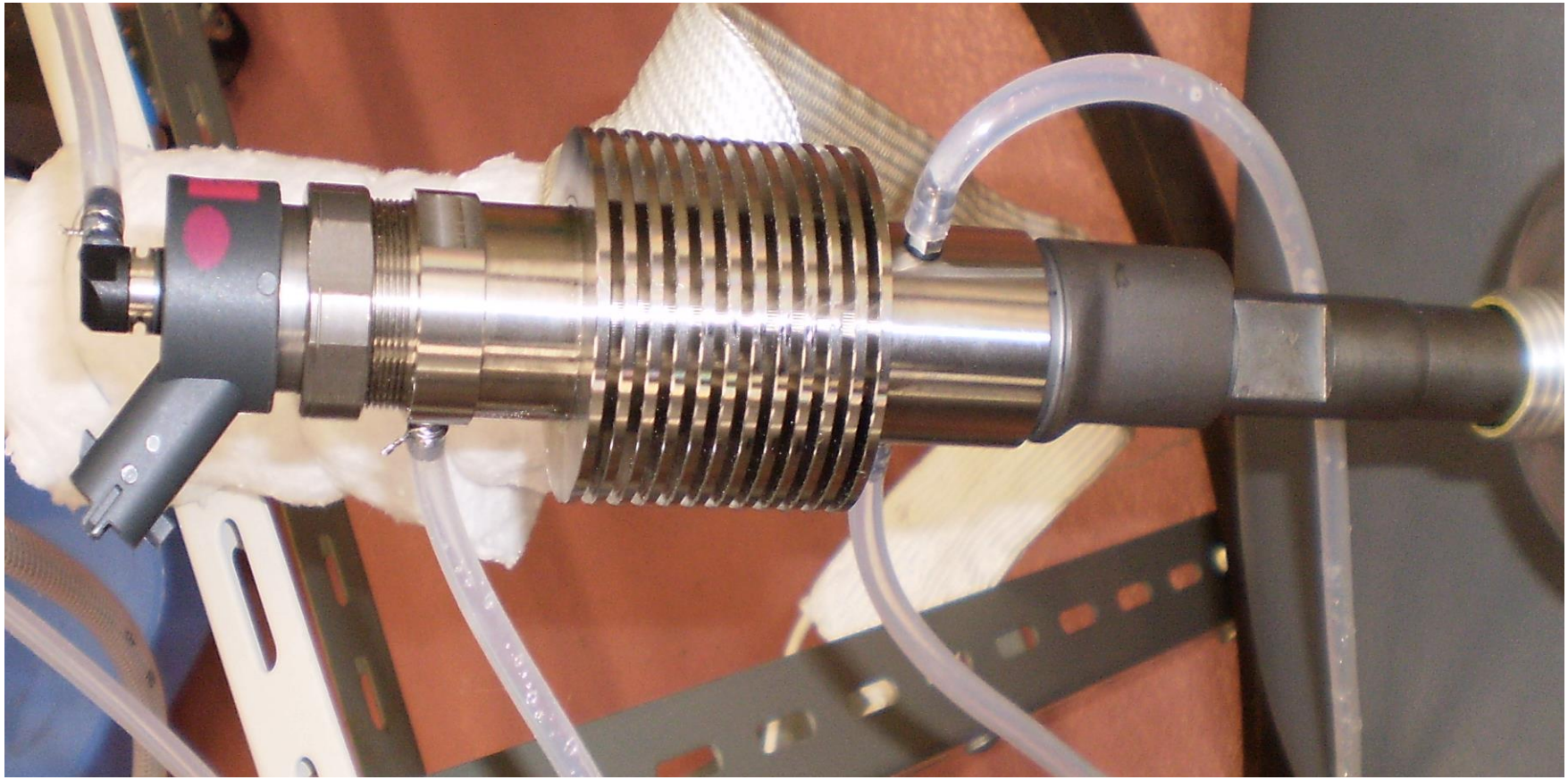

Figure 6. The Modified Bosch Common Rail Diesel Injector used for injecting subcooled water.

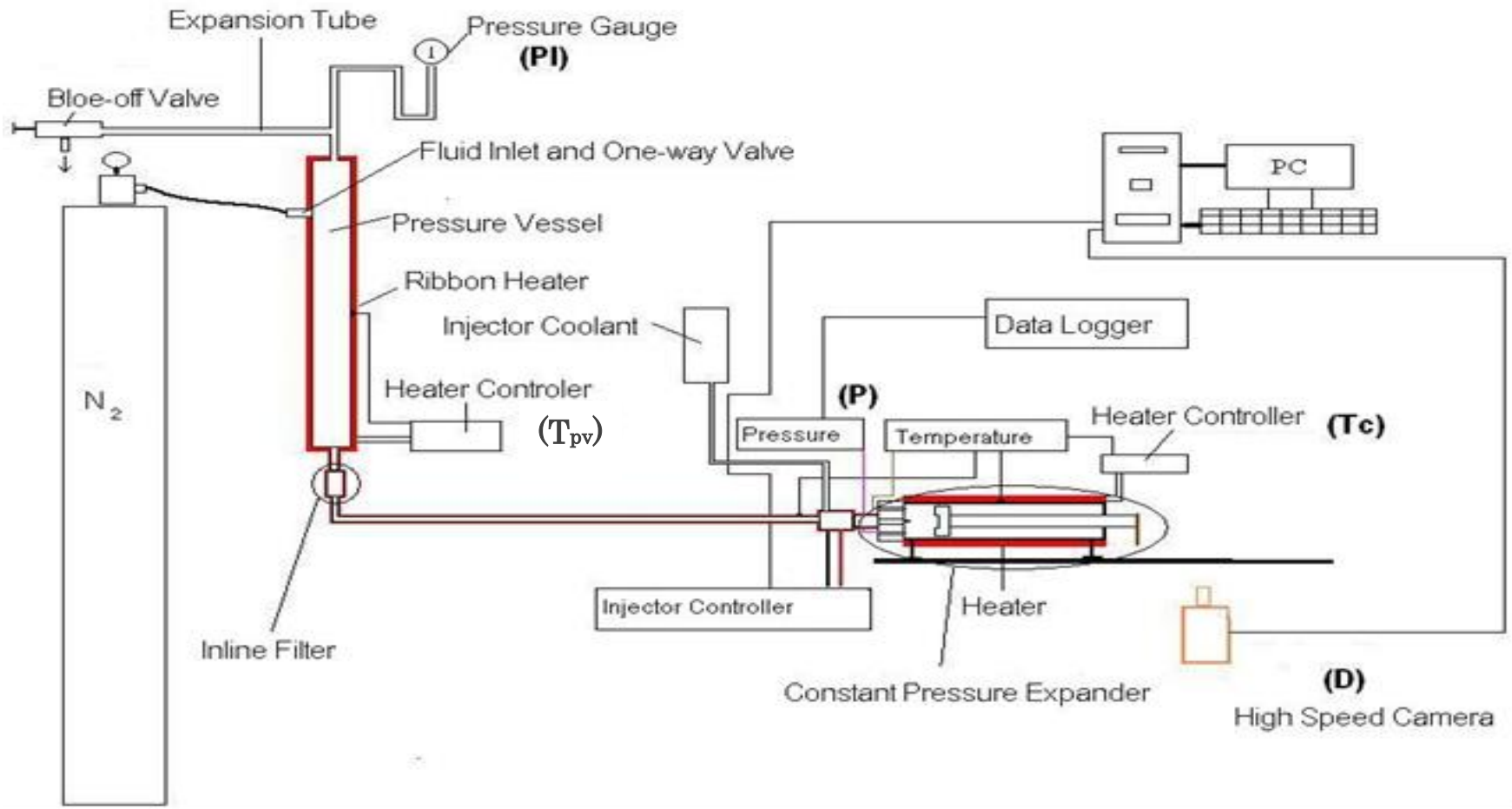

Figure 7. The Experimental Set-up for investigating the SLFB process.

3.5.2.1 The apparatus

While stable injector operation was achieved, the injector remains prone to rusting due to the high temperature of the water that is used and the dissolved oxygen in this water. Ideally, the injector used in the flash steam engine would be constructed out of materials that provide better rust prevention. For the purpose of maintaining the current injector in a rust-free condition after water injection experiments, the injector was removed from the set-up, and connected to a supply of automotive brake fluid. The injector was then operated with brake fluid to flush out any water within it. The highly hygroscopic nature of the brake fluid helps prevent rusting of the injector internal parts during its non-use. Furthermore, the water solubility of brake fluid allows the injector to be easily flushed with water prior to its use in further subcooled water injection experiments.

With reference to Figure 7, subcooled water was generated and maintained in a pressure vessel heated by an electric ribbon heater and heater controller. The subcooled water was then injected into a constant pressure expander (CPE). This expander was a SMC brand air actuator, which contained a cylinder and a free moving piston. The CPE itself was heated and maintained at predetermined temperatures by a ribbon heater and control system. It was insulated to prevent any heat loss. A head for the CPE was designed and built to accommodate the injector, a pressor sensor, a thermocouple and purge valves. This head was maintained at the same temperature as the CPE. Thermocouples were placed at various points on the surface of the CPE and head to monitor the temperature. The injector was controlled by a pulse generator and pressure data was recorded on a digital data logger.

3.5.2.2 Injector mass flow rate

Prior to the injection experiments, the mass flow rate of the injector was measured. These measurements were carried out for both non-flashing and flashing flows. Figure 8 shows the experimental setup used to investigate the flowrate of the injector. Injections were carried out into an airtight aluminium canister that was maintained at approximately 16ºC by a bath of cold water. The interior of the canister was filled with stainless steel wool to provide a large cold surface area for the flashed vapour to condense on. A rubber bellows was fitted to the canister to absorb any sudden pressure rises that may result from the expanding vapour. The injected mass was determined by measuring the mass of the canister (with bellows attached) prior to injection and then post injection.

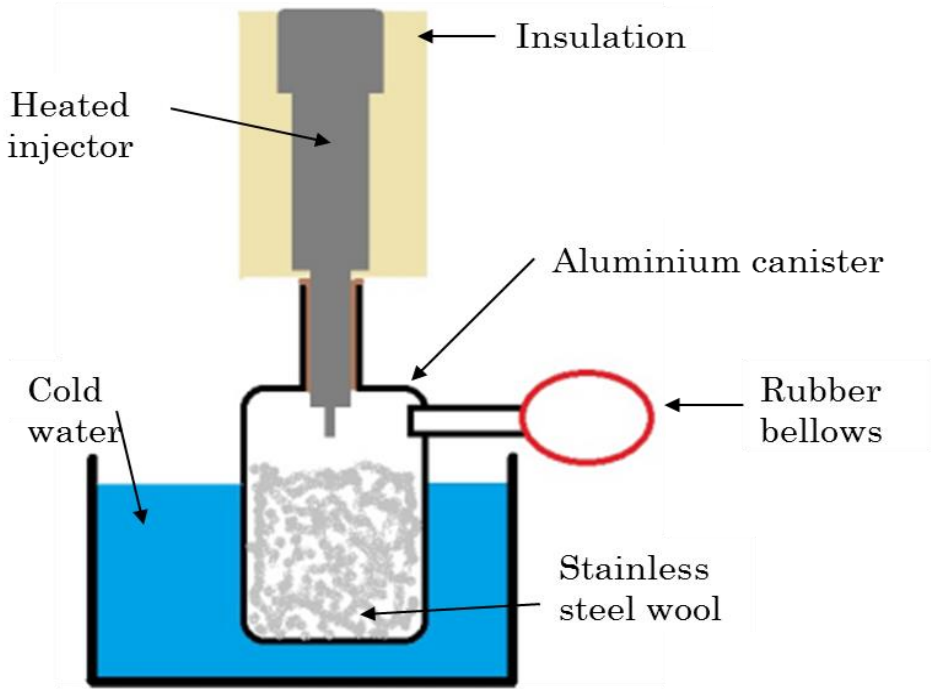

Figure 8. Experimental setup for measuring injector flow rate.

Water held at temperatures of 24ºC (room temperature), 130°C and 240°C (maximum temperature possible with the subcooled water generator) was

injected in 3 different modes namely 5ms x 50 injections, 10ms x 50 injections and 15ms x 50 injections to observe the general trend of mass flow rate variation with the degree of subcooling. Figure 9 shows the results of the variation of mass flow with water temperature.

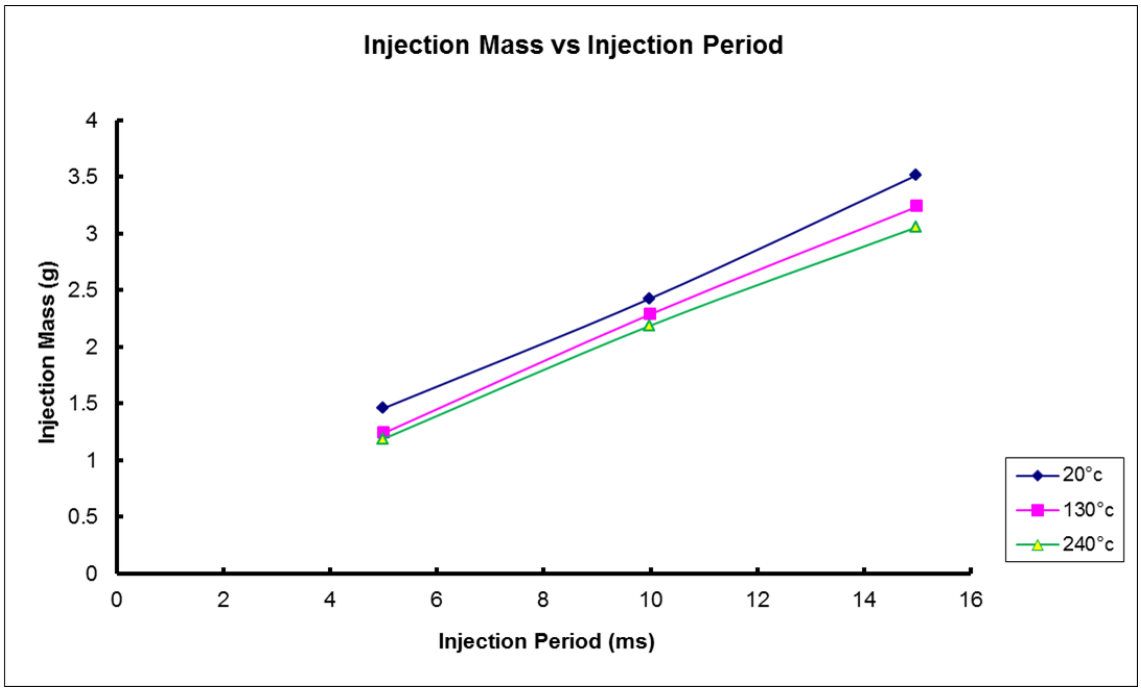

It is observed that the flow rate of the injector decreases for flashing injections. It is known that as the temperature of the subcooled water increases, its flash percentage also increases. It was observed that the injected mass was inversely related to the percentage of flash steam generated.

As future experiments were to be carried out with flashing flows, the goal was to establish a mathematical function that would describe the mass of subcooled water injected for a given injection duration. As the individual injection masses are very small and could not be accurately measured, the mass flow-rate for injections was measured by taking the average of 5 sets of 50 injections, for particular injection durations. The injection durations ranged from 2ms up to 20ms. In order to generate the mass-flow rate function $G(t)_{flow}$, a graph of injected mass vs injection period was plotted and polynomial regression done on this graph to generate the function $G(t)_{flow}$ with a best possible R^2 value. ($R^2 = 0.9969$)

Figure 10 shows the results of the injection experiments for flashing flows for water at 150ºC.

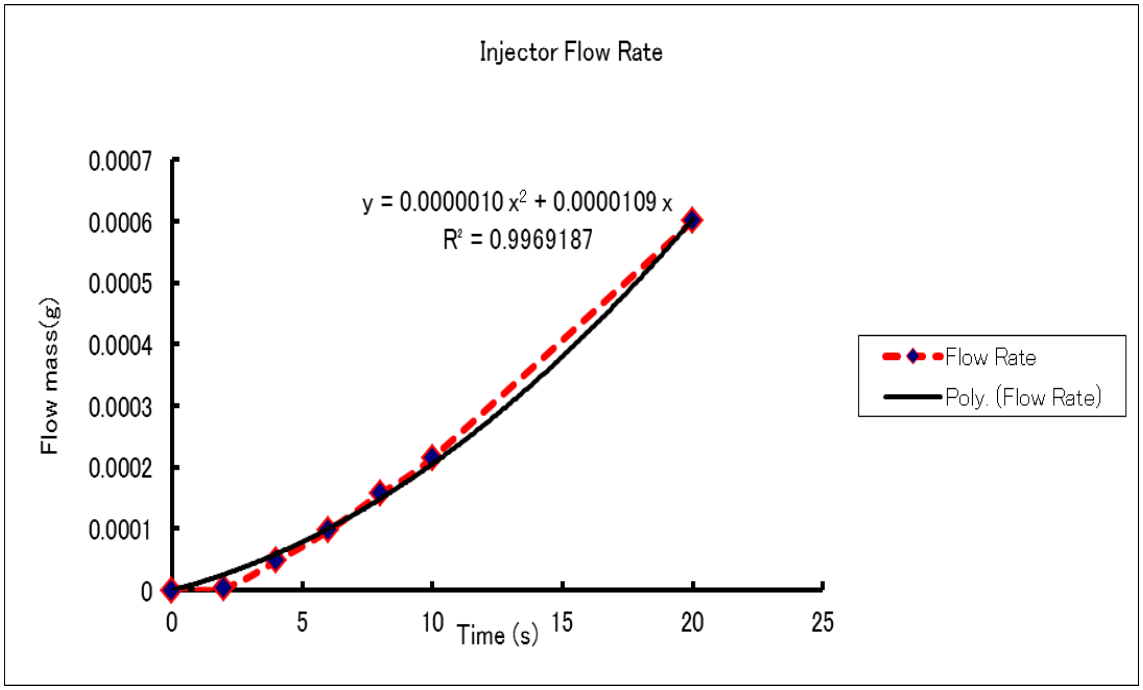

Figure 10. The mass-flow rate for Flashing injections of water at 150ºC.

The mass-flow rate for water at 150ºC can thus be described by:

$$G(t)_{flow(150)} = 0.000001t^2 + 0.0000109t \ \ (g)$$

It was beyond the capabilities of the available equipment to simulate pressure variance in the injection environment when measuring mass-flow rate. The mass-flow rates described by $G(t)_{flow}$ are of injections done in atmospheric pressure. According to the principles of critical flow of subcooled liquids through small diameter pipes, the critical mass-flow rate depends solely on the pressure of the liquid in the reservoir once a choke plane is generated in the flow path. If the reservoir pressure is low, the flashing occurs within the pipe prior to the exit and if the pressure is high enough the flashing occurs at the exit of the pipe. The mass-flow rate cannot be increased any further by decreasing the pressure at the pipe exit (downstream). Thus only the upstream pressure affects the mass-flow rate. In the case of the SLFB engine injections, the very fact that flashing occurs (at either the exit of the nozzle or within the nozzle) leads to

chocked flow and renders the flashing mass-flow rate immune to the pressure fluctuations downstream of the flash generated choked plane. Therefore the in-cylinder pressure fluctuations have no influence on the flashing mass-flow rate as long as flashing occurs throughout the duration of the injection. Back-pressure would only influence the mass-flow rate in the case of non-chocked flows, i.e. if the in-cylinder pressure is higher than the saturation pressure of the liquid exiting the injector nozzle, as in this situation flashing would cease and non-choked flows would result.

3.5.2.3 The constant pressure expander (CPE)

A commercially available air actuator was modified for use in the experiment. The modifications made were mainly to the head of the actuator to allow the attachment of the injector and various other sensors and components. The CPE used for these experiments are shown in Figure 11 and the modifications to the head are shown in Figure 12

Figure 11. The modified SMC Air Actuator

Figure 12. The modifications to the head.

3.5.2.4 The injection experiment procedure

Pure distilled water was heated in a pressure vessel up to a temperature of 240ºC and maintained in a subcooled state at a vapour pressure of 5MPa by compressed Nitrogen. A pressure of 5MPa was used in order to achieve adequate injection mass flow rate and to ensure that the level of subcooling was high enough that flashing only occurred at, or very close to the exit of the injector nozzle tip orifices and not within the injector or delivery pipes. Each injection experiment consisted of 50 consecutive injection events. The injected mass was varied by varying the injection duration. The first set of experiments used a 15ms *ON* duration with a 1ms *OFF* duration between each injection. Experiments were carried out using a Constant Pressure Expander (CPE) with wall temperatures (T_c) of 80ºC, 120ºC, 130ºC, and 140ºC. The start of the injections simultaneously triggered the gathering of pressure data by the high speed data logger and high speed video camera. The data gathered from the pressure sensor output and the video from the high-speed camera were used to plot a Pressure vs Volume graph for each injection experiment. This graph was then used to calculate the indicated work (W_i) done by the expanding steam for the duration of the injections. It became apparent that the subcooled water was losing heat to the CPE head prior to injection and accurate knowledge of the injected water temperature could not be established. Consequently, the temperature of the CPE head on to which the injector was connected needed to be at the same temperature T_{pv} as the subcooled liquid. This mitigated any heat loss from the subcooled liquid prior to injection. The temperature at which the CPE could safely be maintained for extended periods of time was 130°C and so the temperature of the subcooled water was also maintained at 130°C and injection experiments repeated for 50 X 10ms *ON* and 1ms *OFF* followed by 50 X 5ms *ON* and 1ms *OFF*. Injection experiments were also carried out with non-flashing injection of 50 X 5ms ON and 1ms OFF for water temperatures (T_{pv}) of 70ºC and 90ºC with a T_c temperature of 130ºC. Figure 13 illustrates the experimental procedure of the CPE injection experiments. It is worthy of note that the temperature of the injected liquid is the same as the temperature of the injector T_{inj} and the subcooled water generating pressure vessel T_{pv} if no heat loss occurs on its journey between the pressure vessel and the injector.

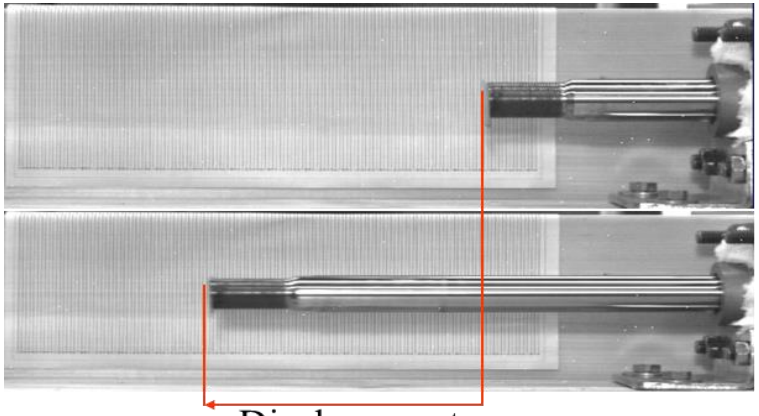

Displacement

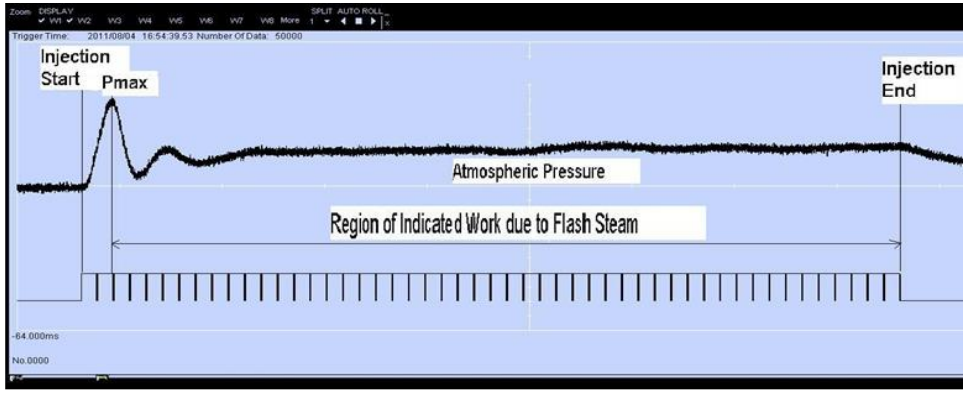

Pressure sensor data with respect to injection timing

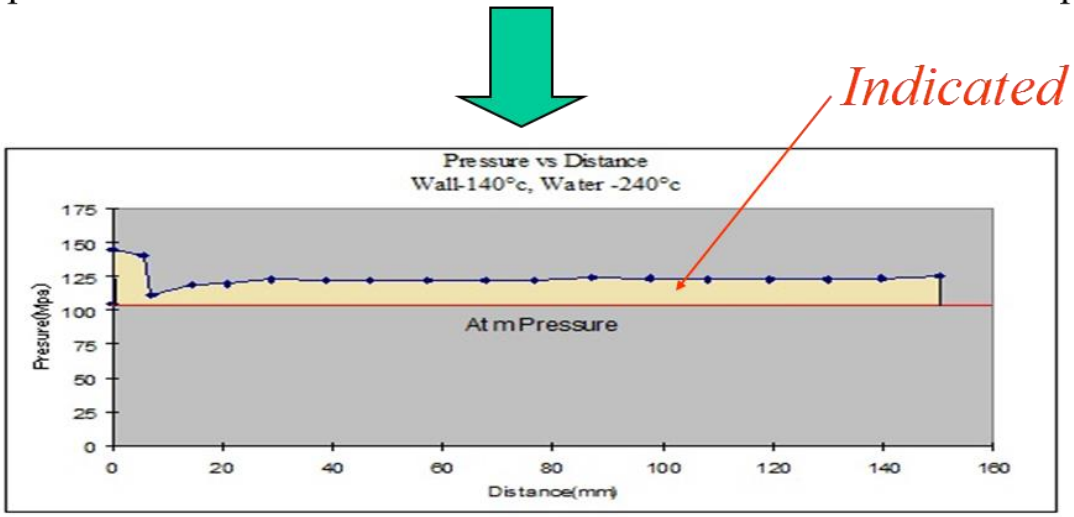

Figure 13. The Experimental procedure of Stage 2.

3.5.2.5 Results

The Indicated work was calculated according to equation (1). v_i is the volume of the CPE at injection initiation and v_f at the end of injection. P is the constant pressure at which expansion takes place within the CPE.

$$W_i = \int_{v_i}^{v_f} P \; dv \tag{1}$$

The enthalpy of Flash steam was calculated according to equation (2). This enthalpy is a function of the pressure within the cylinder as is the specific enthalpy of the liquid at the final vapour pressure, and is thus denoted as $H_{fs}(P_{cyl})$ and $h_{fvp}(P_{cyl})$ respectively.

$$H_{fs}(P_{cyl}) = \left(h_{isl} - \; h_{fvp}(P_{cyl})\right) \cdot \; m_i \tag{2}$$

In the CPE experiments, the expansion occured at a constant pressure, thus $P_{cyl} = constant$ and this constant pressure was used to determine the h_{fvp}.
The efficiency with which the enthalpy of Flash steam was converted to work was calculated according to equation (3). E_v is termed the efficiency value.

$$E_v = \left[\frac{W_i}{H_{fs}}\right] \cdot \; 100 \tag{3}$$

An E_v value of 100 relates to the work output being equal to the enthalpy of flash steam generated by the injected mass of subcooled liquid. Values larger than 100 indicated an input of energy in addition to that of the flash steam energy. Figure 14 shows the efficiency values at various CPE wall temperatures.

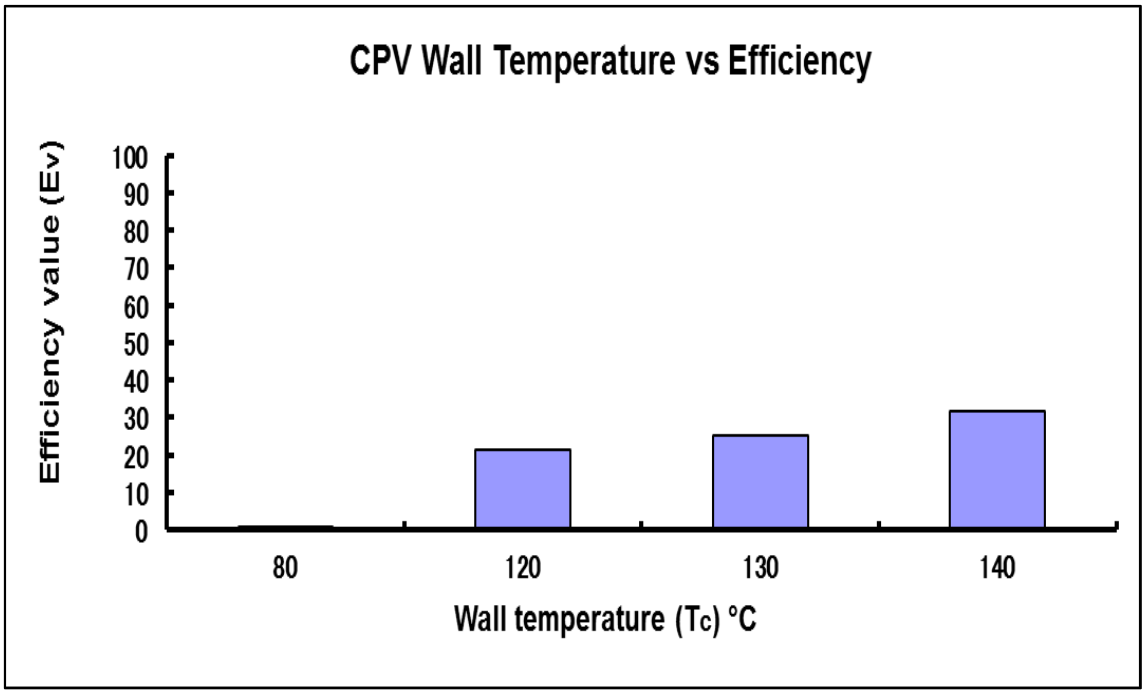

Figure 14. The efficiency of conversion of flash steam enthalpy to expansion work within the CPE for injections of subcooled water at a temperature of 240°C (T_{pv})

It can be seen that a wall temperature of 80ºC all but removes the work output of flashing. This is due to condensation of the flash steam. Furthermore it is clear that as the wall temperature increases, the efficiency also increases. The relatively low efficiencies can be attributed to heat lost from the subcooled water prior to it being injected. Figure 15 shows the efficiency values when the injections were carried out at near adiabatic conditions. Here, the subcooled water was at a temperature of 130°C (T_{pv}) as was the CPE temperature (T_c) and the injector temperature(T_{inj}).

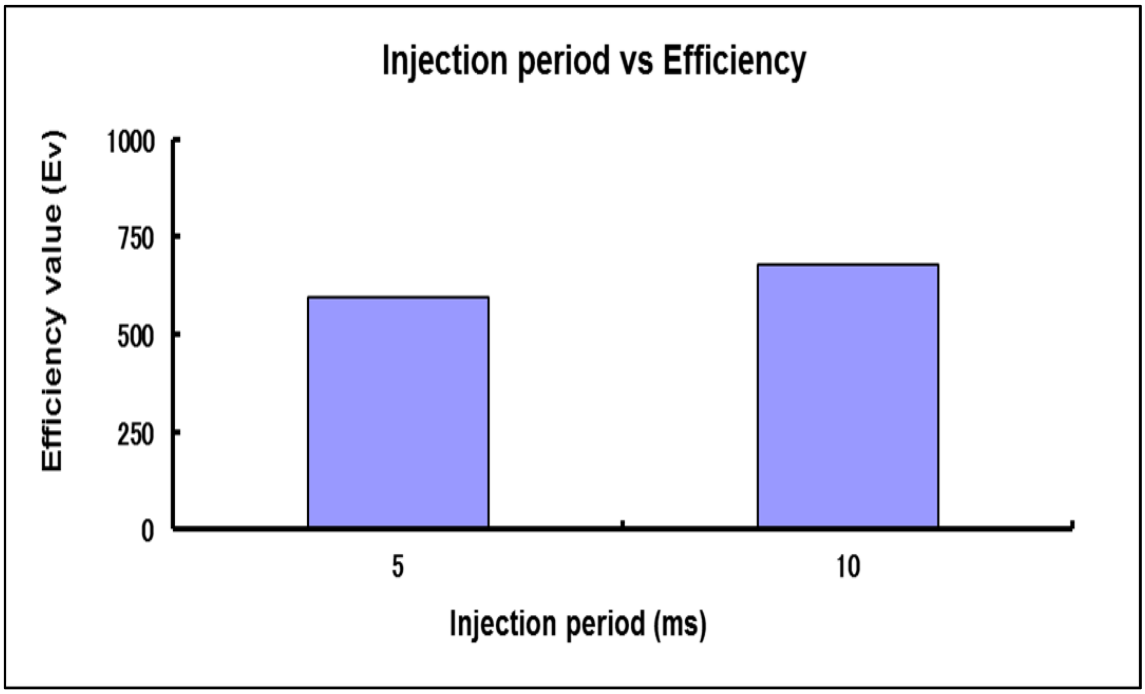

Figure 15. The results of the experiment carried out under near adiabatic conditions where no heat is gained or lost by the injected fluid prior to it being injected

By the definition of efficiency value in equation (3), it can be determined that an additional source of energy input was present as the indicated work output was larger than that possible from flash steam alone. This additional work is the multiphase convective boiling of unflashed water off the CPE walls (Q_{cb}). This convective boiling input may be described by equations (4) and (5).

$$Q_{cb} = h_{CB}(T_s - T_l) \cdot A_{cl} \tag{4}$$

$$Q_{cb} = B_s \cdot L \tag{5}$$

T_s and T_l are the temperatures of the surface and liquid striking the surface respectively. A_{cl} , L_l and C refer to the area covered by the liquid striking the surface, the latent heat of vaporisation of the liquid striking the surface and the coefficient of heat transfer respectively.

The speed of boiling can be described by equation (6).

$$B_s = \frac{h_{CB}(T_s - T_l) \cdot A_{cl}}{L} \tag{6}$$

The boiling speed B_s is the determining factor in the ablity of convective boiling to contribute to power output as engine speeds increase.
Figure 16 shows the indicated work for non-flashing injections in comparison to a flashing injection. The CPE wall temperature is at 130ºC and the injected water temperatures are at 70ºC, 90ºC and 130ºC.

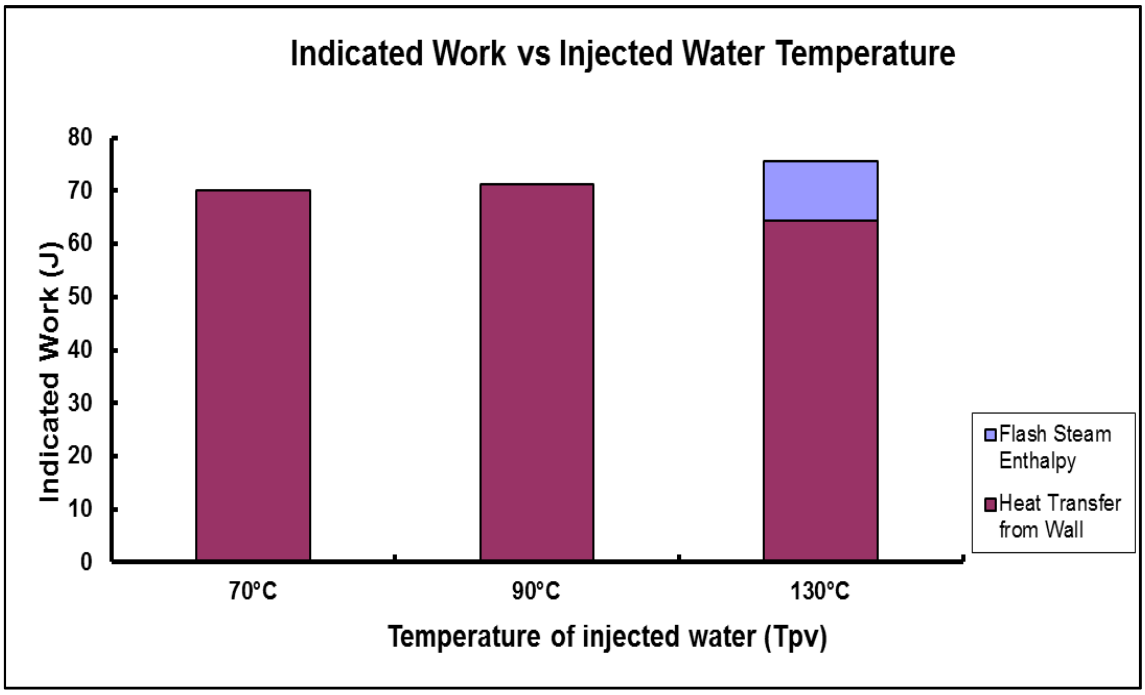

Figure 16. The results of non-flashing injections when compared to flashing injections into the CPE with a wall temperature of 130°C.

While there is no significant change in the convective boiling work output for temperatures of 70°C and 90ºC, the contribution of convective boiling off the wall reduces when flashing occurs. As noted earlier, the contribution of convective boiling is dependent on the mass of liquid striking the hot wall, the surface area of the wall it covers and the boiling speed (convection). Flashing causes a chocked flow, reducing the mass flow rate of the injector. So less liquid strikes the hot wall. Furthermore, the liquid phase of the wet steam exiting the injector is at a relatively higher temperature than the non-flashing injections. As boiling

speed is dependent on the temperature difference between the bulk of the liquid and the hot surface, i.e. the larger the difference the larger the convection. The smaller temperature difference between the wall and the liquid phase of the flashed water further reduces the contribution of convective boiling. When taking into account the reduction in mass flow rate of the injector due to flashing flow (choked flow), the reduction in liquid water striking the walls and other effects such as reduced boiling speed, a total reduction of more than 11% in convective boiling work is expected. However the results show a reduction of only 8.89%. Research in the field of heat transfer has shown that spray cooling can increase Critical Heat Flux (CHF) values and more efficiently transfer heat off hot surfaces when compared to liquid jets of the same mass flux [13],[14],[15],[16]. Investigations by the authors into the injection patterns of non-flashing and flashing injections from the injector indicates a significant widening of the spray cone angle due to flashing. This would in theory translate to a larger area of the heated internal surface of the cylinder being impacted by the unflashed liquid portion. Furthermore, research on flash boiling and atomization has shown enhanced atomization through flashing [6],[7],[8]. It can thus be hypothesized that the smaller than expected decrease in convective boiling which in effect is an improvement in convective boiling for flashing injections was due in part to the enhancement of heat transfer from the walls of the CPV resulting from flash induced atomization of the liquid striking the walls. Figure 17a shows a non-flashing injection at a liquid temperature of 70ºC and Figure 17b shows a flashing injection at a subcooled liquid temperature of 130ºC.

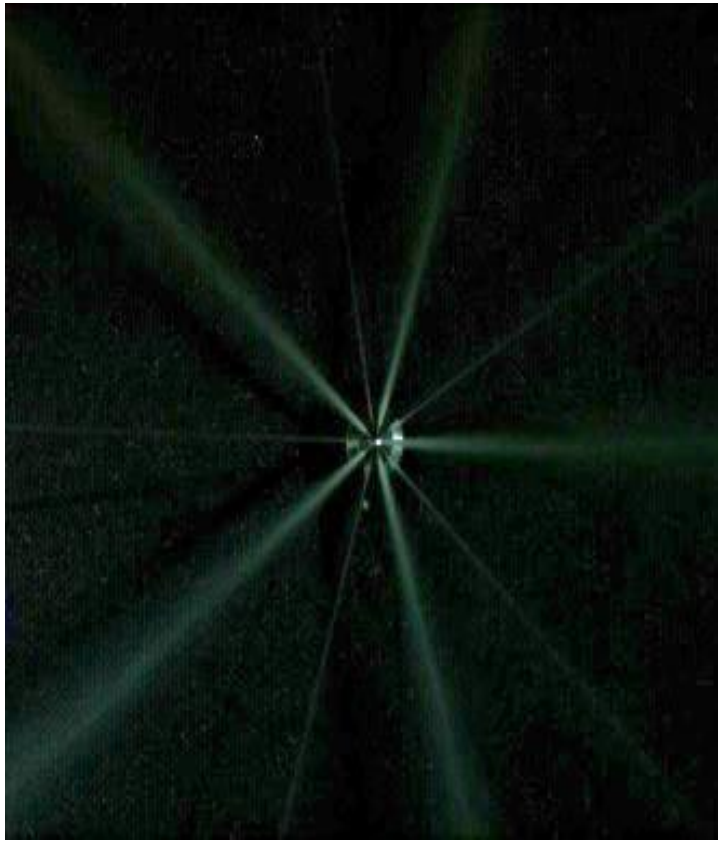

Figure 17a. A Non-Flashing injection from the constructed injected. T_{inj} at 70ºC.

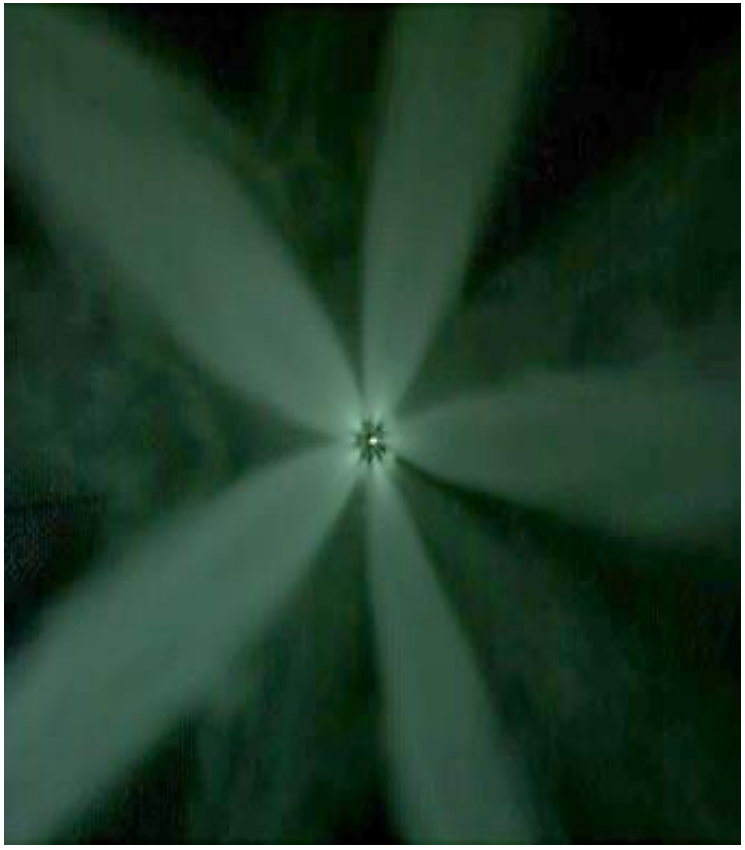

Figure 17b. A Flashing injection from the constructed injected. T_{inj} at 130ºC

3.5.3 Stage 3: The Powering Of an Engine with the SLFB Cycle

In order to investigate the repeatability of the findings of stage 2 in a reciprocating piston engine (the power generation unit of the WHR system), an experimental engine was built. As with the injector construction, the fabrication of a complete engine was beyond the capabilities of the author, so the modification of a commercially available single cylinder engine was undertaken. The engine chosen was a Yamaha 7CN. The head of this engine was removed and a new block for the new power unit, mounted in its place. A piston extension for this unit was attached onto the piston of the 7CN. This in effect gave an engine with the same stroke as the 7CN but with a smaller bore diameter. The specifications of each engine are listed in Table 2.

Table 2. Specifications of the 7CN and the new engine hereafter referred to as FB1.

Specifications	Yamaha 7CN	FB1
Bore	67mm	35mm
Stroke	49mm	49mm
Swept Volume	173cm³	47cm³

Heating fins were attached onto the injector holder, boiling plate and cylinder block. The cylinder block and above were encased in an insulated aluminium casing and hot gasses were fed through this casing to provided heating for the various heated surfaces and components of the FB1. Figure 18 shows the cross-sectional view of the FB1.

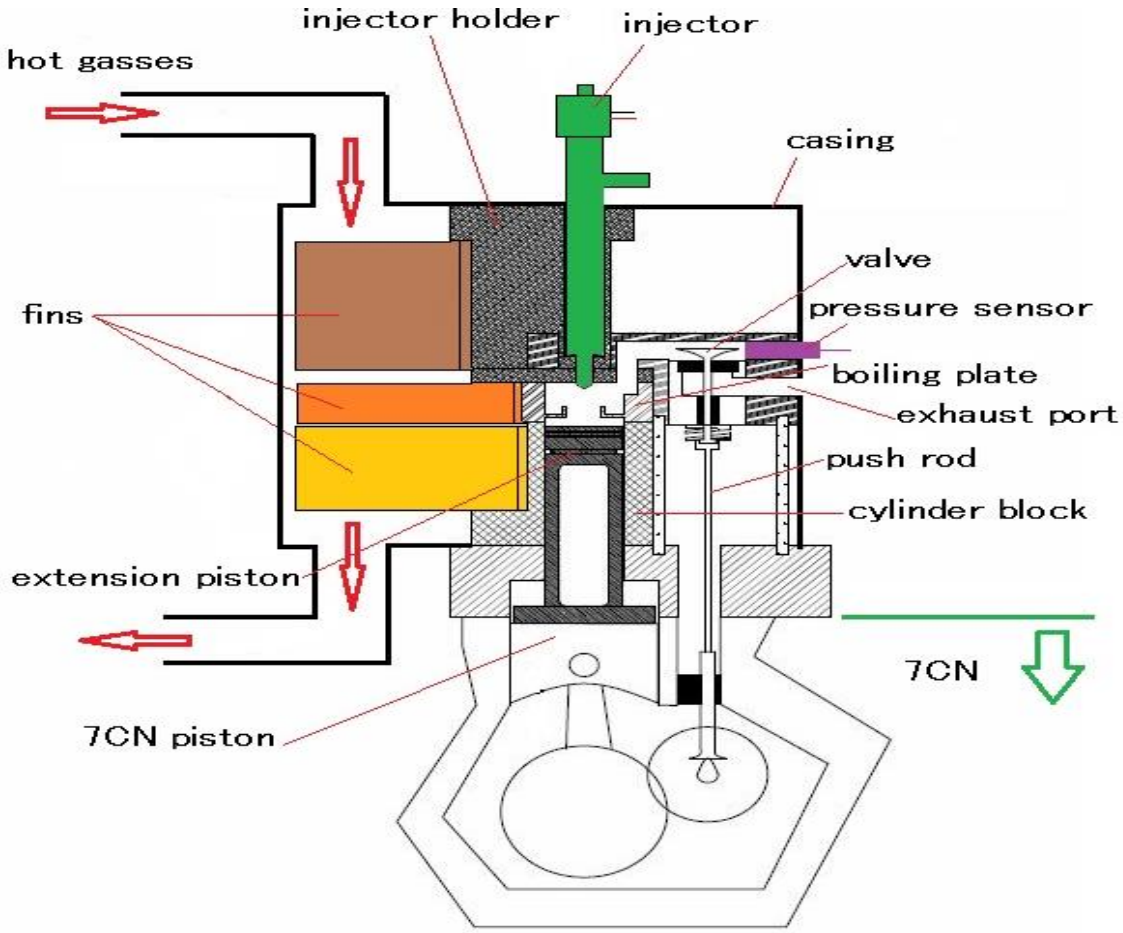

Figure 18.The FB1 with casing, fins, pressure sensor and injector attached.

3.5.3.1 Procedure

The experimental conditions for investigating the SLFB cycle in a piston engine are listed in Table 3 and Figure 19 shows the experimental setup.

Table 3. The experimental conditions.

Working fluid	Water
Working fluid temperature(T_{pv})	150±3 ºC (controllable variable)
Injector temperature(T_{inj})	150±3 ºC and 180±11 ºC (controllable variable)
Boiling plate temperature(T_{bp})	195 ºC ~ 297 ºC (non-controllable variable)
Cylinder wall temperature(T_{blo})	149 ºC ~ 253 ºC (non-controllable variable)
Injection period	10ms and 20ms (controllable variable)
Injection pressure (gauge pressure)	8 MPa (constant)

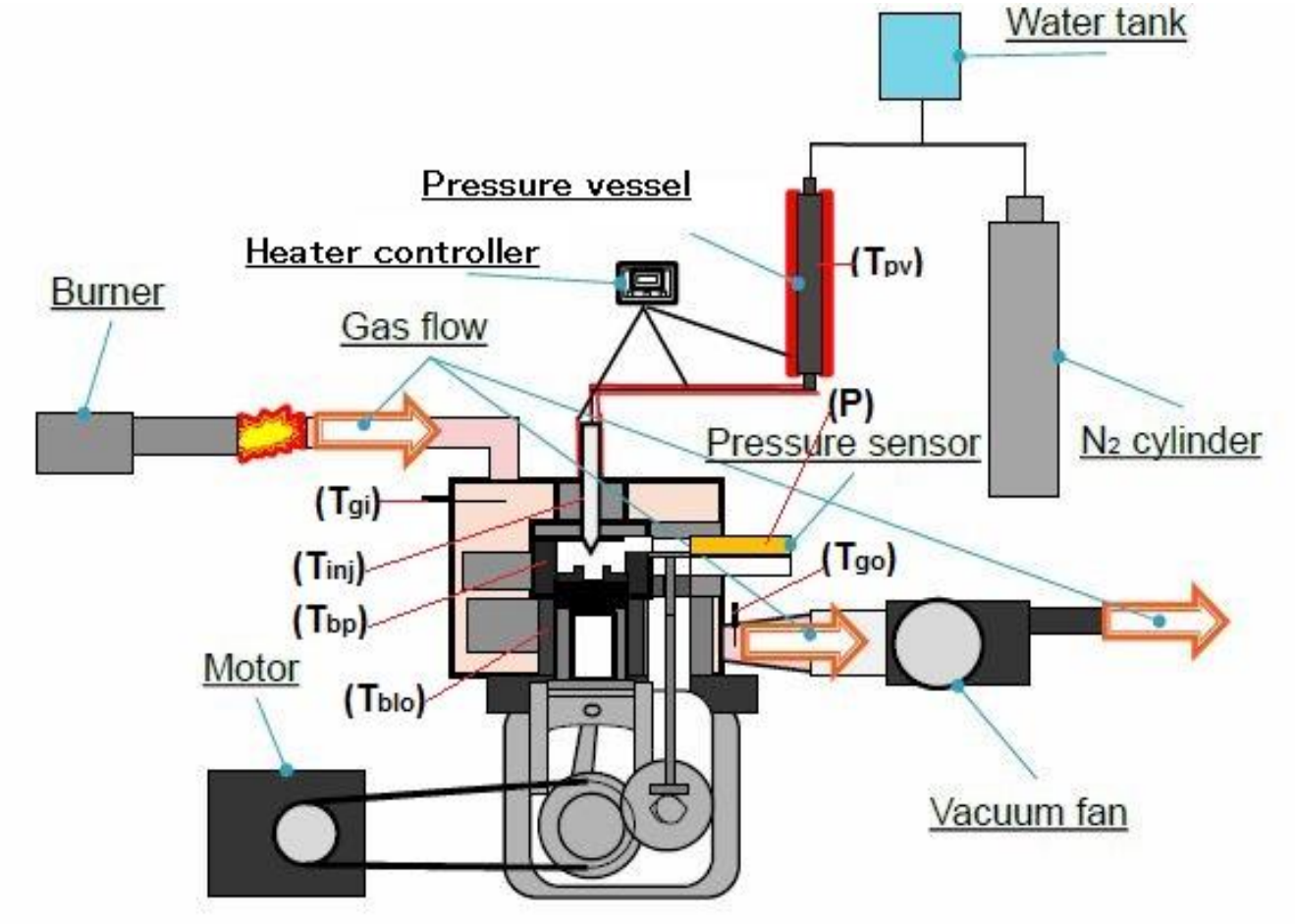

Figure 19. The experimental setup used to investigate the SLFB cycle.

The experiment was carried out by injecting measured amounts of high temperature subcooled water, by altering injection timing, directly into the heated boiling plate section with the piston stationary at 5º ATDC. Injection durations were set at 10ms and 20ms. Heating for the power unit was provided by a gas burner and vacuum fan combination and heat input was controlled by fan speed and burner output adjustment. This heating set-up was chosen as it was analogous to the proposed system that would gain its heat from automotive exhaust. The temperatures of the injector(T_{inj}), the boiling plate(T_{bp}), block(T_{blo}), pressure vessel(T_{pv}), heating gases at inlet(T_{gi}) and heating gases at outlet(T_{go}) were logged as was the in-cylinder pressure(P). Injections were carried out at water temperatures of 150°C and 180°C(T_{pv}). The exact temperature of injected water was taken to be the values of T_{inj} at the beginning of an injection as this was a more accurate measure of the injected liquid temperature, as was learned in *stage 2*. The experiments were carried out as single injection events.

3.5.3.2 Results

For single injection events, the engine was seen to turn over successfully. Figures 20a to 20d show the pressure versus volume charts of 10ms duration injections and Figures 21a to 21d are of 20ms duration injections. The pressures indicated are gauge pressures. The dead volume of the expansion region has been ignored and only the volume swept by the piston has been considered. At the first 10ms injection of water at 148ºC, the engine did not complete a full cycle. However all injections thereafter did.

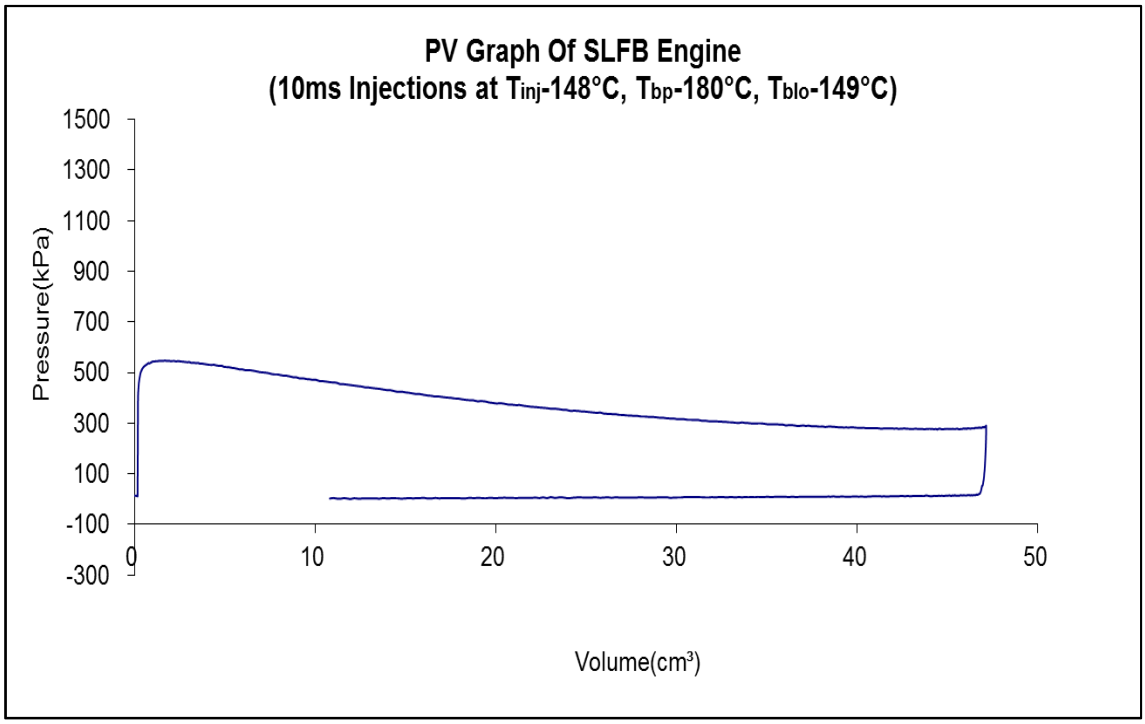

Figure 20a. PV chart for the engine cycle for a 10ms injection of subcooled water at 148ºC(T_{inj}).

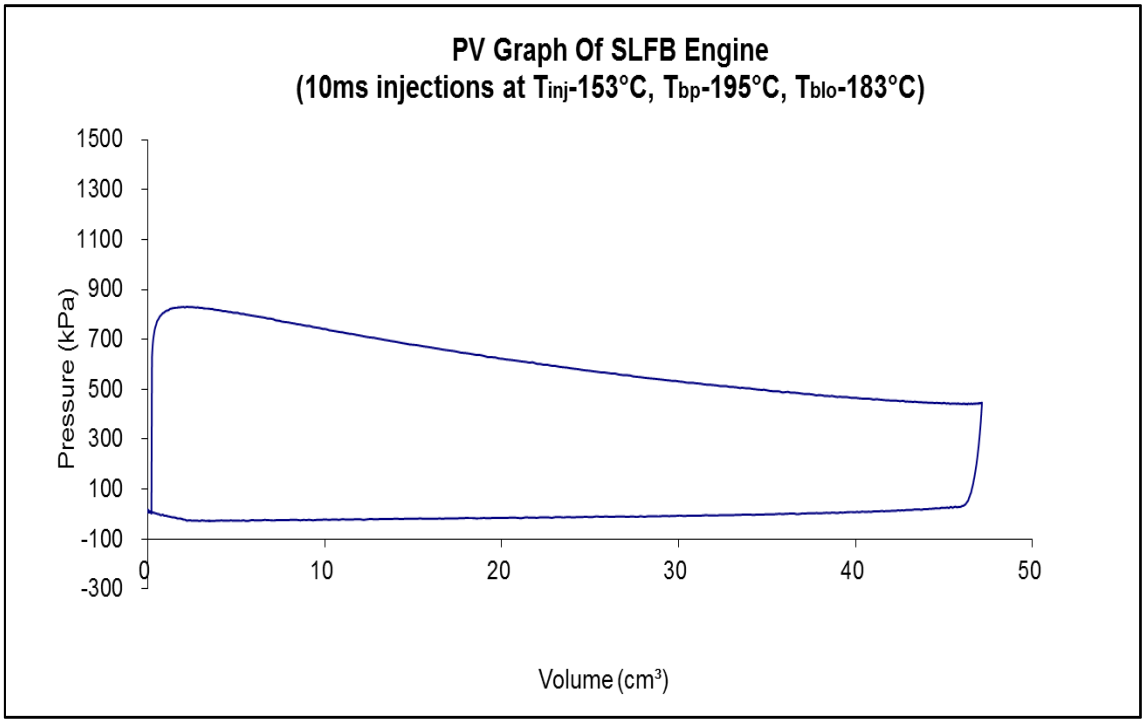

Figure 20b. PV chart for the engine cycle for a 10ms injection of subcooled water at 153ºC(T_{inj})

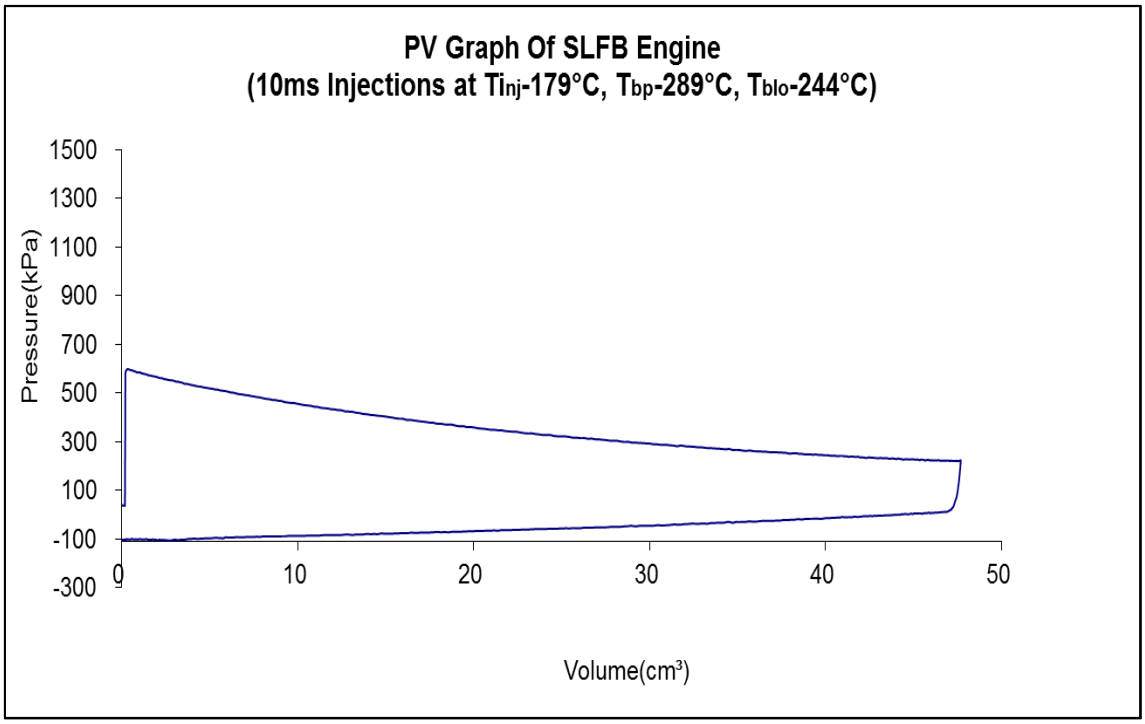

Figure 20c. PV chart for the engine cycle for a 10ms injection of subcooled water at 179ºC(T_{inj}).

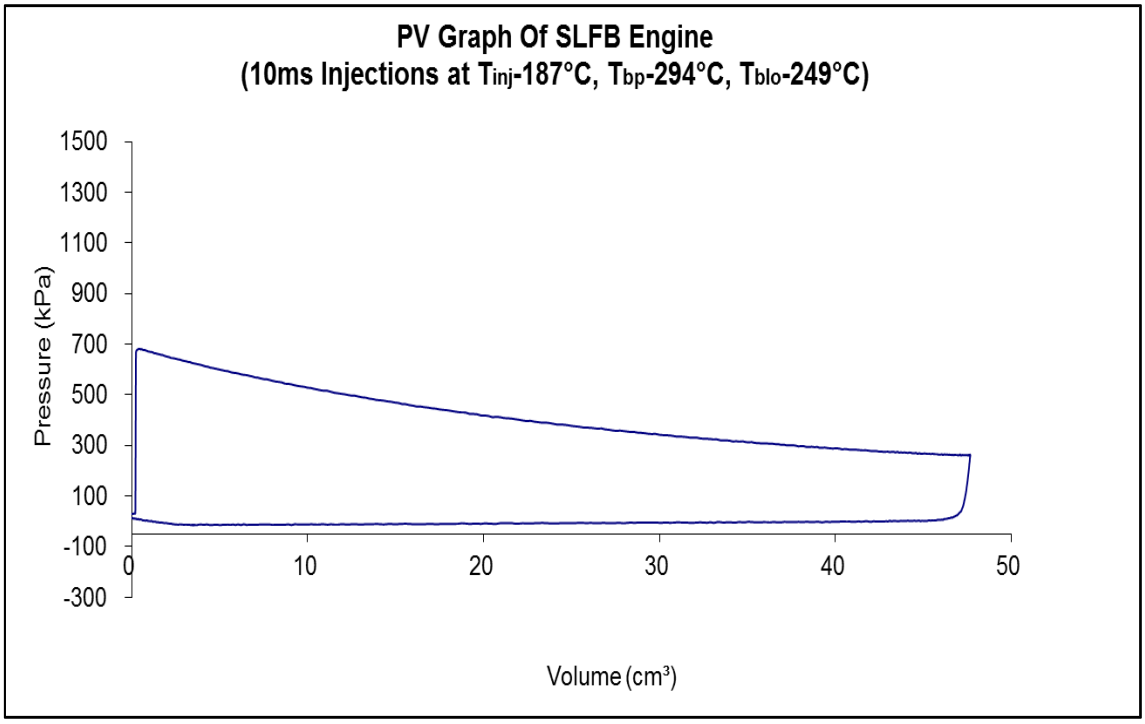

Figure 20d. PV chart for the engine cycle for a 10ms injection of subcooled water at 187ºC(T_{inj}).

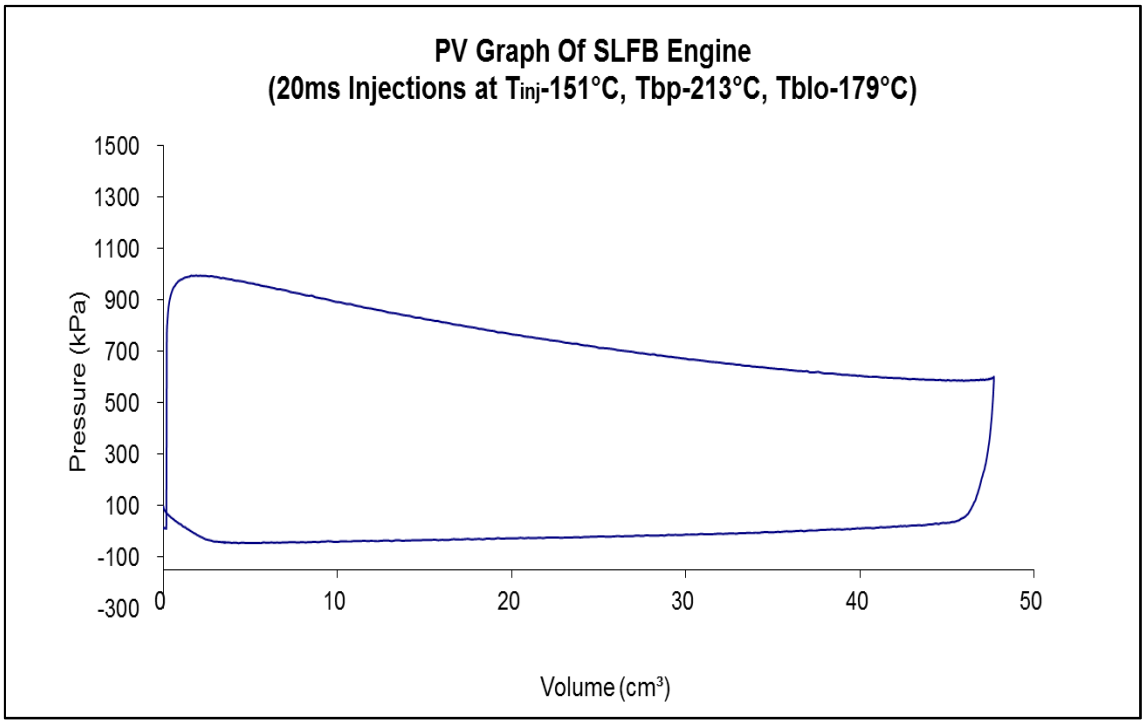

Figure 21a. PV chart for the engine cycle for a 20ms injection of subcooled water at 151ºC(T_{inj}).

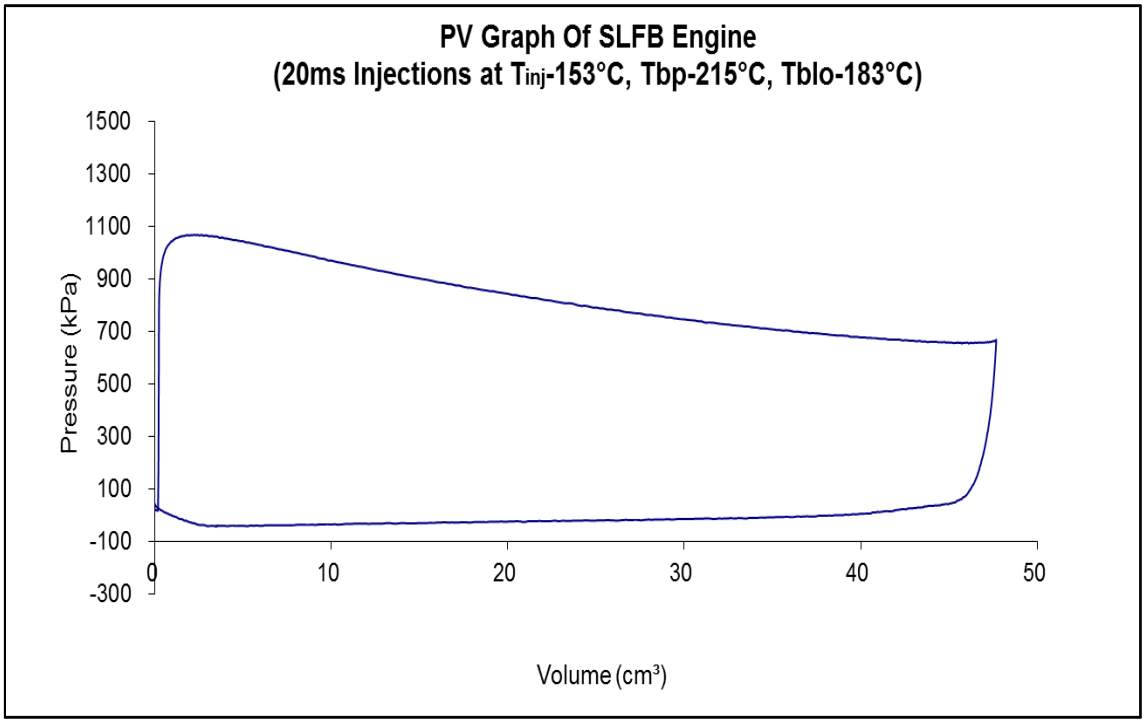

Figure 21b. PV chart for the engine cycle for a 20ms injection of subcooled water at 153ºC(T_{inj}).

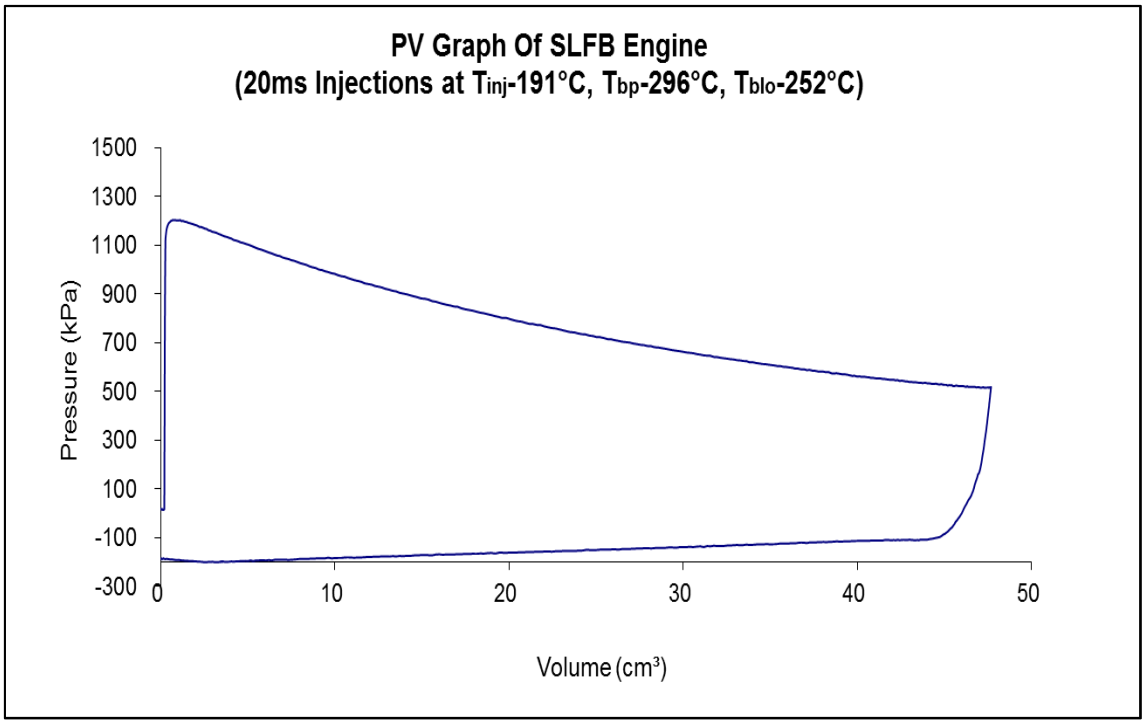

Figure 21c. PV chart for the engine cycle for a 20ms injection of subcooled water at 191ºC(T_{inj}).

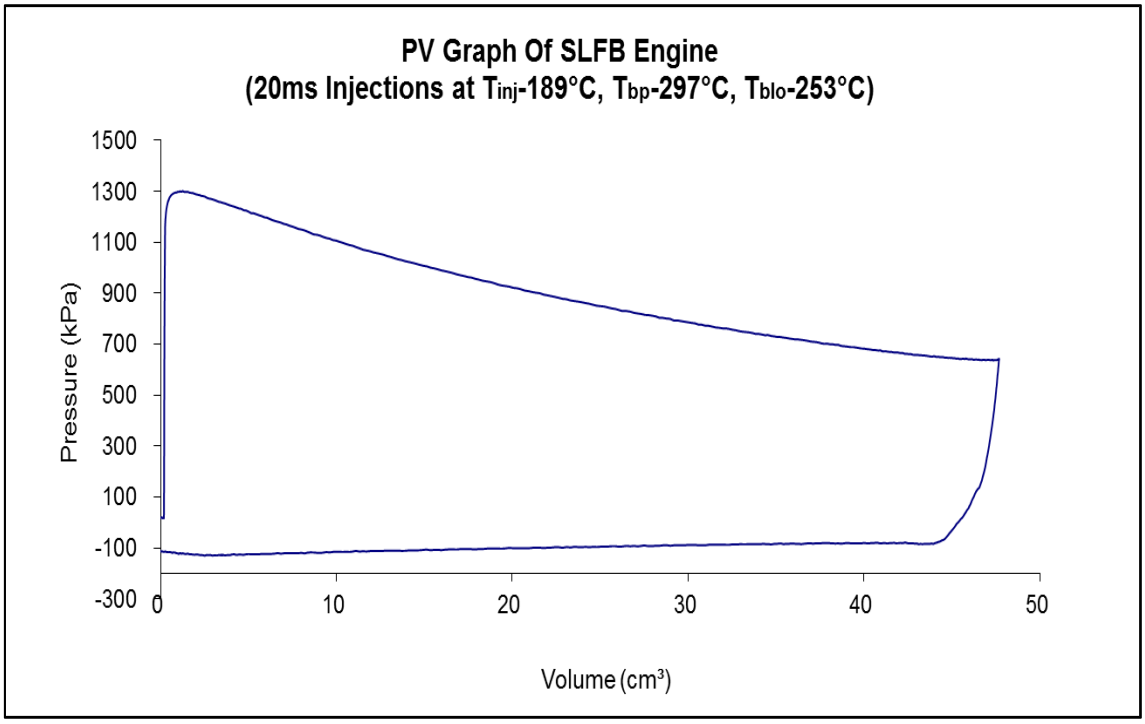

Figure 21d. PV chart for the engine cycle for a 20ms injection of subcooled water at 189ºC(T_{inj}).

The pressure data was sampled at 0.5º intervals of the crank rotation. Due to the heating system employed by this engine, exact, arbitrary control of the temperature of the various parts of the engine namely the injector holder, boiling plate and engine block was not possible. Figures 22a to 22d show Pressure vs Time charts during the power stroke for each 10ms injection and Figures 23a to 23d for 20ms duration injections. The pressure data shown is for a duration of 200ms from the start of injection. Injection was initiated 5º ATDC and exhaust valve opening at 5º BBDC.

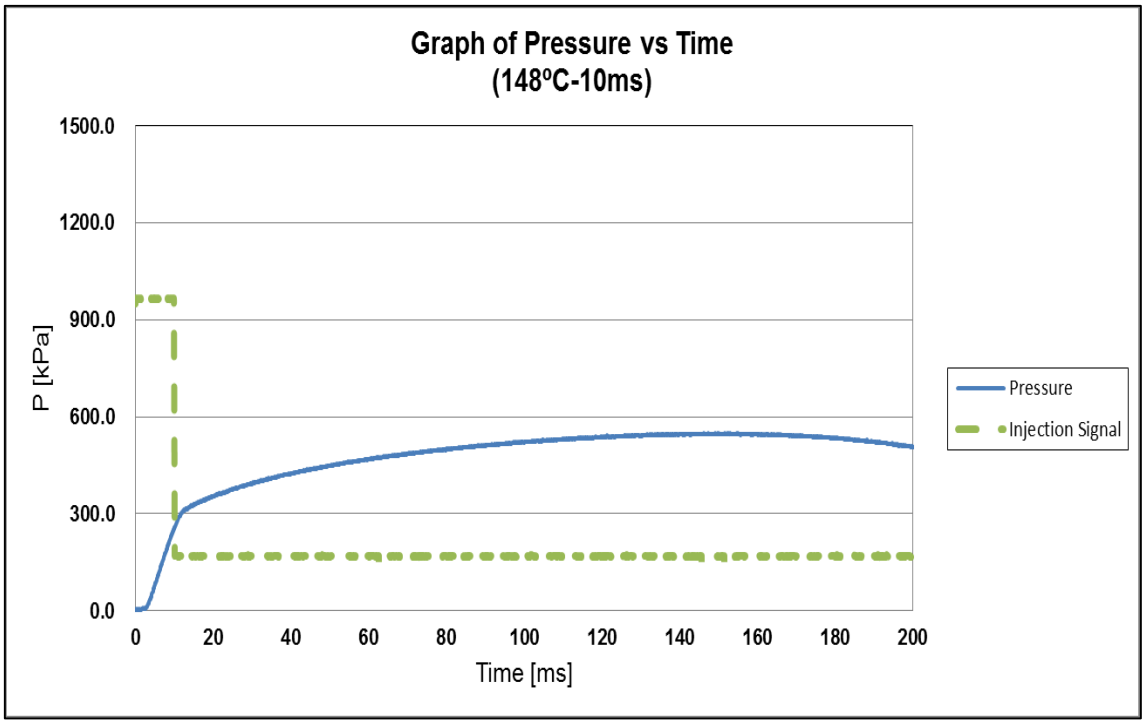

Figure 22a. Detail of pressure rise with respect to time during the power stroke for a 10ms injection at 148ºC(T_{inj}) and T_{bp} at 180ºC.

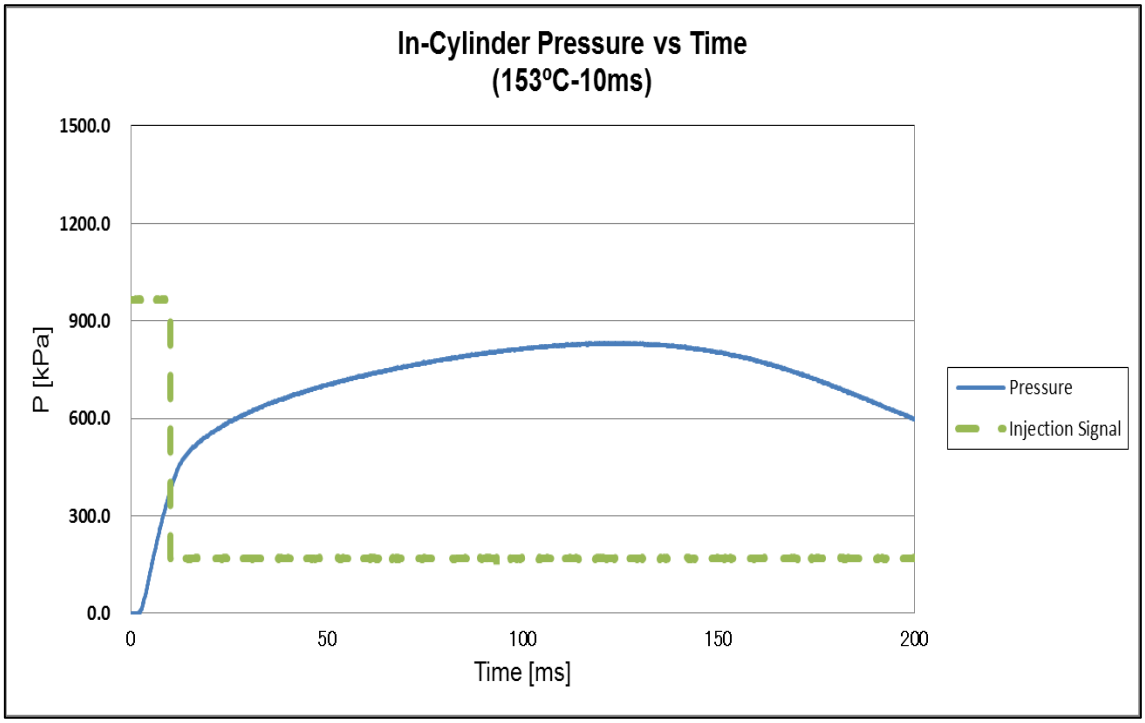

Figure 22b. Detail of pressure rise with respect to time during the power stroke for a 10ms injection at 153ºC(T_{bp}) and T_{bp} at 195ºC.

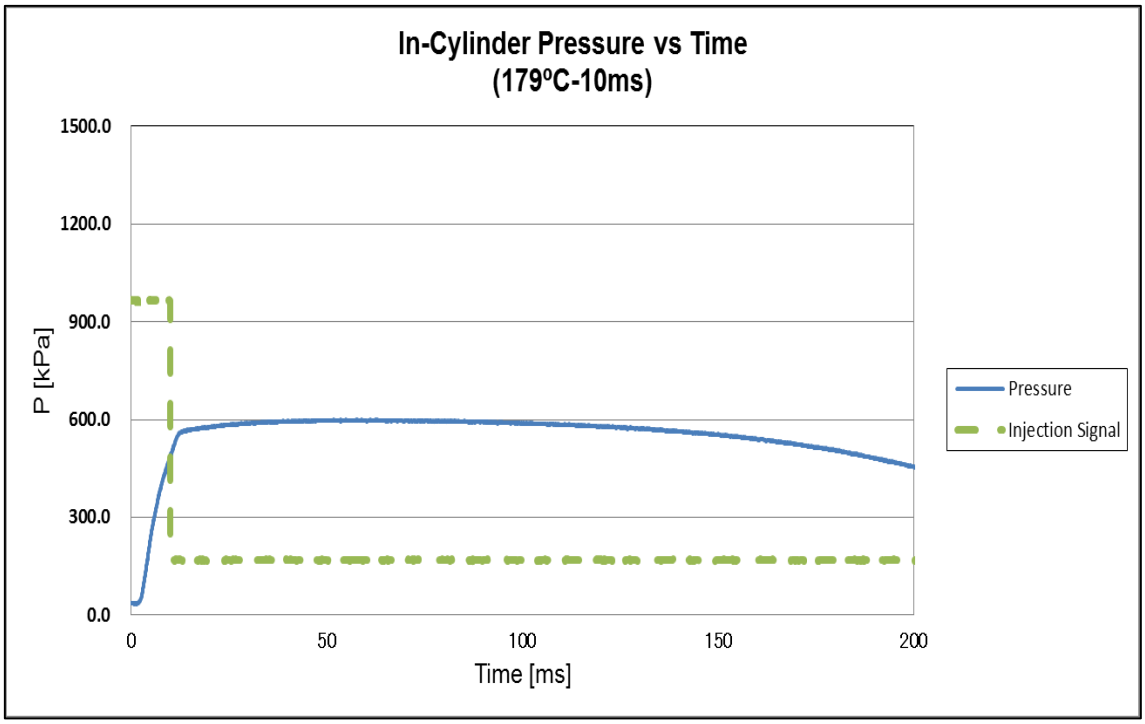

Figure 22c. Detail of pressure rise with respect to time during the power stroke for a 10ms injection at 179ºC(T_{inj}) and T_{bp} at 289ºC.

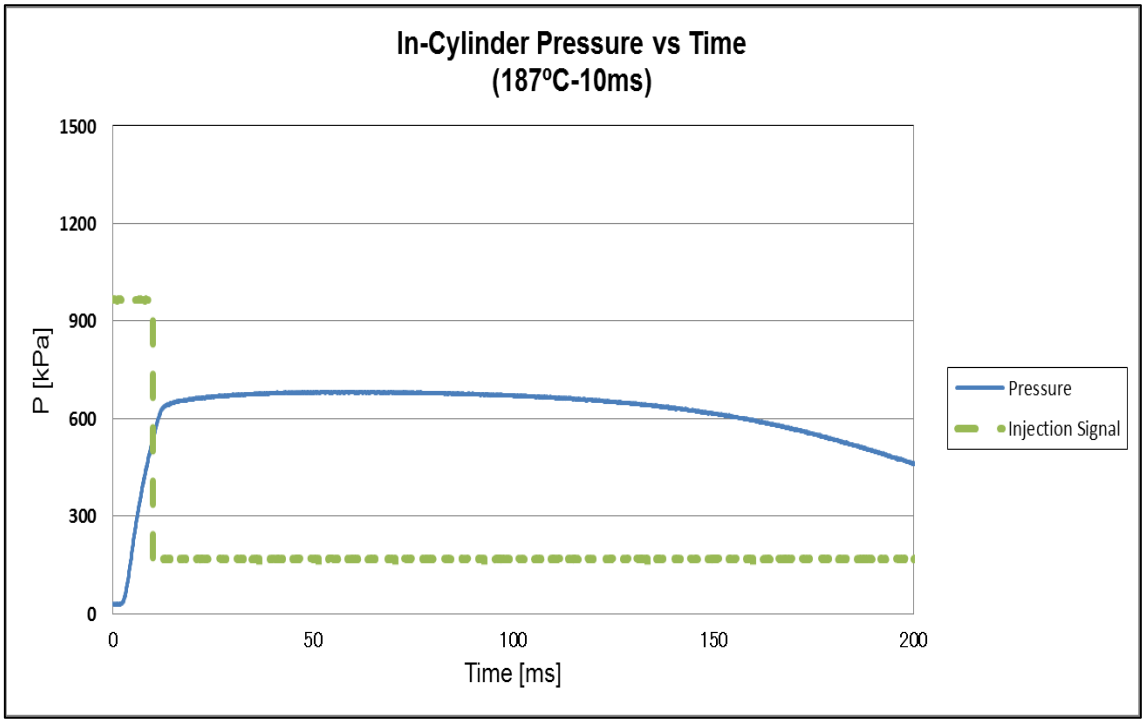

Figure 22d. Detail of pressure rise with respect to time during the power stroke for a 10ms injection at 187ºC(T_{inj}) and T_{bp} at 294ºC.

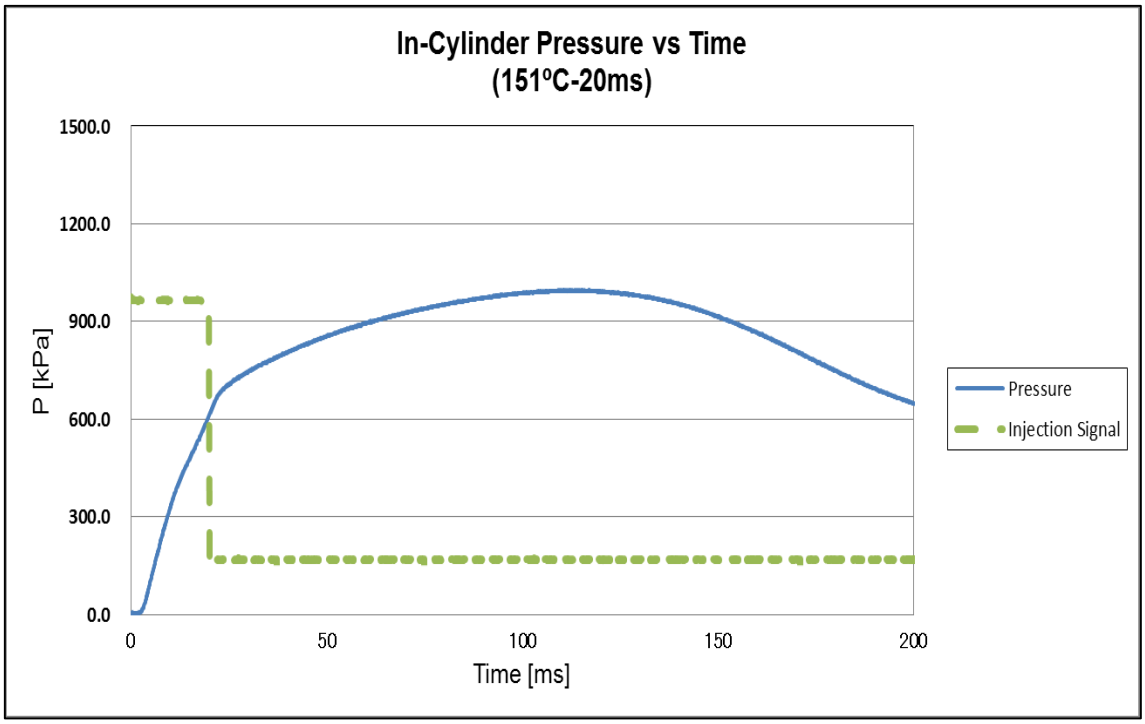

Figure 23a. Detail of pressure rise with respect to time during the power stroke for a 20ms injection at 151ºC(T_{inj}) and T_{pv} at 213ºC.

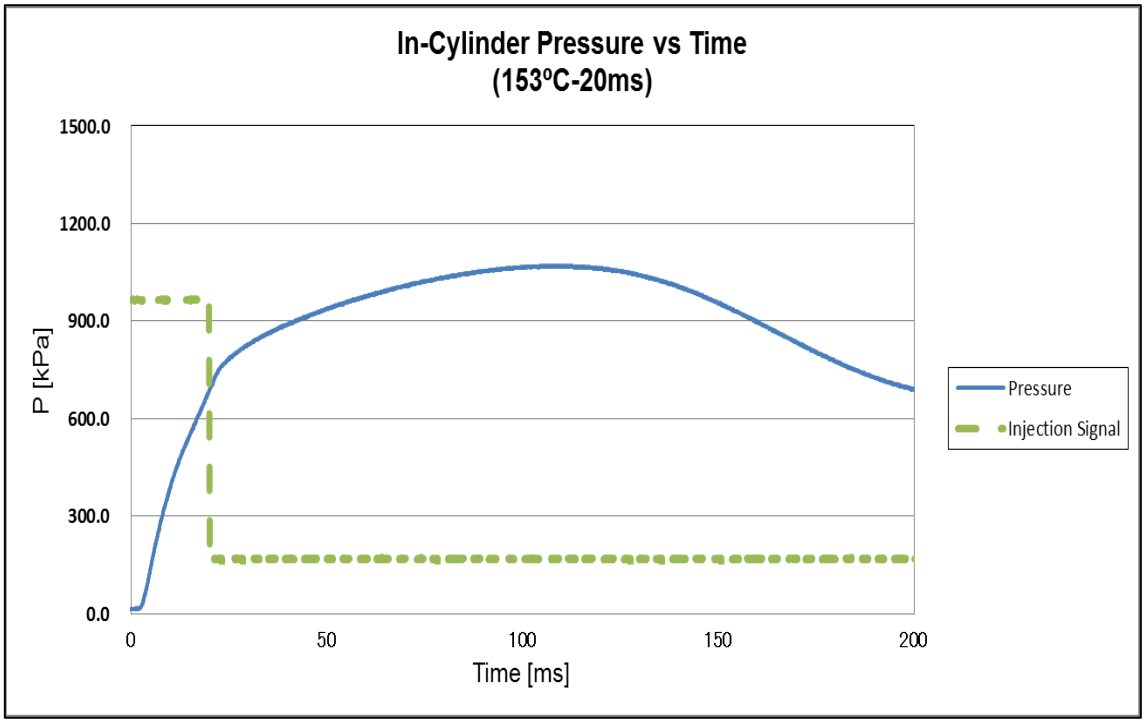

Figure 23b. Detail of pressure rise with respect to time during the power stroke for a 20ms injection at 153ºC(T_{inj}) and T_{pv} at 215ºC.

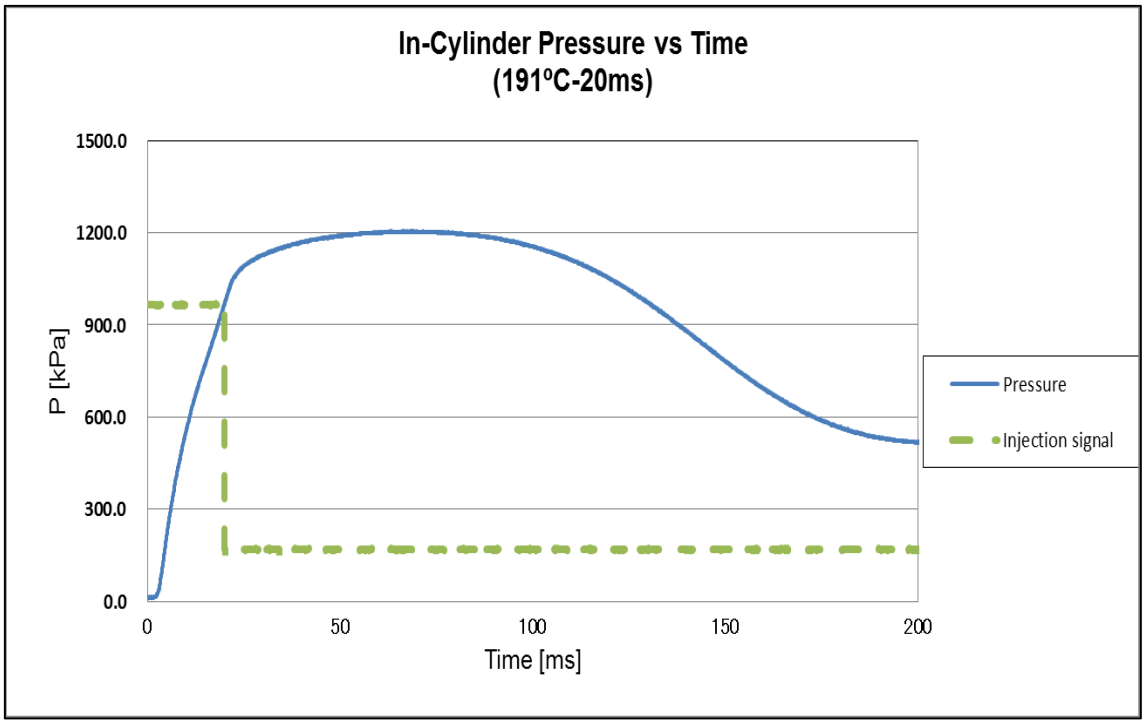

Figure 23c. Detail of pressure rise with respect to time during the power stroke for a 20ms injection at 191ºC(T_{inj}) and T_{bp} at 296ºC.

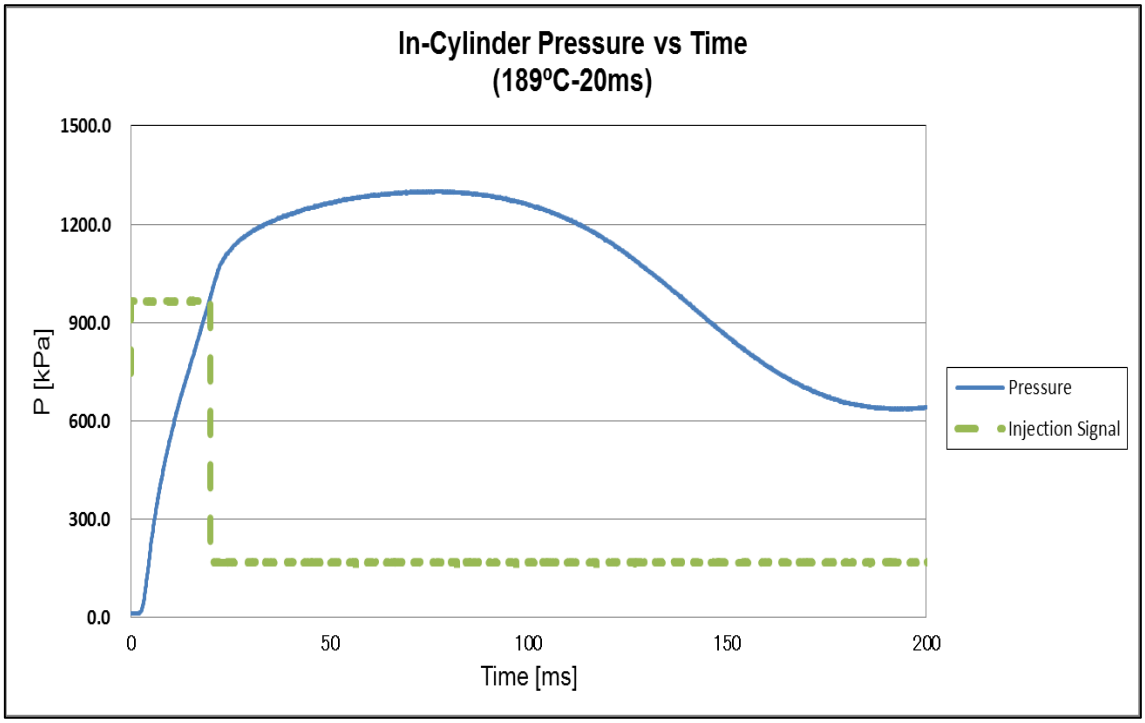

Figure 23d. Detail of pressure rise with respect to time during the power stroke for a 20ms injection at 189ºC(T_{inj}) and T_{bp}at 297ºC.

With reference to Figures 23a to 23d, it is noteworthy that flashing occurs only within the injection period and results in the initial steep pressure gradient. Once injection is complete, a positive but smaller pressure gradient continues to be observed in all experiments for varying durations of time during the expansion phase. This indicates additional heat input into the working fluid within the cylinder. As convective boiling is the source of this additional heat input, this additional heat input with respect to boiling plate temperature is illustrated by Figure 24. ΔP in Figure 24 may be defined by equation (7).

$$\Delta P = P_{peak} - P_{ei} \tag{7}$$

P_{peak} and P_{ei} refer to the peak in-cylinder pressure and the pressure at the end of injection respectively. Thus ΔP is representative of the contribution of the convective boiling input.

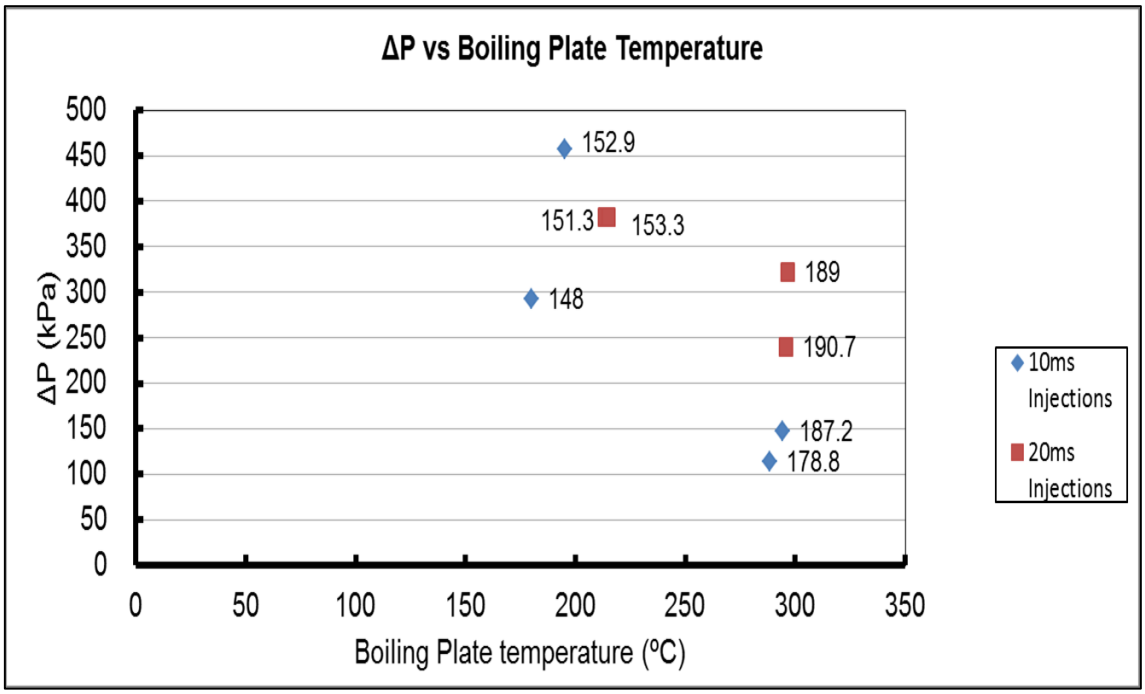

Figure 24. ΔP with relation to the boiling plate temperature. Data labels indicate injection temperature.

It can be seen from Figure 24 that ΔP increases with increasing boiling plate temperatures of 180ºC ~ 215ºC but then significantly falls off for boiling plate

temperatures of 289ºC ~ 297ºC. This fall is more pronounced for smaller injection masses (10ms).

In contrast to the CPE experiment where flashing occurred at a constant pressure, the heat release from flashing within the cylinder of the engine is time variable as it happens at ever increasing in-cylinder pressures. The amount of heat held by the flash steam (H_{fs}) can only be determined empirically from the known information of in-cylinder pressure and injector mass flow rate. The flashing mass flow rate of the injector has already been established experimentally, and is represented by the time variable function$G(t)_{flow}$. The specific enthalpy of flash steam is dependent on the in-cylinder pressure seen by the subcooled fluid as it enters the cylinder. The time variable in-cylinder pressure function ($P_{cyl}(t)$) was established from experiment data (pressure sensor data) and was then used to calculate the time dependent specific enthalpy ($h_{fvp}(t)$). Thus the total flash steam enthalpy (H_{fs}) released during an injection period t may be represented by Equation (8).

$$H_{fs} = \int_0^t [h_{isl} - h_{fvp}(t)] \quad G(t)_{flow} \quad dt \tag{8}$$

It is worthy of note that the flashing mass-flow is not influenced by in-cylinder pressures as long as flashing continues to occur during injection. This is because flashing flows through the injector are chocked flows. Furthermore, flashing heat release is only calculated from this mass-flow rate for the duration that flashing occurs and not the entire duration of injection.

The efficiency value for each experiment was calculated according to Equation (3).

Figure 25 shows the relationship of the efficiency of flash energy conversion to indicated work, in relation to the boiling plate temperature.

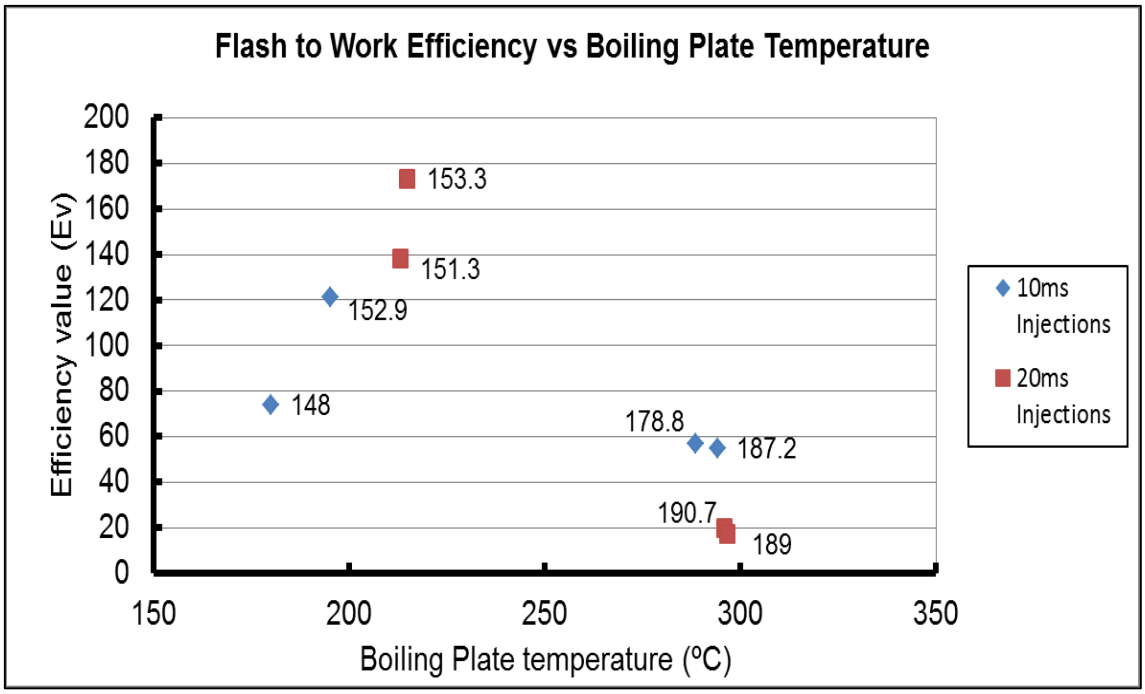

Figure 25. The Efficiency of conversion of Flash energy to work in relation to the boiling plate temperature. The data labels indicate the injection temperatures.

It can be seen from the results that the efficiency tends to increase with boiling plate temperature increase and injected mass of fluid, up to around 215ºC but then falls drastically at boiling plate temperatures of around 290ºC. The relationship of injected mass to efficiency is also seen to invert at these high temperatures. This can be explained by the Leidenfrost effect where the significantly large temperature difference between the boiling plate surface and the boiling point of the liquid hitting it, generates an insulating vapour layer between the hot surface and the liquid striking it. This prevents the liquid from rising in temperature and delays boiling. This relatively cooler liquid (due to it being generated at a lower saturation pressure) mixes with the fresh in-flow of hotter working fluid and causes dissipation. Figures 26a to 26c demonstrates this Dissipation effect. This effect is seen to be more pronounced at higher injection masses and can be attributed to larger masses of the liquid phase remaining in the boiling plate. According to simulations done by Steffen et al on a TLC powered piston engine [2], residual liquid mass within the dead space of a hydro-cyclone separator has a similar effect causing the reduction in the isentropic efficiency of the engine. The results of this experiment reflect this.

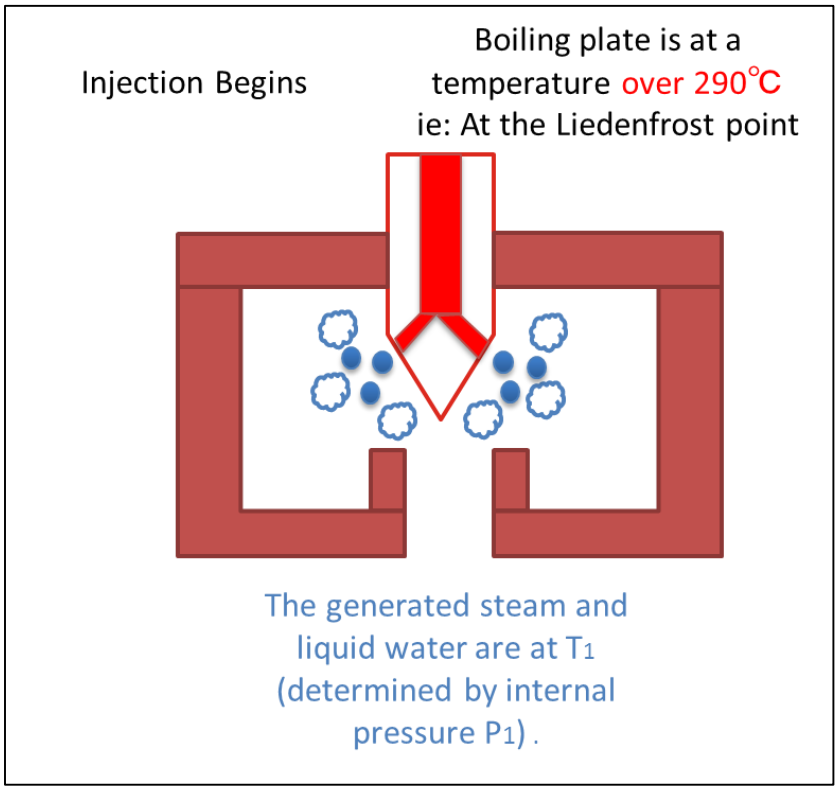

Figure 26a.Stage 1 of the process that leads to Dissipation

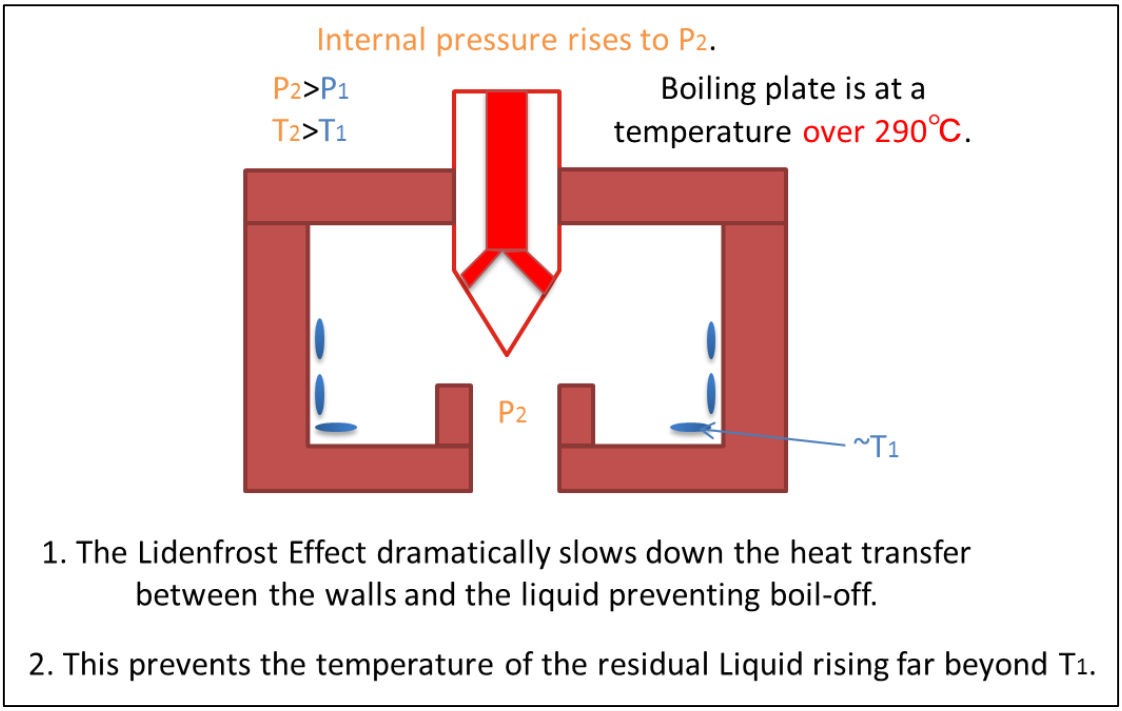

Figure 26b. Stage 2 of the process that leads to Dissipation.

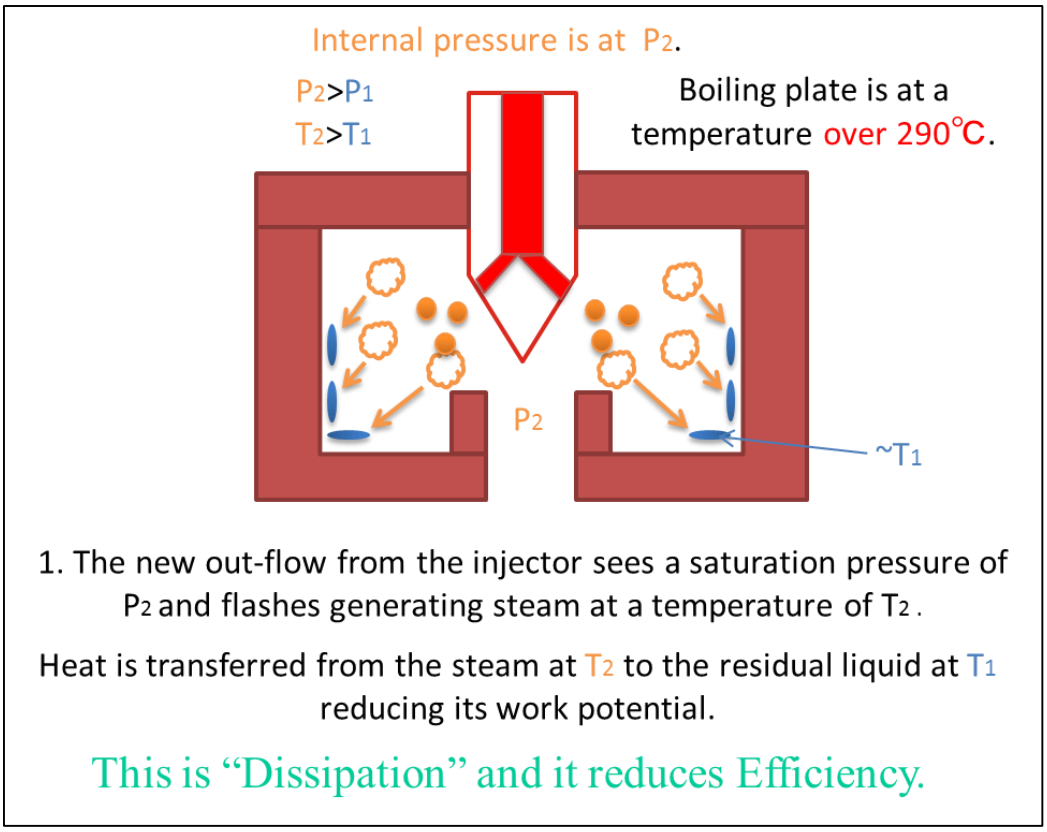

Figure 26c. Stage 3 of the Process that leads to Dissipation.

Tables 4a and 4b show the temperature of the various parts of the FB1 engine just prior to injection.

Tables 4a. Temperatures of various parts of the FB1 engine for 10ms injections.

Injection		Temperature [℃]		
		Injector	Boiling Plate	Block
150 [℃]	10 [ms] (First)	148.0	180.0	149.0
	10 [ms] (Second)	152.9	195.1	183.4
180 [℃]	10 [ms] (First)	178.8	288.5	244.3
	10 [ms] (Second)	187.2	294.1	249.1

Tables 4b. Temperatures of various parts of the FB1 engine for 20ms injections

Injection		Temperature [℃]		
		Injector	Boiling Plate	Block
150 [℃]	20 [ms] (First)	151.3	213.2	178.7
	20 [ms] (Second)	153.3	214.9	182.5
180 [℃]	20 [ms] (First)	190.7	295.8	251.5
	20 [ms] (Second)	189.0	296.7	252.9

Figure 27 shows the relationship of flash energy conversion efficiency to the injection temperature.

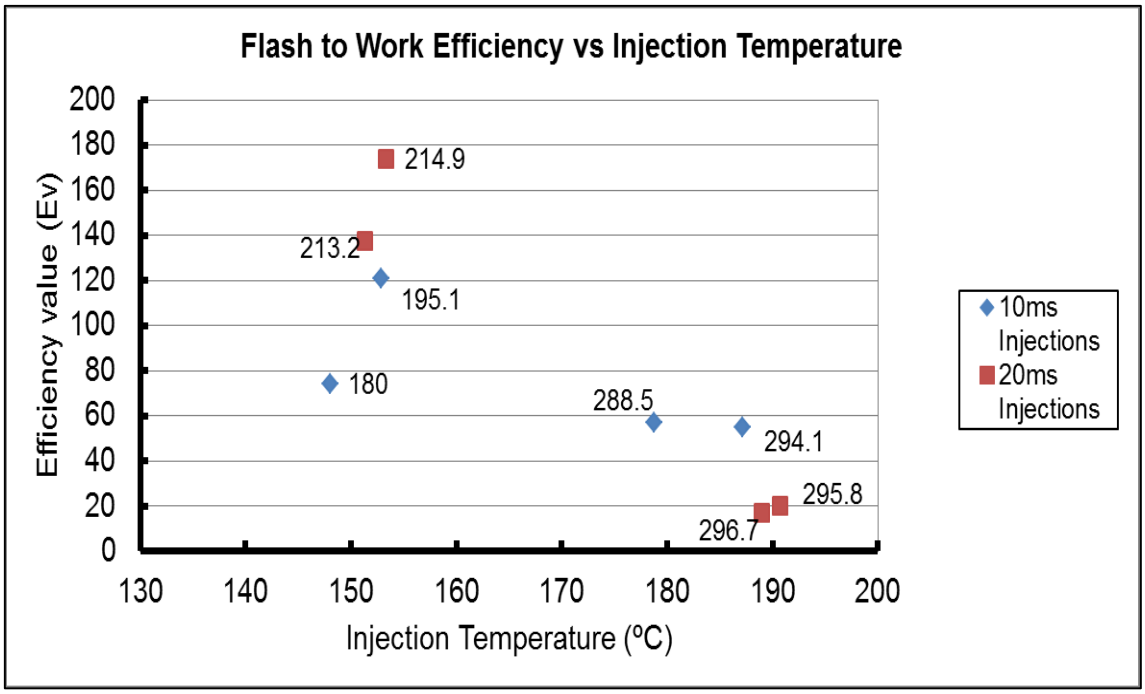

Figure 27. The Efficiency of conversion of Flash energy to work in relation to the injected liquid temperature. The data labels indicate boiling plate temperatures.

A similar relationship to that seen between the flash to work efficiency and boiling plate temperature is also observed between the injection temperature and flash to work efficiency. With reference to tables 4a and 4b, it must be noted that due to the nature of the heating system, the boiling plate temperature is not arbitrary to the injector temperature which is taken to be the injected fluid temperature. Thus the effect of the high boiling plate temperature dominates here as well. In addition to this effect, Steffen et al [2] also found that higher injection temperatures resulted in efficiency decreases due to higher exergy losses caused by spontaneous evaporations in the dead volume. This could also be a contributing factor to the efficiency reduction observed in the SLFB engine with high injection temperatures. The indicated power is calculated from the indicated work and the time taken to produce that work. In all cases except for the very first injection were the engine did not complete a full cycle, the time t_{cyc} is taken as the period for one complete cycle and W_i is the indicated work for that single cycle. For the incomplete cycle of the first injection, t_{cyc} was taken as the time duration the engine was in rotation. Indicated power is described by equation (9)

$$p_i = {}^{W_i}/_{t_{cyc}} \tag{9}$$

Figure 28 shows the relationship between the peak in-cylinder pressure and indicated power. It is clear from this that power output is proportional to peak in-cylinder pressure and that higher peak in-cylinder pressures are generated by larger injection masses, higher boiling plate temperatures and if overall trends are taken, on injection temperatures. Figure 29 shows the relationship of peak in-cylinder pressure to injected liquid temperature, and Figure 30 shows the relationship of peak in-cylinder pressure to boiling plate temperature.

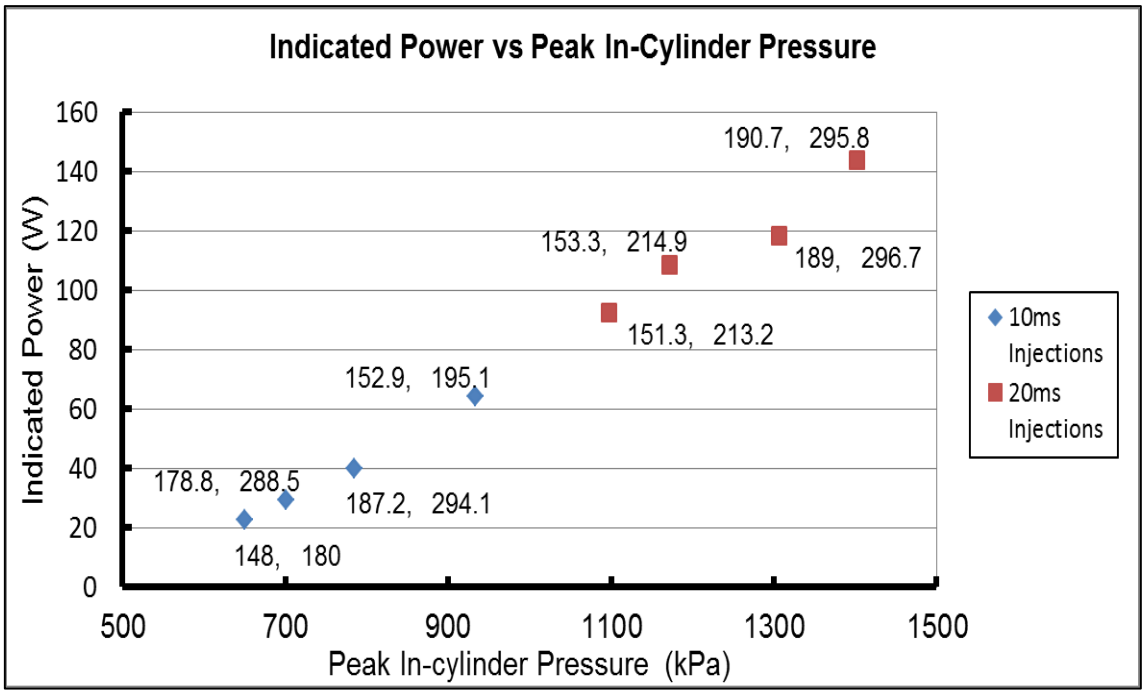

Figure 28. Engine power output in relation to In-Cylinder peak pressure.Data labels indicate the injection temperature and boiling plate temperatures respectively.

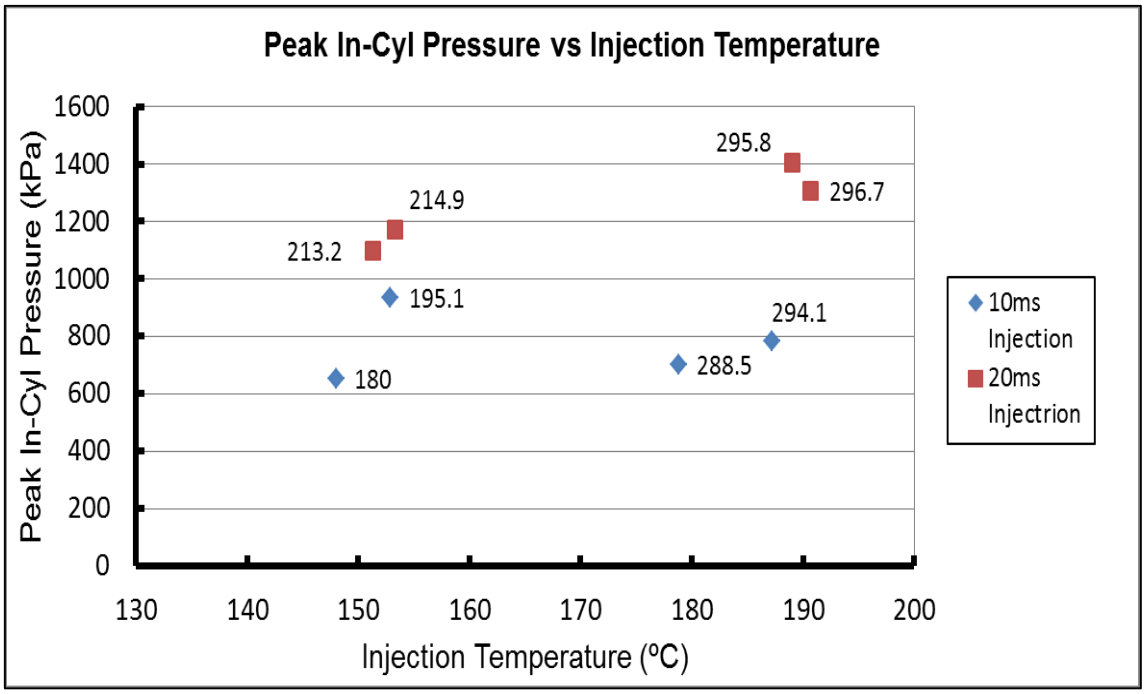

Figure 29. Peak In-Cylinder Pressure in relation to the injected liquid temperature. Data labels indicate boiling plate temperature.

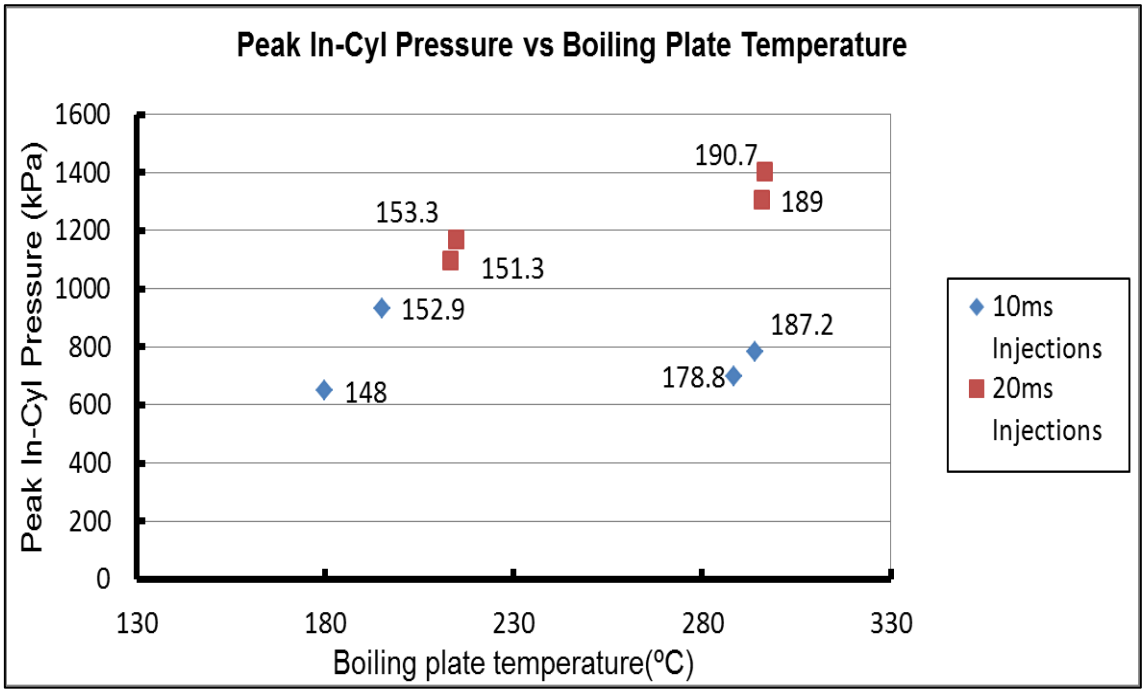

Figure 30. Peak In-Cylinder Pressure in relation to the Boiling Plate temperature. Data labels indicate injection temperature.

While it may seem from Figure 30 that higher boiling plate temperatures result in a higher peak in-cylinder pressures, it must be noted that the boiling plate temperatures are a non-controllable variable in this experiment and higher boiling point temperatures have corresponding higher injection temperatures as well. Thus it is highly plausible that the higher peak in-cylinder pressures at boiling plate temperatures of 289ºC ~ 297ºC are a result higher injection temperatures alone. This argument is further strengthened by the trend seen in Figure 24 of reducing convective boiling input with increasing boiling plate temperatures.

3.6 DISCUSSION

It has been established that the TLC has the potential to efficiently generate power as a WHR system. It has also been shown by some researchers [4] albeit in simulations to be superior to the ORC systems [9],[10],[12]. The SLFB cycle was envisioned to improve upon the standard TLC.

The existence of wet steam is one of the major issues with TLC cycles running at low subcooled temperatures. Such devices as cyclone separators have been proposed for removing the liquid portion of the working fluid prior to it being introduced into the expansion unit [2] and shows promise. However it is not without drawbacks due to dead volume related exergetic losses [2]. The SLFB cycle eliminates the need for separating the two phases. It also helps mitigate any heat losses from the working fluid which should lead to a cycle working at higher efficiencies than the standard TLC. It is also expected to overcome the efficiency drop with increased stroke volume that standard TLC engines suffer from, due to the need for increased injection durations [2]. The SLFB engine achieves this by the convective boiling process which continues to generate steam throughout the power stroke.

The results of the experiment have proven the SLFB piston engine to have a greater efficiency than the TLC powered piston engine with a cyclone separator if all other factors such as the working fluid (water), the efficiency of the heat exchanger, work required to power the high pressure pump and mechanical losses of the piston engine remain the same. Consequently the SLFB powered piston engine is expected to be superior in exergic efficiency to the supercritical ORC as well.” [2] [4]. In order to realise this, the convective boiling process of the SLFB cycle needs to be optimized as do the parameters of the piston engine

such as its stroke length, boiling surface temperature, injection pattern and timing, exhaust valve timing and location, the ideal operating engine speed (in order for convective boiling to be able to contribute) and engine load control (so that the in-cylinder pressure needed to overcome load doesn't surpass the saturation pressure of the boiling plate or block temperatures).

Figure 31 shows the TS chart comparison of the ideal SLFB cycle to that of the current engine working under the same conditions. The cycle shown in Figure 31 (in orange) achieved a flash to work conversion efficiency value (E_v) of 174 which translates to 100% of the flash energy being converted to work and convective wall boiling contributing an additional 74% of the flash energy input. The shaded region (in orange) of the observed cycle is only hypothesised to be as such as this region contains both flashing and convective boiling occurring simultaneously and their interactions are beyond the capabilities of the current experimental setup to quantify. It can however be determined that increasing the convective boiling speed would result in a higher peak in-cylinder pressure resulting in a higher power output. Equation (5) confirms this fact. Furthermore, increasing the stroke length will allow more work to be extracted from the expanding steam as steam generation through convective boiling is an ongoing process throughout the entire power stroke. This should therefore result in an improvement in efficiency.

As noted by Steffen et al, the dead volume causes exergetic losses which leads to an overall reduction in efficiency. The SLFB engine is not immune to this as is clearly seen in the very first injection experiment of 10ms at 148ºC which has a significantly smaller efficiency to the second experiment at roughly the same parameters. In this first injection experiment, the dead space of the boiling plate contains only dry air. However subsequent injections were made into a saturated low pressure steam environment.

The ideal design of the boiling plate would need to improve boiling effectiveness while reducing its dead volume. The observed effect of improved heat transfer between the wall and liquid striking it due to flash induced atomization is a bonus and should be taken into consideration when designing the boiling surface.

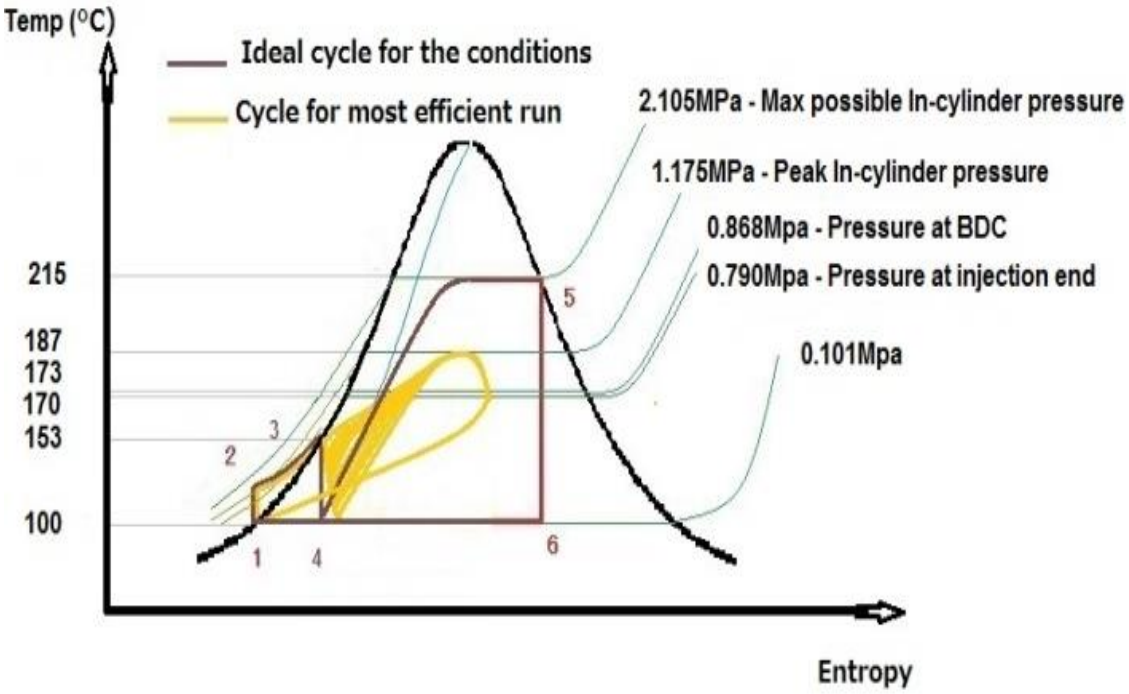

Figure 31. Comparison between the ideal cycle and the most efficient cycle achieved.

Future research will concentrate on enhancing the convective boiling process and the optimizing of boiling plate design and the piston engine's operating parameters for maximum efficiency.

3.7 CONCLUSION

The SLFB cycle is capable of producing power efficiently through a combination of flash evaporation and convective boiling. However, heat losses from the high temperature subcooled liquid prior to injection must be minimised in order to realise high efficiencies. The application and repeatability of this cycle was confirmed in a piston engine. Under optimized boiling plate temperatures, it is capable of surpassing the efficiency of a TLC powered piston engine with a hydro-cyclone separator operating under the same working fluid temperatures. The power output of the experimental SLFB piston engine is directly related to the mass of injected working fluid and its temperature, for temperatures of 180ºC ~ 215ºC. The efficiency of the engine is directly related to the mass and temperature of injected working fluid for boiling plate temperature of 180ºC ~ 215ºC but inverts in relationship at boiling plate temperatures of 289ºC ~ 297ºC due to the influence of the Leidenfrost effect and heat dissipation into the

residual liquid mass. The effective removal of the residual liquid mass during the exhaust stroke is expected to improve the overall efficiency of the engine.

REFERENCES

1. R. Saidur,M. Rezaei,W.K. Muzammil,M.H. Hassan,S. Paria,M. Hasanuzzaman Technologies to recover exhaust heat from internal combustion engines “Renewable and Sustainable Energy Reviews, Volume 16, Issue 8, October 2012, Pages 5649–5659, doi:10.4271/2014-01-2592
2. Michael Steffen, Michael Löffler, Karlheinz Schaber, “Efficiency of a new Triangle Cycle with flash evaporation in a piston engine”, Energy, Volume 57, 1 August 2013, Pages 295-307, ISSN 0360-5442, doi:10.1016/j.energy.2012.11.054.
3. Ngoc Anh Lai, Johann Fischer, “Efficiencies of power flash cycles”, Energy, Volume 44, Issue 1, August 2012, Pages 1017-1027, ISSN 0360-5442, doi:10.1016/j.energy.2012.04.046.
4. Johann Fischer, “Comparison of trilateral cycles and organic Rankine cycles”, Energy, Volume 36, Issue 10, October 2011, Pages 6208-6219, ISSN 0360-5442, doi:10.1016/j.energy.2011.07.041.
5. Henrik Öhman, Per Lundqvist, “Theory and method for analysis of low temperature driven power cycles”, Applied Thermal Engineering, Volume 37, May 2012, Pages 44-50, ISSN 1359-4311, doi:10.1016/j.applthermaleng.2011.12.046.
6. Eran Sher, Tali Bar-Kohany, Alexander Rashkovan, “Flash-boiling atomization”, Progress in Energy and Combustion Science, Volume 34, Issue 4, August 2008, Pages 417-439, ISSN 0360-1285, doi:10.1016/j.pecs.2007.05.001.
7. A. Günther, K.-E. Wirth, “Evaporation phenomena in superheated atomization and its impact on the generated spray”, International Journal of Heat and Mass Transfer, Volume 64, September 2013, Pages 952-965, ISSN 0017-9310, doi:10.1016/j.ijheatmasstransfer.2013.05.034.
8. Jianqin Fu, Jingping Liu, Chengqin Ren, Linjun Wang, Banglin Deng, Zhengxin Xu, “An open steam power cycle used for IC engine exhaust gas energy recovery”, Energy, Volume 44, Issue 1, August 2012, Pages 544-554, ISSN 0360-5442, doi:10.1016/j.energy.2012.05.047.

9. Hui Xie, Can Yang, “Dynamic behavior of Rankine cycle system for waste heat recovery of heavy duty diesel engines under driving cycle”, Applied Energy, Volume 112, December 2013, Pages 130-141, ISSN 0306-2619, doi:10.1016/j.apenergy.2013.05.071.
10. Sipeng Zhu, Kangyao Deng, Shuan Qu, “Energy and exergy analyses of a bottoming Rankine cycle for engine exhaust heat recovery”, Energy, Volume 58, 1 September 2013, Pages 448-457, ISSN 0360-5442, doi:10.1016/j.energy.2013.06.031.
11. V. Pandiyarajan, M. Chinna Pandian, E. Malan, R. Velraj, R.V. Seeniraj, “Experimental investigation on heat recovery from diesel engine exhaust using finned shell and tube heat exchanger and thermal storage system”, Applied Energy, Volume 88, Issue 1, January 2011, Pages 77-87, ISSN 0306-2619, doi:10.1016/j.apenergy.2010.07.023.
12. Alberto Boretti, “Recovery of exhaust and coolant heat with R245fa organic Rankine cycles in a hybrid passenger car with a naturally aspirated gasoline engine”, Applied Thermal Engineering, Volume 36, April 2012, Pages 73-77, ISSN 1359-4311, doi:10.1016/j.applthermaleng.2011.11.060
13. Jungho Kim, “Spray cooling heat transfer: The state of the art”, International Journal of Heat and Fluid Flow, Volume 28, Issue 4, August 2007, Pages 753-767, ISSN 0142-727X, doi:10.1016/j.ijheatfluidflow.2006.09.003.
14. K. Oliphant, B.W. Webb, M.Q. McQuay, “An experimental comparison of liquid jet array and spray impingement cooling in the non-boiling regime”, Experimental Thermal and Fluid Science, Volume 18, Issue 1, September 1998, Pages 1-10, ISSN 0894-1777, doi:10.1016/S0894-1777(98)10013-4.
15. Yu.A. Buyevich, V.N. Mankevich, “Cooling of a superheated surface with a jet mist flow”, International Journal of Heat and Mass Transfer, Volume 39, Issue 11, July 1996, Pages 2353-2362, ISSN 0017-9310, doi:10.1016/0017-9310(95)00249-9.
16. Ruey-Hung Chen, Louis C Chow, Jose E Navedo, “Effects of spray characteristics on critical heat flux in subcooled water spray cooling”, International Journal of Heat and Mass Transfer, Volume 45, Issue 19, September 2002, Pages 4033-4043, ISSN 0017-9310, doi:10.1016/S0017-9310(02)00113-8.

Definitions/Abbreviations

$ATDC$	After top dead center
$AWHR$	Automotive waste heat recycling
A_{cl}	Area covered by liquid
$BBDC$	Before bottom dead center
B_s	Convective boiling speed
h_{CB}	Constant of heat transfer
CHF	Critical heat flux
CPE	Constant pressure expander
E_v	Efficiency value
H_{fs}	Enthalpy of flash steam
$h_{fs}\%$	Percentage of specific enthalpy in flashed steam
L_{fvp}	Latent heat of vaporization at final vapour pressure
L	Latent heat of vaporization of liquid striking the surface
m_i	Injection mass
P_{cyl}	In-cylinder pressure
P_{ei}	In-cylinder pressure at end of injection
p_i	Indicated power
P_{max}	Maximum pressure of working fluid
P_{min}	Minimum pressure of working fluid
P_{peak}	Peak in-cylinder pressure
Q_{cb}	Heat from convective boiling
TDC	Top dead center
TLC	Trilateral cycle
T_c	Temperature of CPE wall.
T_{blo}	Temperature of block
T_{bp}	Temperature of boiling plate
T_{gi}	Temperature of heating gasses at inlet
T_{go}	Temperature of heating gasses at outlet
T_{inj}	Temperature of injector
T_l	Temperature of liquid striking surface
T_{max}	Maximum temperature of working fluid
T_{min}	Minimum temperature of working fluid
T_{pv}	Temperature of pressure vessel
T_s	Temperature of surface
v_f	Final volume
v_i	Initial volume
WHR	Waste heat recovery
W_i	Indicated work
h_{fvp}	Specific enthalpy of liquid at final vapour pressure
h_{isl}	Initial specific enthalpy of subcooled liquid
t_{cyc}	Time taken for one cycle of rotation
x	Quality of vapour

Chapter 4: The Fundamentals Governing the Operation and Efficiency of a Subcooled Liquid Flash, Boiling (S.L.F.B) Cycle Powered Reciprocating Engine for Automotive Waste Heat Recovery

4.1 INTRODUCTION

It has been established that the SLFB cycle is capable of generating power [1] and some of the fundamental phenomenon governing the cycle have been proven and others discovered. Theoretically, it has the potential for higher efficiencies in power production than the RC or the ORC [2], [3]. Experimentation carried out thus far has been for single cycle operations of the engine and further investigation is required in multi-cycle operation. Multicycle operation will provide an insight into the other fundamentals governing the efficiency of a reciprocating engine operating on the SLFB cycle.

4.1.1 The Subcooled Liquid Flash, Boiling Cycle

The ideal SLFB cycle is illustrated in Figure 1, and as it applies to a reciprocating engine may be summarized by Figure 2.

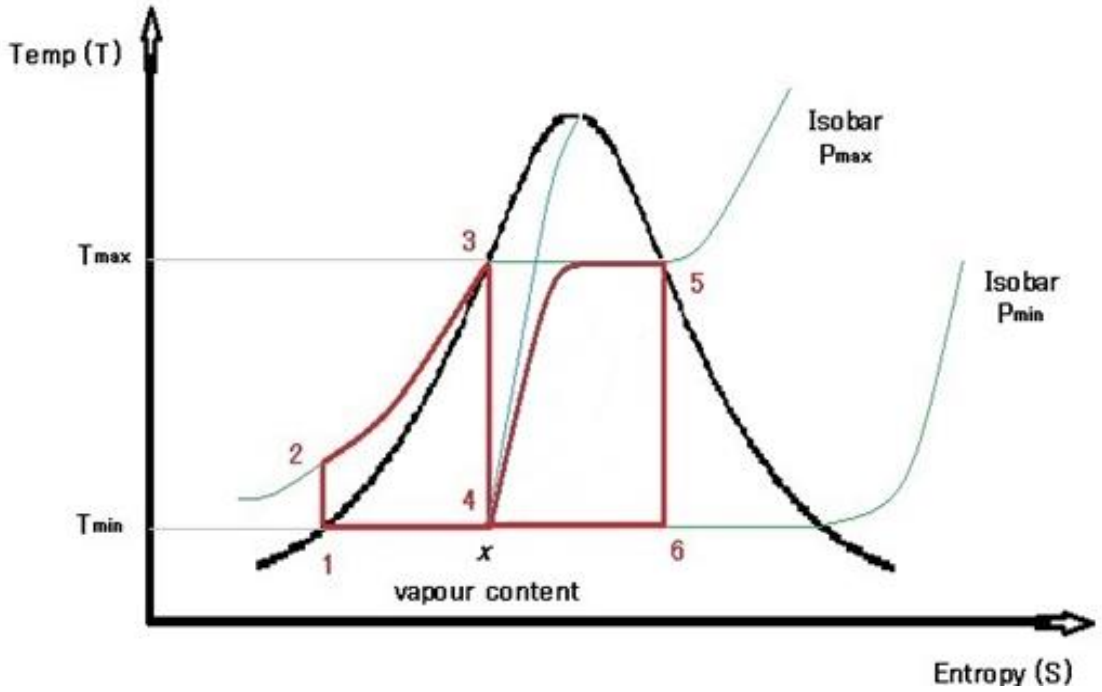

Figure 1. The TS Diagram of the ideal SLFB Cycle

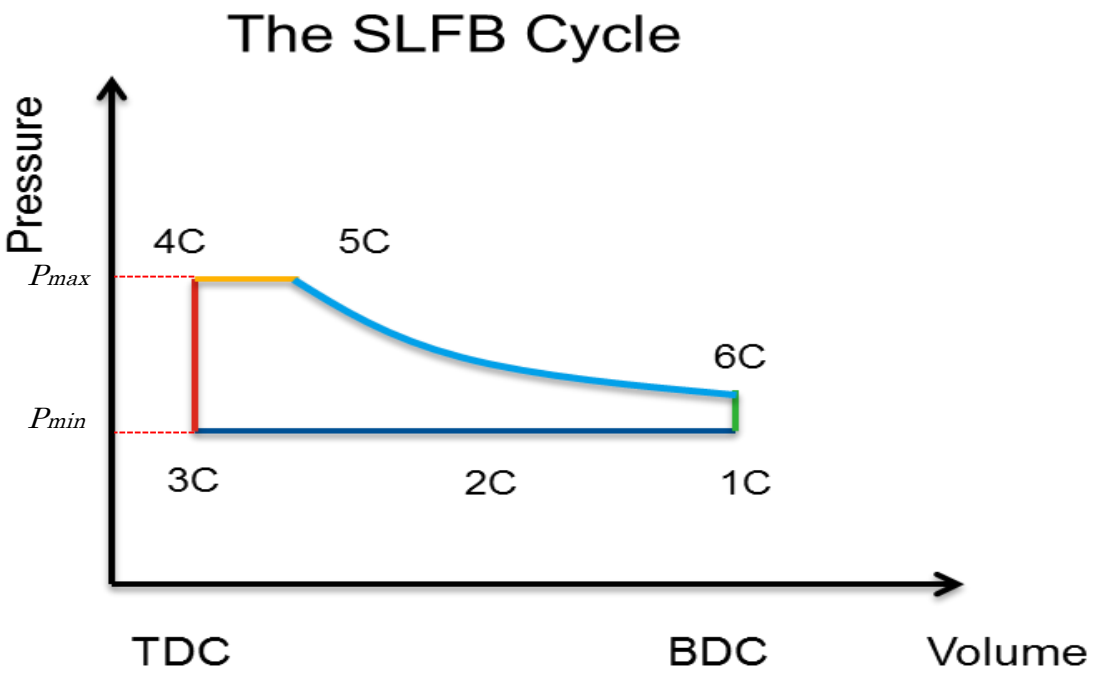

Figure 2. The PV Diagram of the ideal SLFB Cycle in a Piston Engine.

The SLFB cycle researched in this paper has similarities to the Trilateral Cycle (TLC) [2],[3],[4],[5]. Research done on the TLC has shown it to be superior [4] to the well-established ORC [5],[6],[7]. Both the SLFB and TLC use a phenomenon known as “Flashing” to generate an expandable vapour which in turn can be used in an expansion engine.

With reference to Figure 1, the stages of the SLFB Cycle may be described as follows:

- 1-2 is the isentropic compression of the liquid phase to a maximum pressure $\boldsymbol{P_{max}}$ by an isentropic pump. The pump compresses the liquid to a pressure high enough to maintain it in a subcooled state at $\boldsymbol{T_{max}}$.

- 2-3 is the isobaric heating of the liquid phase up to the temperature $\boldsymbol{T_{max}}$. At state 3 the liquid is in a superheated state.

- 3-4 is the isentropic expansion of the vapour generated from "flashing". In this process, wet saturated steam is generated as the temperature of the working fluid drops to the temperature $\boldsymbol{T_{min}}$ and pressure $\boldsymbol{P_{min}}$ with vapor content $\boldsymbol{x}$.

- 4-5 is the multiphase convective boiling of the wet portion of steam generated in process stage 3-4, from the heated walls of a specially designed component within the expansion unit. The vapour generated is capable of reaching a maximum pressure of $\boldsymbol{P_{max}}$ determined by the wall temperature($\boldsymbol{T_{max}}$).

- 5-6 is the isentropic expansion of the vapour generated.

- 6-1 is the complete condensation of the vapour back to state 1.

With reference to Figure 2:

- 3c-4c is Flashing Heat Release.
- 4c-5c is Convective Boiling Heat Addition.
- 5c-6c is Adiabatic Expansion
- 6c-1c is Exhaust.
- 1c-2c-3c is Condensation, Pressurisation and Heating.

The TLC is represented by process stages 1-2-3-4 in Figure 1. The SLFB Cycle augments the output of the TLC through multiphase convective boiling of the unflashed liquid generated in stage 3-4, which in the TLC would be discarded. This makes the SLFB Cycle inherently more efficient than the TLC.

The principle of operation of the SLFB engine is illustrated in Figure 3.

- High temperature subcooled water is delivered directly into the expansion unit using a fast response electro-mechanical injector.

- Work is generated in the power unit from two processes;
  (a) The *Flashing* of the superheated working medium and
  (b) The *Multiphase Convective Boiling* of the unflashed liquid portion by heat transfer from heated surfaces within the power unit.

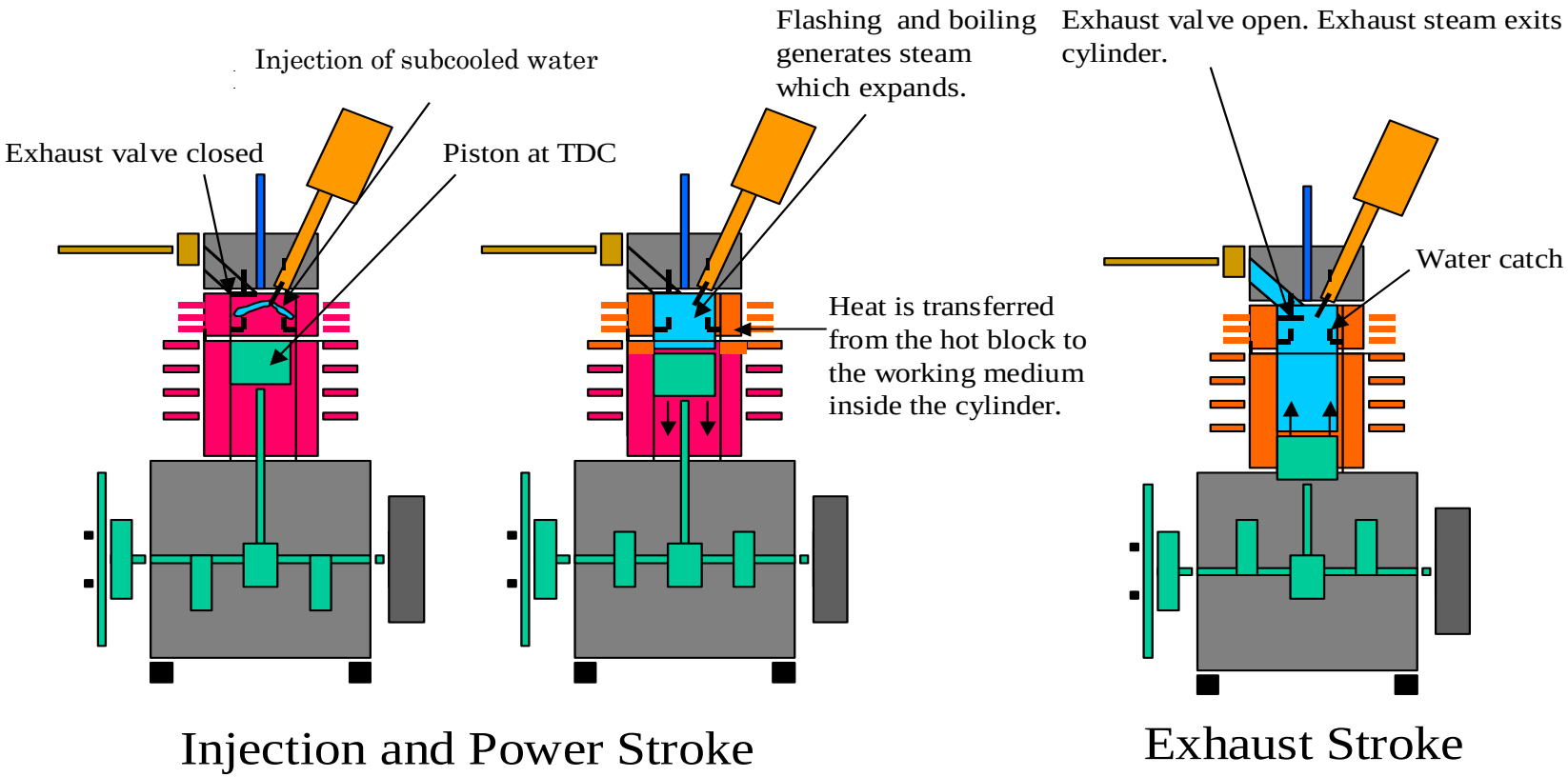

Figure 3. The 2-Cycle SLFB piston engine.

4.1.1.1 Flashing

When a high temperature subcooled liquid is released into an environment with a vapour pressure lower than the pressure required to maintain the liquid in its subcooled state, the liquid phase can hold less heat and discards this excess heat by converting a certain portion of the liquid into the gas phase. This phase change is an almost instantaneous process known as “Flashing”. Flash steam enthalpy is the difference between the enthalpies of the liquid phase of the subcooled water and the liquid phase of the water at the lower vapour pressure to which it falls after flashing has taken place. The vapour content of the wet steam generated by flashing can be described by equation (1).

$$x = \frac{h_{isl} - h_{fvp}}{L_{fvp}} \tag{1}$$

x is the vapour quality of the steam generated. The heat possessed by this vapour is described by equation (2)

$$h_{fs} = \ h_{isl} - h_{fvp} \tag{2}$$

Thus the enthalpy of Flash steam may be calculated according to equation (3). This enthalpy is a function of the pressure within the cylinder as is the specific enthalpy of the liquid at the final vapour pressure, and is thus denoted as $H_{fs}(P_{cyl})$ and $h_{fvp}(P_{cyl})$ respectively.

$$H_{fs}(P_{cyl}) = \left(h_{isl} - \ h_{fvp}(P_{cyl})\right) \cdot \ m_i \tag{3}$$

4.1.1.2 Multiphase convective boiling

The convective boiling of the unflashed liquid that occurs within the heated part of the engine may be described by equations (4) and (5).

$$Q_{cb} = h_{CB}(T_s - T_l) \cdot A_{cl} \tag{4}$$

$$Q_{cb} = B_s \cdot L \tag{5}$$

T_s and T_l are the temperatures of the surface and liquid striking the surface respectively. A_{cl} , L_l and C refer to the area covered by the liquid striking the surface, the latent heat of vaporisation of the liquid striking the surface and the coefficient of heat transfer respectively.

The speed of boiling may be described by equation (6).

$$B_s = \frac{h_{CB}(T_s - T_l) \cdot A_{cl}}{L_l} \tag{6}$$

The boiling speed B_s is the determining factor in the ablity of convective boiling to contribute to power output as engine speeds increase.

The Efficiency E_{sw} describes the efficiency with which the total enthalpy of injected subcooled water is converted to work in the engine. This is described by Equation 7.

$$E_{sw} = \frac{w_i}{H_s} \tag{7}$$

$\mathrm{H_s}$ is the total enthalpy of the subcooled water and $\mathrm{w_i}$ is the indicated work.

4.1.2 Single Event Experiment Results

Single event experiments carried out on the flash engine (The FB1) showed that both Flashing and Convective Boiling contributed to the power output of the engine as was theorised. It was seen from the results that the efficiency E_v of the engine tended to increase with boiling plate temperature increase and injected mass of fluid, up to around 215ºC but then fell drastically at boiling plate temperatures of around 290ºC. This was attributed to the Leidenfrost Effect which causes a buildup of "*residual mass"* of relatively cooler liquid within the expansion engine. This residual mass buildup led to *"dissipation",* which is a loss of flash steam heat to the relatively cooler residual mass. This effect was seen to be more pronounced for larger injection masses.
Furthermore, the engine efficiency was seen to decrease for both small and large injected masses with the onset of the Leidenfrost effect. Furthermore, the engine efficiency was shown to decrease more significantly for larger masses. Figure 4 illustrates this.

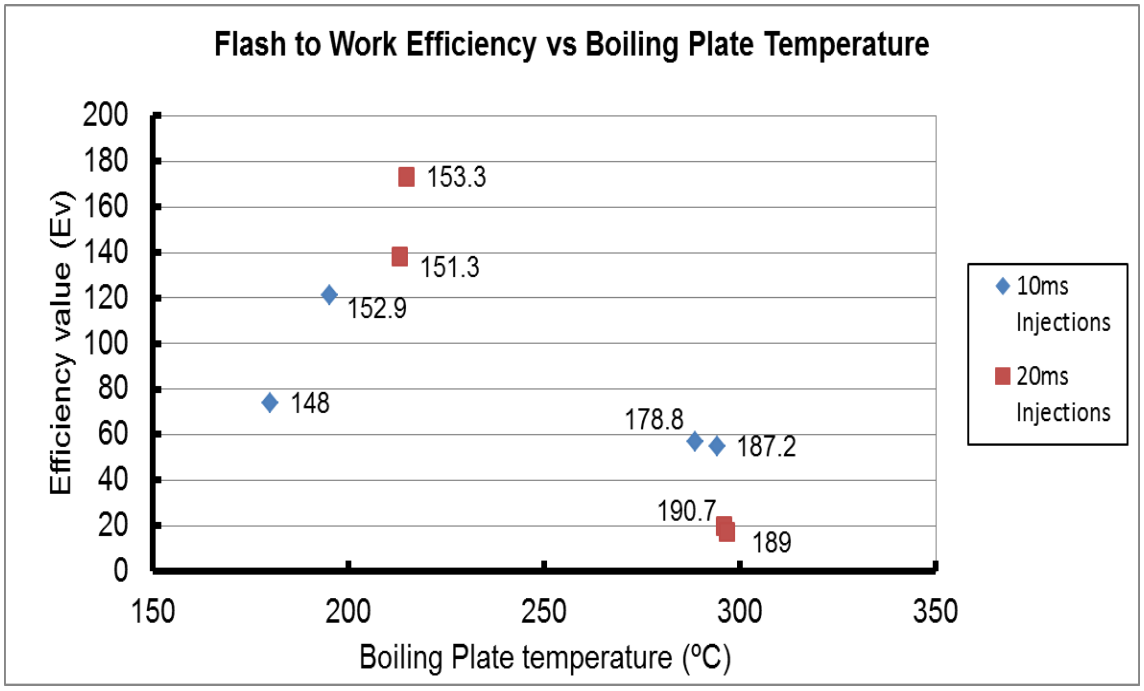

Figure 4. The Efficiency of conversion of Flash energy to work in relation to the boiling plate temperature for single event experiments. Data labels indicate injection temperature.

The efficiency with which the enthalpy of Flash steam was converted to work was calculated according to equation (8). E_v is termed the efficiency value.

$$\mathrm{E_v} = \left[\frac{\mathrm{W_i}}{\mathrm{H_{fs}}}\right] \cdot \ 100 \tag{8}$$

An E_v value of 100 relates to the engine's work output being equal to the enthalpy of flash steam generated by the injected mass of subcooled liquid. Values larger than 100 indicated an input of energy in addition to that of the flash steam energy, in other words the input from Convective Boiling.

4.2 AIM

To investigate the SLFB Cycle in cyclic operation of a reciprocating piston engine.

4.3 PROCEDURE

The engine shown in Figure 5 was used for running the experiments. The FB1 engine is the result of a modification of a commercially available single cylinder Yamaha 7CN engine. The head of this engine was removed and a new block for the new power unit, mounted in its place. A piston extension for this unit was attached onto the piston of the 7CN which in effect gave an engine with the same stroke as the 7CN but with a smaller bore diameter. Heating fins were attached onto the injector holder, boiling plate and cylinder block. The cylinder block and above were encased in an insulated aluminium casing. The experiments were then carried out using the experimental setup seen in Figure 6. The specifications of each engine are listed in Table 1.

Table 1. Specifications of the 7CN and the new FB1 engine.

Specifications	Yamaha 7CN	FB1
Bore	67mm	35mm
Stroke	49mm	49mm
Swept Volume	173cm³	47cm³

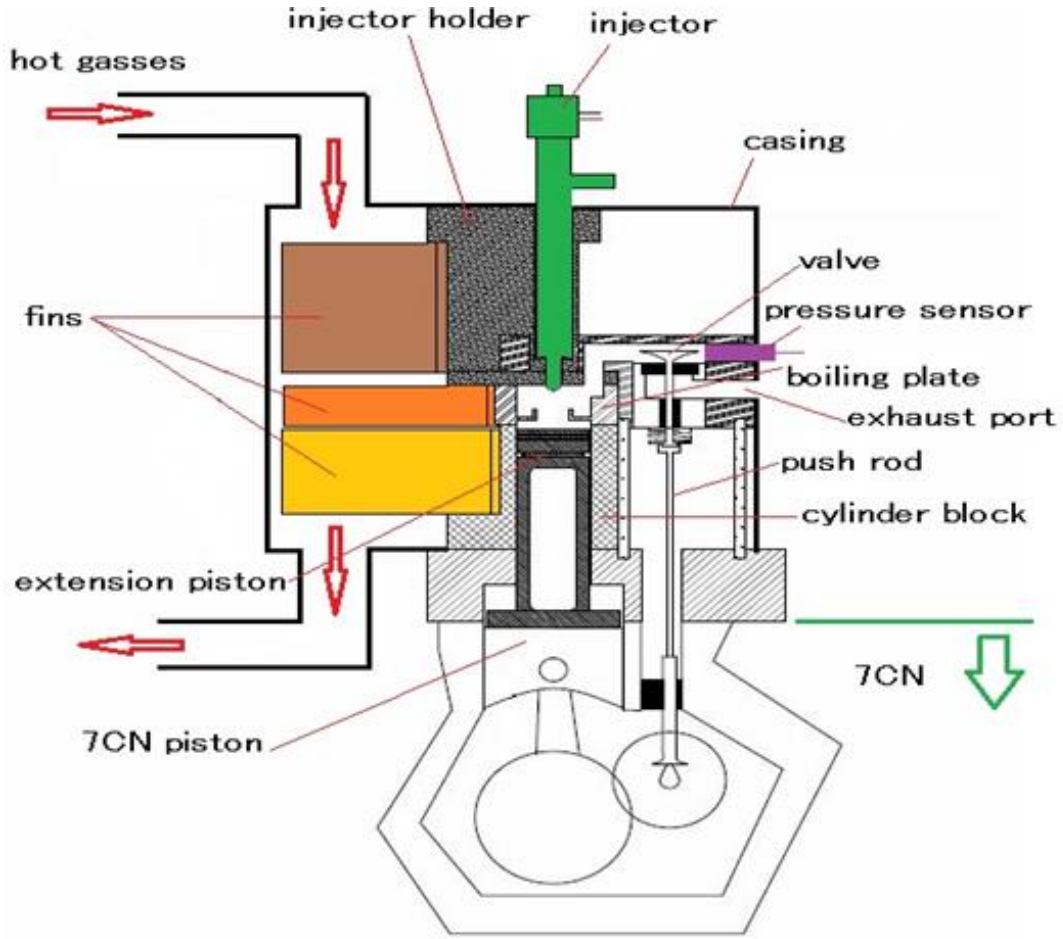

Figure 5.The FB1 with casing, fins, pressure sensor and injector attached.

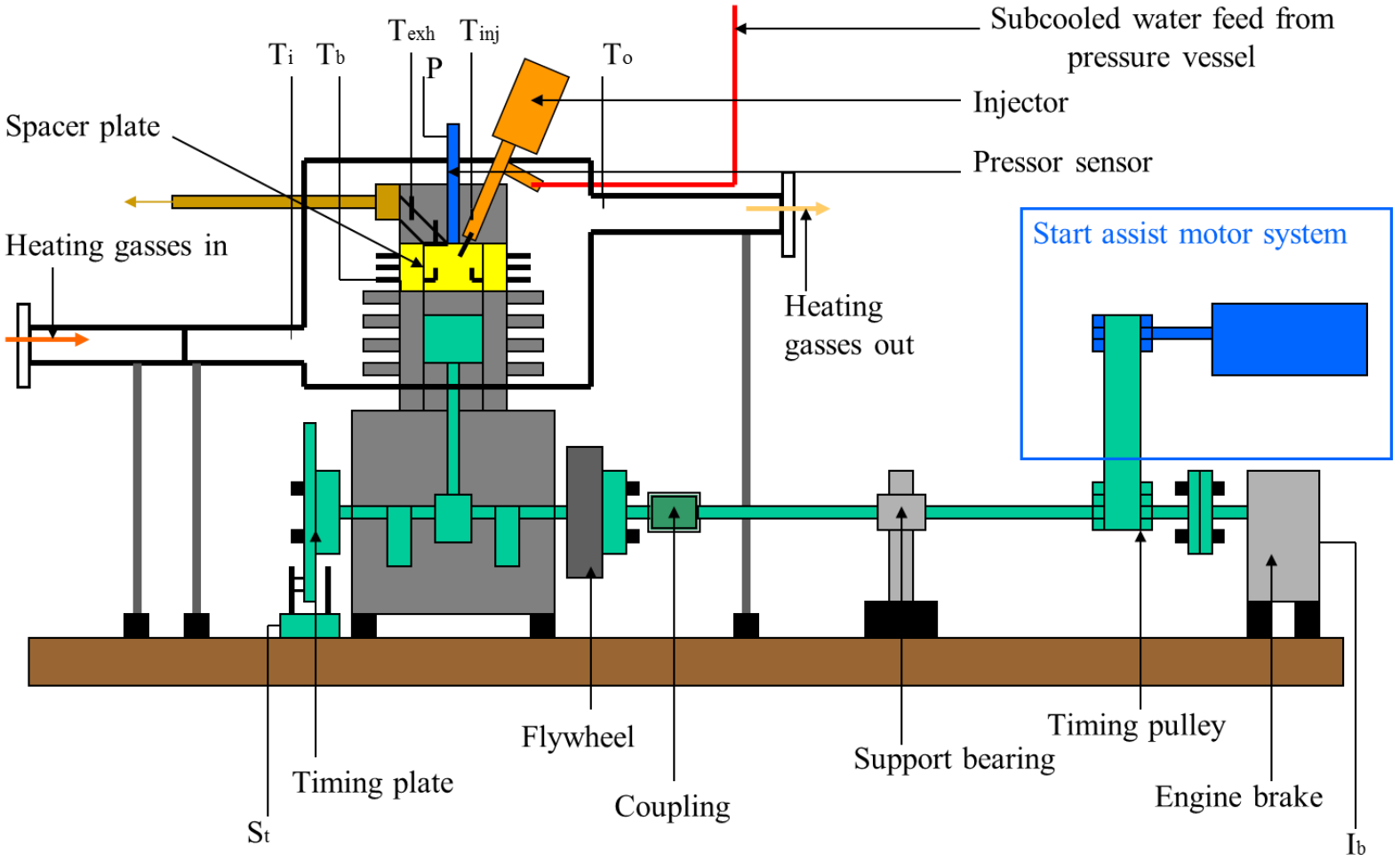

Figure 6. The experimental setup used to investigate the SLFB cycle

The experiment was carried out by injecting measured amounts of high temperature subcooled water, by altering injection duration, directly into the heated boiling plate at 5º ATDC. Injection durations per cycle were set at 20ms and 30ms for single injections and 10i-5-10i-5-10i, 20i-5-5i-5-5i for split injections. The “i” indicates the duration for which the injector solenoid was energized, thus 10i-5-10i-5-10i indicates three 10ms periods of injection with 5ms of non-injection between them. Heating for the power unit was provided by a gas burner and vacuum fan combination and heat input was controlled by fan speed and burner output adjustment. The temperatures of the injector(T_{inj}), the boiling plate (T_{bp}), block (T_{blo}), heating gases at inlet (T_{gi}) and heating gases at outlet (T_{go}) were logged as was the in-cylinder pressure(P). Injections were carried out at subcooled water temperatures (T_{pv}), of 150°C and 180°C. The exact temperature of injected water was taken to be the temperature of the injector (T_{inj}) at the beginning of an injection. Once the engine started turning over, a brake (load) was applied and data acquisition started. The experimental conditions are listed in Table 2.

Table 2. The experimental conditions.

Working fluid	Water
Working fluid temperature($\mathrm{T_{pv}}$)	150±3 ºC 180±3 ºC
Injector temperature($\mathrm{T_{inj}}$)	150±3 ºC (20ms,30ms) 180±10 ºC (20ms,30ms) 200±12 ºC (10-10-10ms,20-5-5ms)
Boiling plate temperature($\mathrm{T_{bp}}$)	195 ºC ~ 285 ºC
Cylinder wall temperature($\mathrm{T_{blo}}$)	149 ºC ~ 247 ºC
Injection period	10ms and 20ms 10-10-10ms 20-5-5ms
Subcooled water pressure (gauge pressure)	8 MPa

The split injection experiments were carried out at approximately equal Injector and Boiling Plate temperatures. The single injection experiments were also carried out at approximately equal injector and Boiling Plate temperatures which were different to the split injections.

The injection masses with relation to injection pattern are shown in Table 3.

Table 3. Injected masses.

Injection Pattern	Injected mass (g)
20ms (150°C)	0.622
20ms (180°C)	0.589
30ms (150°C)	1.210
30ms (180°C)	0.945
10i-5-10i-5-10i (200°C)	0.621
20i-5-5i-5-5i (200°C)	0.777

The efficiency of the engine was determined according to the definition of E_{sw} from Equation 7. The Efficiency E_{sw} describes the efficiency with which the total enthalpy of injected subcooled water is converted to work in the engine.

4.4 RESULTS

The engine was successfully run under load for all the above injection patterns. Figures 7a and 7b show samples of in-cylinder pressure data for single 30ms injections and Figures 8a and 8b show single 20ms injections. Both are for multi-cycle engine operation.

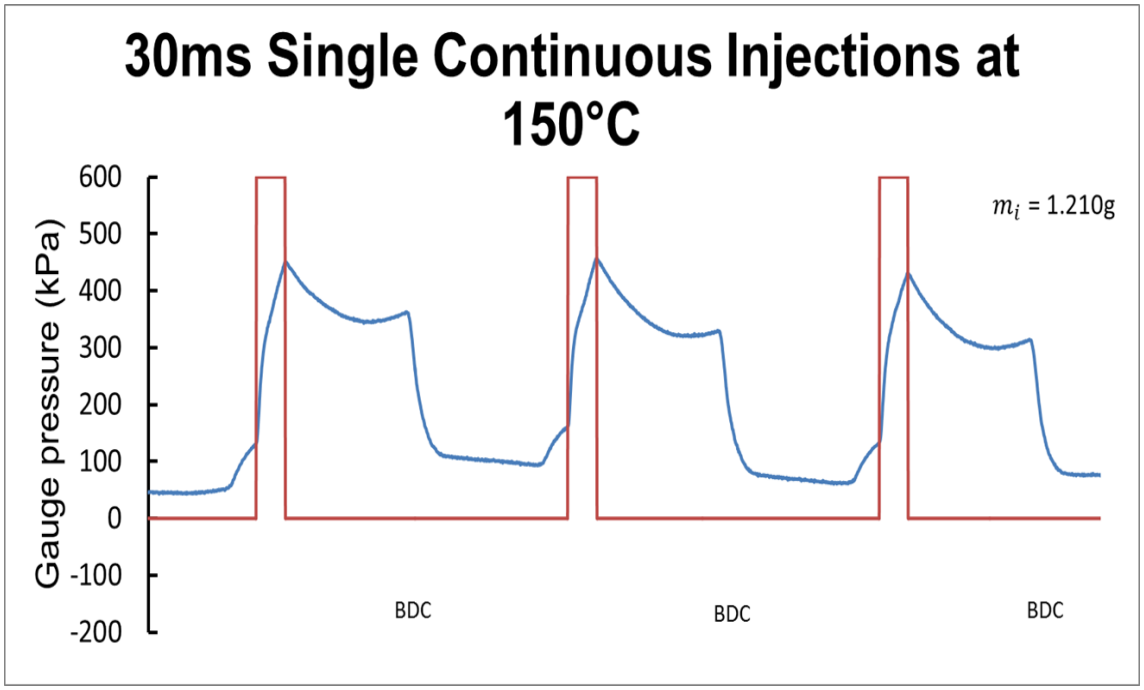

Figure 7a. Pressure information with relation to piston position for the engine cycles of single 30ms injections of subcooled water at 150ºC (T_{inj}).

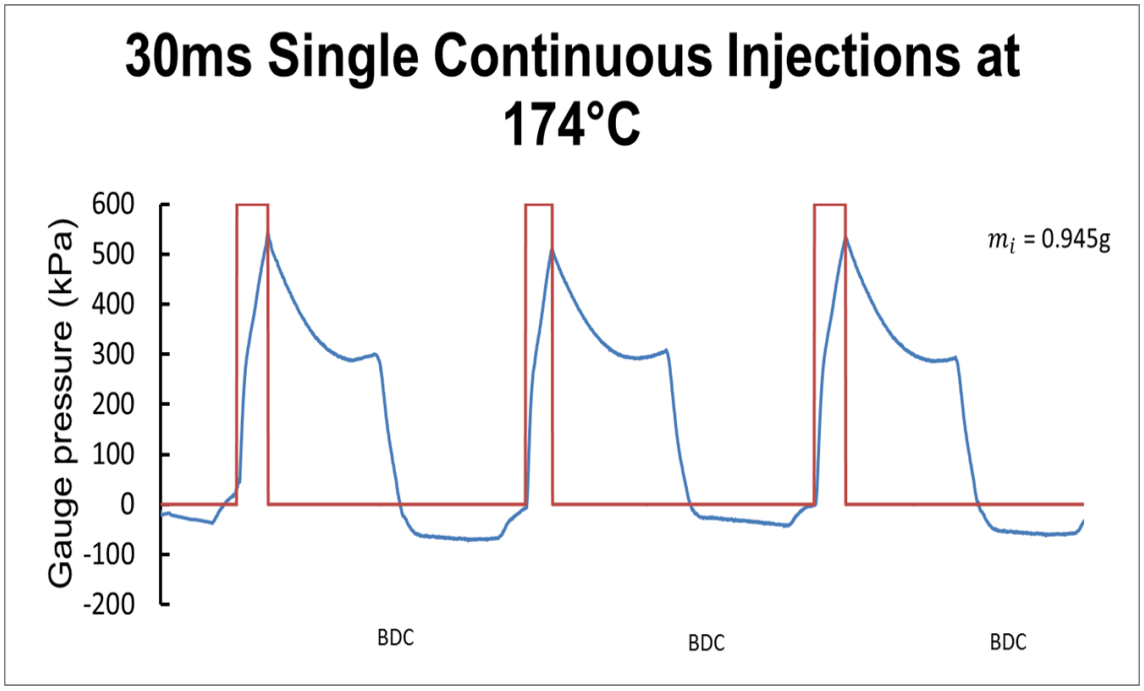

Figure 7b. Pressure information with relation to piston position for the engine cycle of single 30ms injections of subcooled water at 174ºC (T_{inj}).

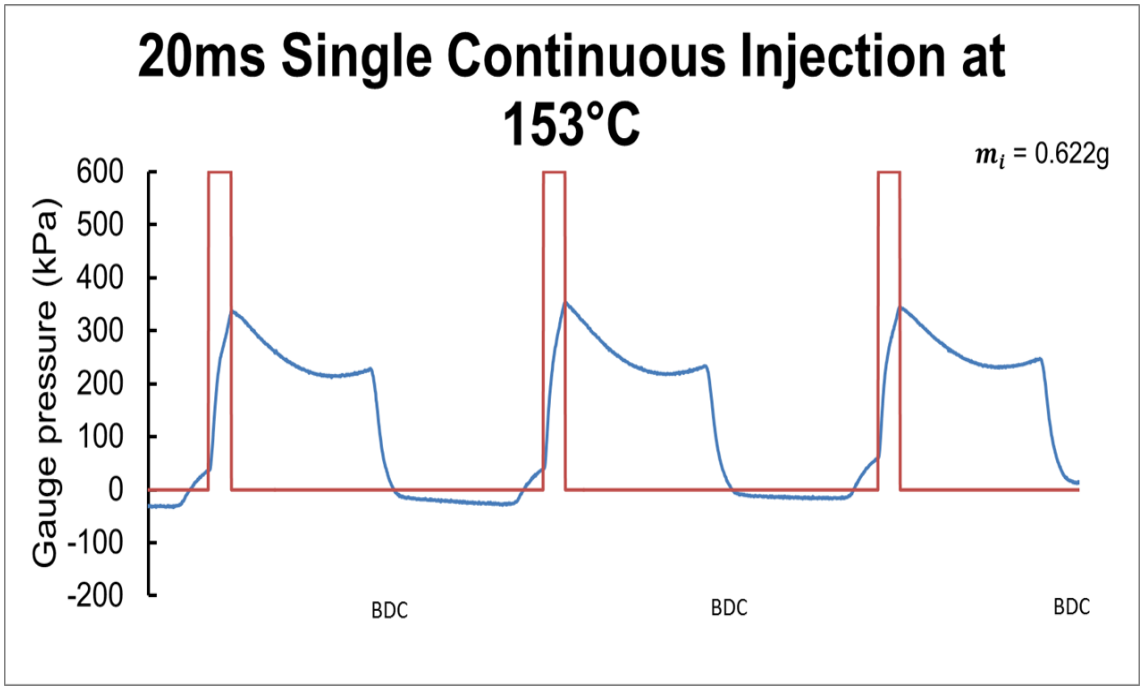

Figure 8a. Pressure information with relation to piston position for the engine cycle of single 20ms injections of subcooled water at 153ºC (T_{inj}).

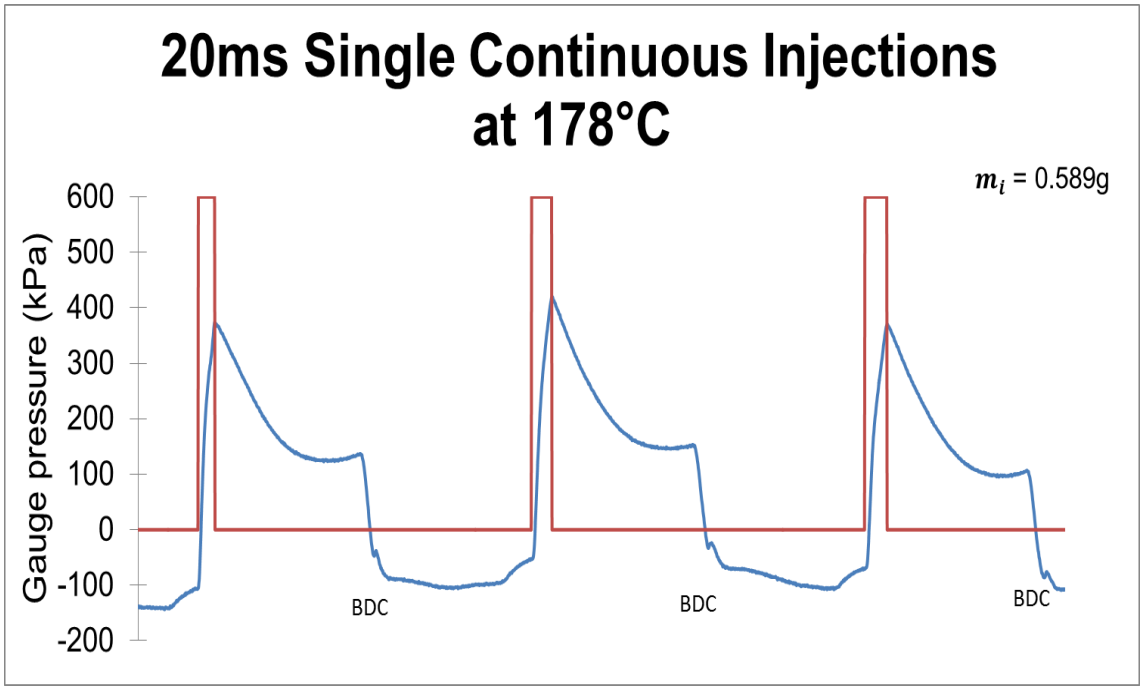

Figure 8b. Pressure information with relation to piston position for the engine cycle of single 20ms injections of subcooled water at 178ºC($\boldsymbol{T_{inj}}$).

With single injections, it was seen that injections with the higher injection masses and temperatures of subcooled water generated higher in-cylinder pressures and as a result higher power outputs. At low temperatures of subcooled water, smaller masses of water were able to achieve higher levels of efficiency ($\mathbf{E_{sw}}$) on average in converting the total enthalpy of injected subcooled water to work than larger injection masses with the same temperature. However, as the temperature of subcooled water increases, smaller masses result in reduced efficiency while larger masses lead to an increase in efficiency. Figure 9 illustrates this.

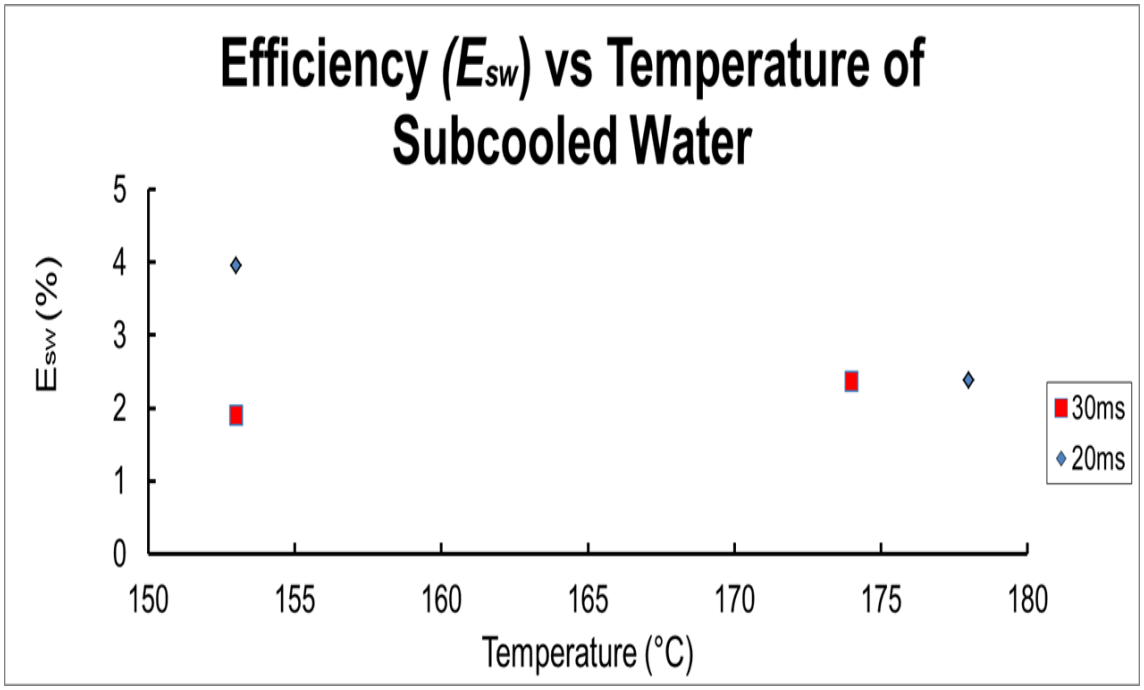

Figure 9. The efficiency of the conversion of the enthalpy of injected water to work.

Figures 10a and 10b show the in-cylinder pressure data for split injections of 10i-5-10i-5-10i and 20i-5-5i-5-5i respectively.

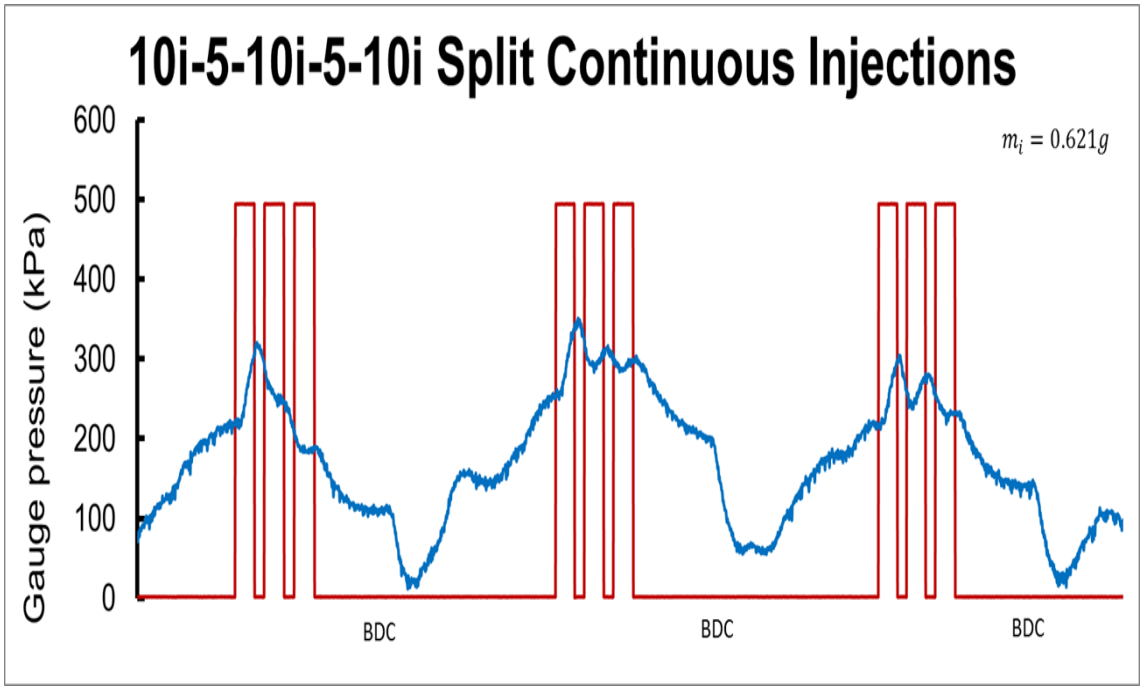

Figure 10a. Pressure information with relation to piston position for the engine cycle of 10i-5-10i-5-10i injections of subcooled water at an average temperature of 210ºC($\boldsymbol{T_{inj}}$).

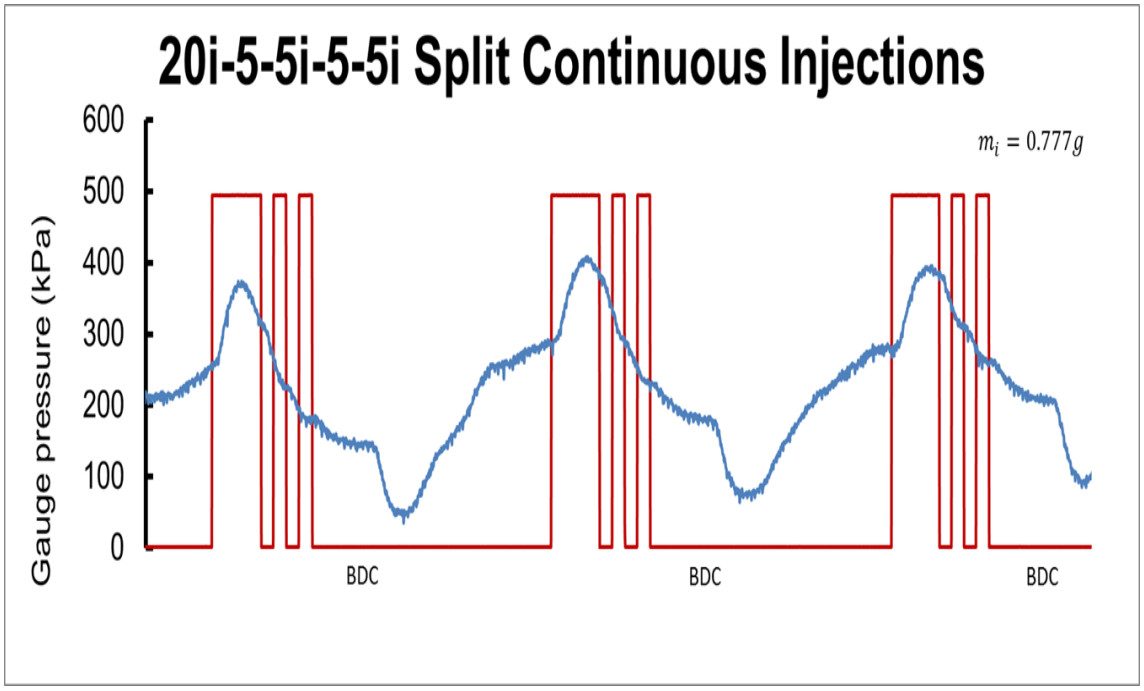

Figure 10b. Pressure information with relation to piston position for the engine cycle of 20i-5-5i-5-5i injections of subcooled water at an average temperature of 194ºC(T_{inj}).

With split injections, the 20i-5-5i-5-5i was shown to produce more power per cycle on average than the 10i-5-10i-5-10i as was expected with its larger injection mass. In terms of efficiency (E_{sw}) , the 10i-5-10i-5-10i was shown to achieve higher efficiencies. In fact the 10i-5-10i-5-10i injection mode was shown to be the most efficient of all the injection patterns. It is worthy of note that the horizontal axis of Figures 10a and 10b do not start at the same point within the cycle. Figure 11 illustrates the relationship between the various injection patterns and the average efficiency E_{sw} measured over 30 cycles.

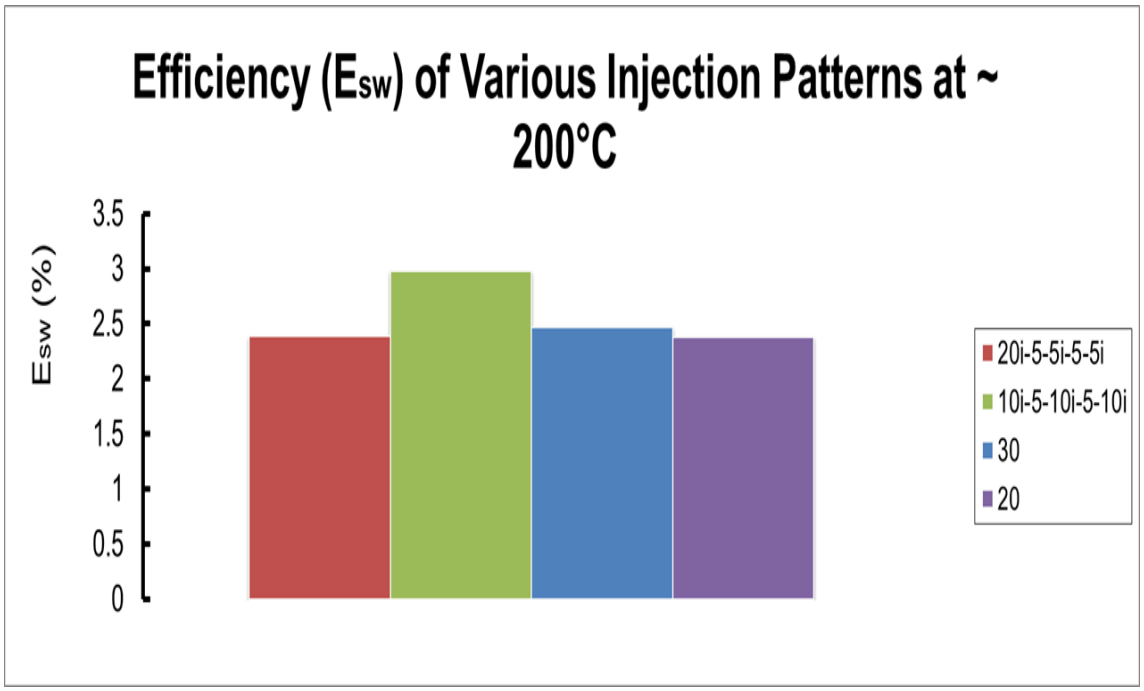

Figure 11.The efficiency of the conversion of the enthalpy of injected water to work for various injection patterns at injection temperatures of 200±10° C.

The 10ms split injection shows the highest average efficiency (E_{sw}) followed by the larger single injected mass of 30ms. The single 20ms injection shows no significant difference to the 20i-5-5i-5-5i split injection.

The changes in temperature of the various components are shown in Figure 12a, 12b and 12c. In Each chart the x-axis begins at the start of injection and the lowest point of the Boiling Plate temperature data indicate the end of injections and the end of the cyclic running of the engine.

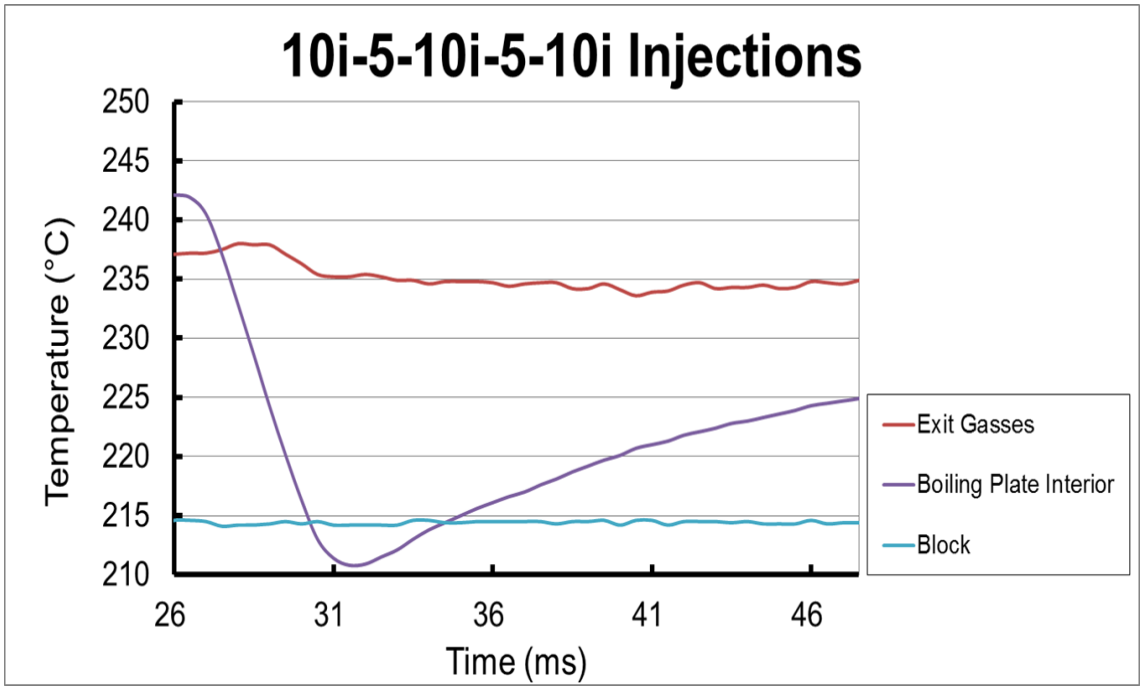

Figure 12a.The change in temperature of the Exit heating gases, the boiling plate and the block for the 10i-5-10i-5-10i injection pattern. Injections begin at the 25ms point.

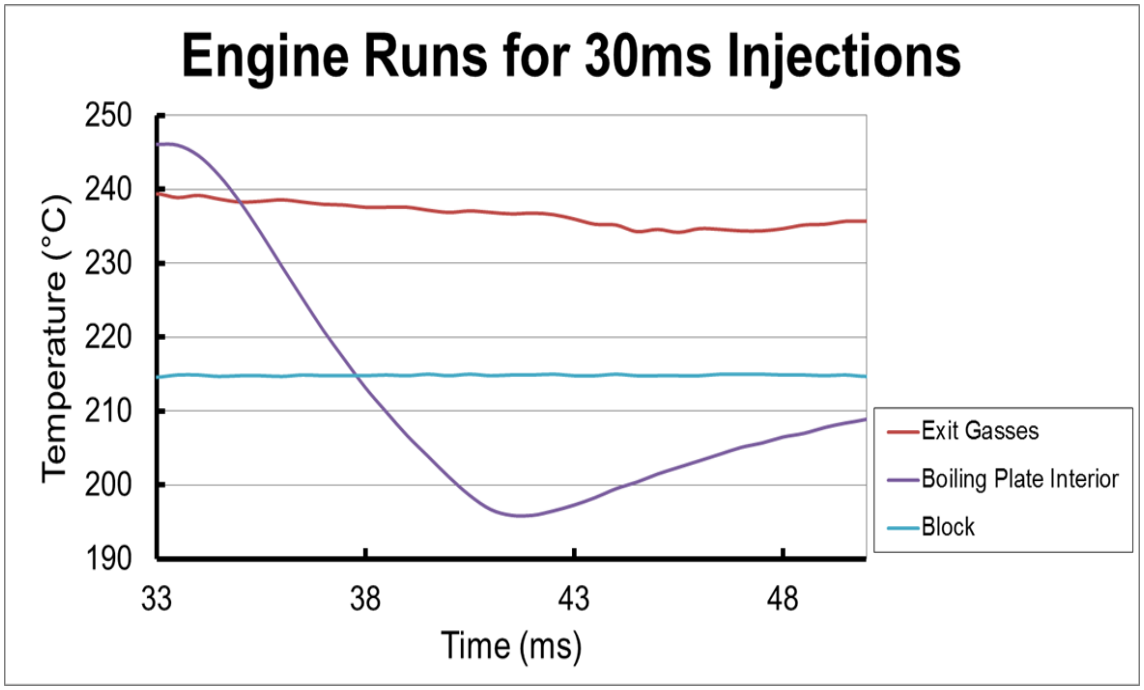

Figure 12b.The change in temperature of the Exit heating gases, the boiling plate and the block for the 30ms injection pattern. Injections begin at the 33ms point.

It can be seen from Figures 12b and 12a that more heat is transferred away from the Boiling Plate for the 30ms single injection than the 10ms split injection.

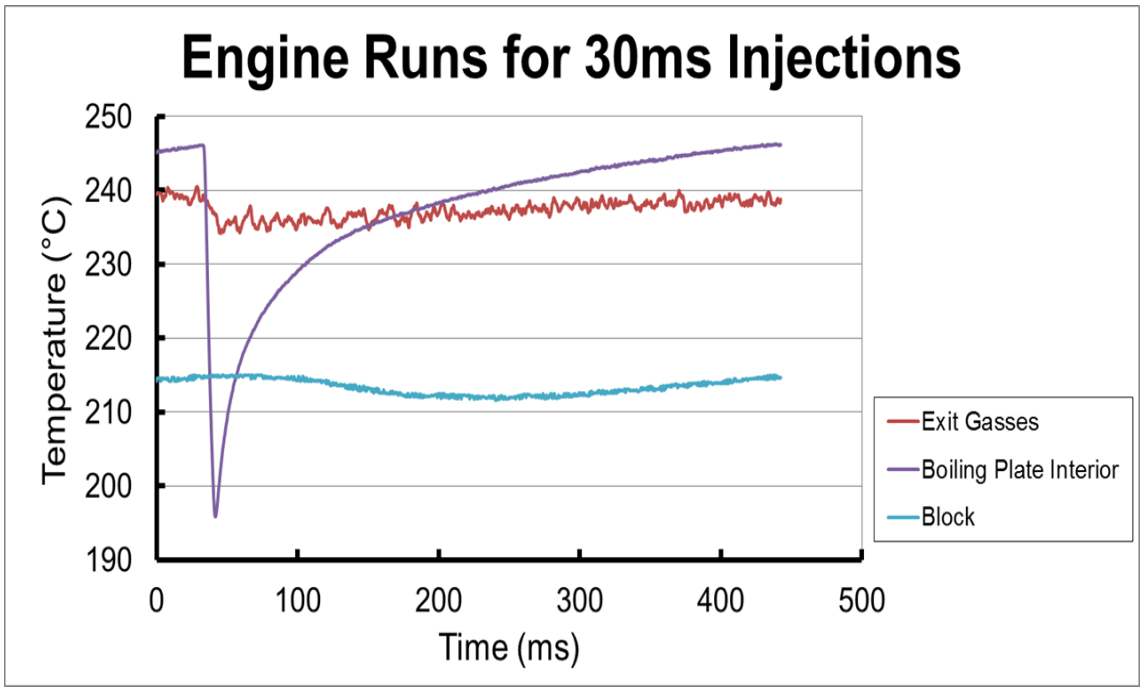

Figure 12c.The change in temperature of the Exit heating gases, the boiling plate and the block for the 30ms injection pattern measured over a longer duration of time.

It is clear from Figure 12c that heat transfer to the working medium is occurring from not only the Boiling Plate but also from the Block.

4.5 DISCUSSION

4.5.1 Results Analysed

Previous single event experiments carried out showed that the conversion of Flash Steam enthalpy (H_{fs}) to work increased in efficiency with increasing temperatures of the subcooled liquid for larger injection masses. Although both large and small injection masses see a significant drop in E_v efficiency beyond the Leidenfrost Point (LFP), smaller masses show a continued fall in E_v with increasing temperatures of subcooled fluid. Larger masses on the other hand seem to show a relative increase, although this cannot be said for certain as the temperature difference between the two injections is only 1°C. Figure 13 illustrates this.

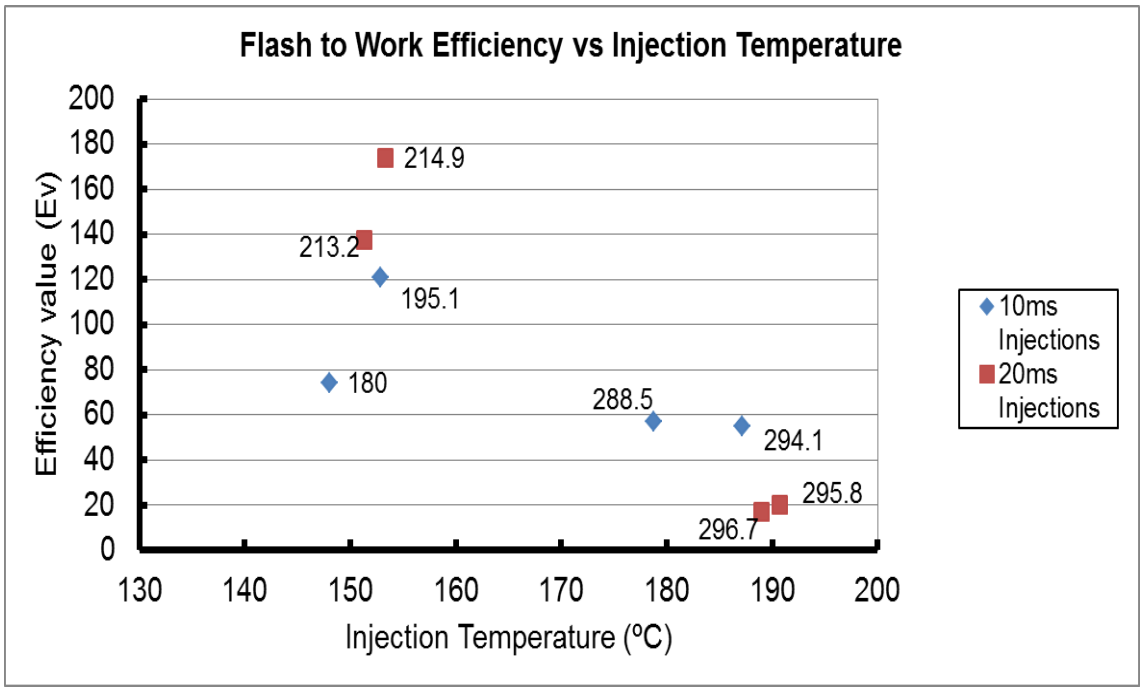

Figure 13. The Efficiency of conversion of Flash energy to work in relation to the Injection temperature for single event experiments. Data labels indicate boiling plate temperatures.

However, when the E_{sw} efficiency analysis is done on the same single event experiment data, smaller injection masses show a higher E_{sw} efficiency than larger masses at similar temperatures as is seen Figure 14.

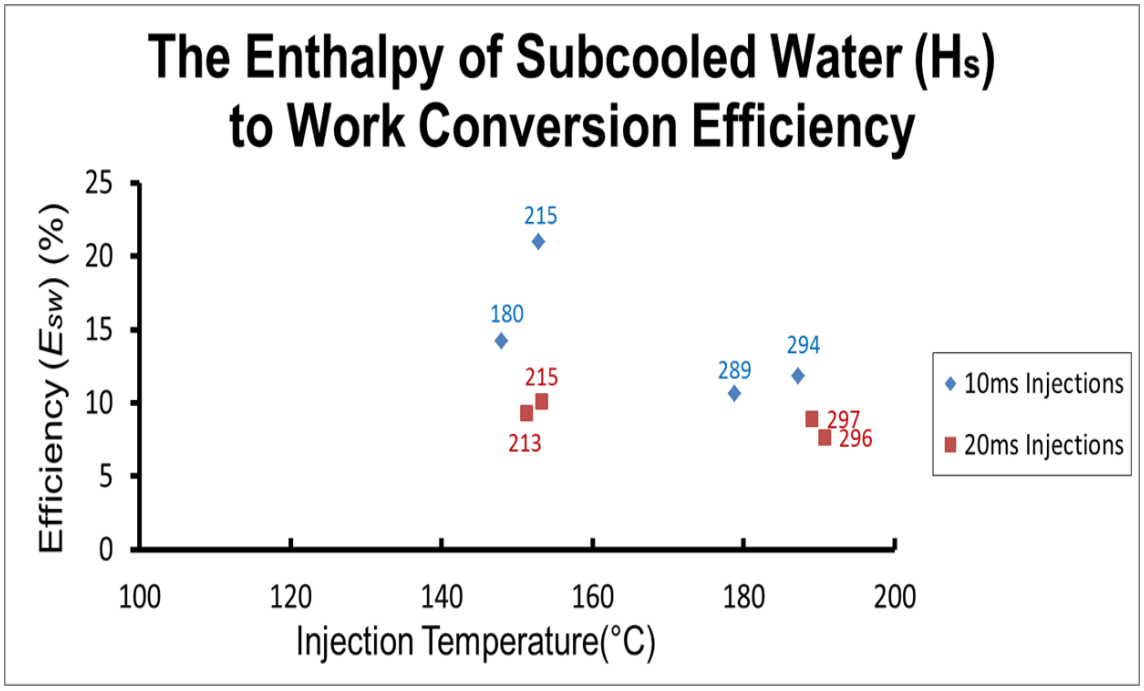

Figure 14. The Efficiency of conversion of the total enthalpy of subcooled water to work in relation to the Injection temperature for single event experiments. Data labels indicate the boiling plate temperature.

As can be seen in Figure 14, the E_{sw} efficiency falls significantly beyond the LFP for smaller injection masses but shows less of a fall for larger injection masses as their temperatures increase. When this is compared to the Figure 9, the commonality observed between the E_{sw} efficiency analysis for single events and multiple cyclic events is that smaller injection masses with low temperatures result in higher E_{sw} efficiencies. This is opposite to the trend seen in Figure 4 of higher E_v efficiencies for larger injection masses below the LFP. This is most probably due to the fact that at low subcooled water temperatures, the work generated by the engine is dominated by convective boiling. Larger injection masses result in higher pressure spikes within the cylinder during injection preventing the latter part of the injected liquid from flashing due to the higher vapour pressures they observe [1]. This results in smaller H_{fs} values.

Furthermore, as the steam generated from convective boiling is dependent on the mass of liquid water available, larger injection masses lead to larger boil-offs giving larger values of W_i and higher E_v efficiencies. E_{sw} efficiencies on the other hand are higher at low temperatures of subcooled water for smaller masses because the lower temperatures of the subcooled water and smaller masses result in smaller H_s values which are independent of all in-cylinder factors. The w_i values are once again dominated by the Convective Boiling output. Thus more efficient convective boiling should result in more Q_{cb}. As Q_{cb} is dependent of the temperature difference $(T_s - T_l)$, smaller injection masses with lower temperatures will result in smaller pressure spikes in-cylinder which in turn will result in lower levels of T_l (unflashed water). Thus the result is more efficient Convective Boiling, larger values of w_i and higher values of E_{sw}. The fall in E_{sw} efficiencies with increasing enthalpy H_s of smaller injection masses is due to the effect of reduced boiling efficiency form a smaller $(T_s - T_l)$ difference due to higher in-cylinder pressures and relatively higher H_s values.

The splitting of the injections are an effective method of increasing efficiency particularly if each injection has enough Flash heat release to maintain positive pressure on the piston as it moves down. This is clearly seen in Figure 11a. However, if the post-injections lack heat release to maintain positive pressure on the piston, this heat release ends up being lost in the exhaust stroke as can be ascertained by comparing the exhaust pressure of Figures 10a and 10b. The 20i-5-5i-5-5i split injections have higher exhaust pressures than the 10i-5-10i-5-10i, indicating an exhausting of useful pressure. It is also clear from this series of experiments that the “Cyclic-build up Residual Mass” of unflashed liquid that doesn’t boil off during each cycle is a significant mode of efficiency loss for a piston engine operating under the SLFB Cycle. The residual mass is the liquid that remains in the boiling plate when the next cycle’s injection begins. As the residual liquid is at a lower temperature than the Flash Steam that results from the injections, heat transfer occurs from the flash steam to the cooler residual liquid reducing the steams potential to do work. This was hypothesized in an earlier paper by the authors [1] as its effects were seen even in single event experiments due the onset of the Leidenfrost effect. In multiple cycle operation this effect is clearly observable from the results seen in Figure 11. The efficiencies across the board are significantly lower than those observed with single event injection experiments below the LFP. It can be seen from Figure

12c that heat transfer also occurs from the engine block to the working medium as it expands within the cylinder. This was not observed in Figures 12a and 12b due to the x-axis durations being shorter. Any temperature drop of the block is delayed due to its large heat capacity and can only be observed over longer durations. This proves that heating the engine block helps contribute to overall heat input into the system. Increasing stroke length should in turn enable this heat input to contribute to work output.

4.5.2 The Subcooled Water Generator

An important component of the SLFB system for automotive applications is the subcooled water generator. A heat exchanger capable of being installed in a car has been tested for its potential for generating the subcooled liquid for the SLFB Engine. In its current state, the heat exchanger only generates subcooled water but one which is capable of generating heated oil for heating the Boiling Plate and the Block of the SLFB engine itself, is planned for the future. A sample of the performance data of the heat exchanger is listed in Table 4. This sample is most representative of a modern gasoline powered sedan's engine operating conditions at highway cruising speeds of 80km/hr (in terms of exhaust temperatures). Figure 15 shows a schematic of the heat exchanger, and Figure 16 shows the experimental setup used for testing the heat exchanger.

The heat exchanger was fed exhaust gases from a 2000cc Mazda LF-VE, 4 cylinder gasoline engine mounted to an engine bench with an engine dynamometer. Experiments were carried out with the engine operating at various load conditions to simulate highway cruising conditions (1300RPM). The throttle position was set at ~10% to 40% of wide open throttle (WOT) and engine speeds was maintained at the desired speed by the dynamometer.

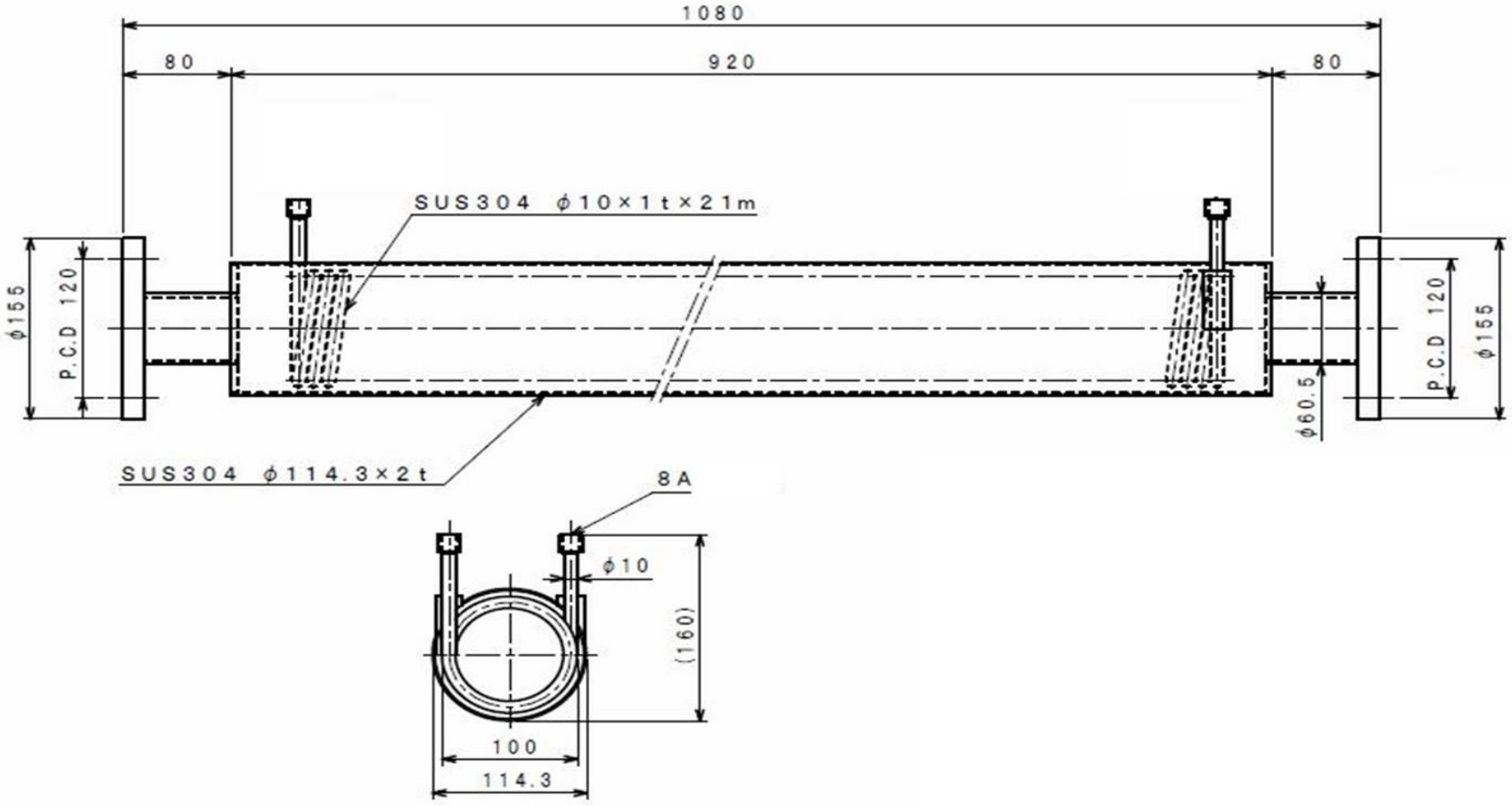

Figure 15. The Subcooled water generator

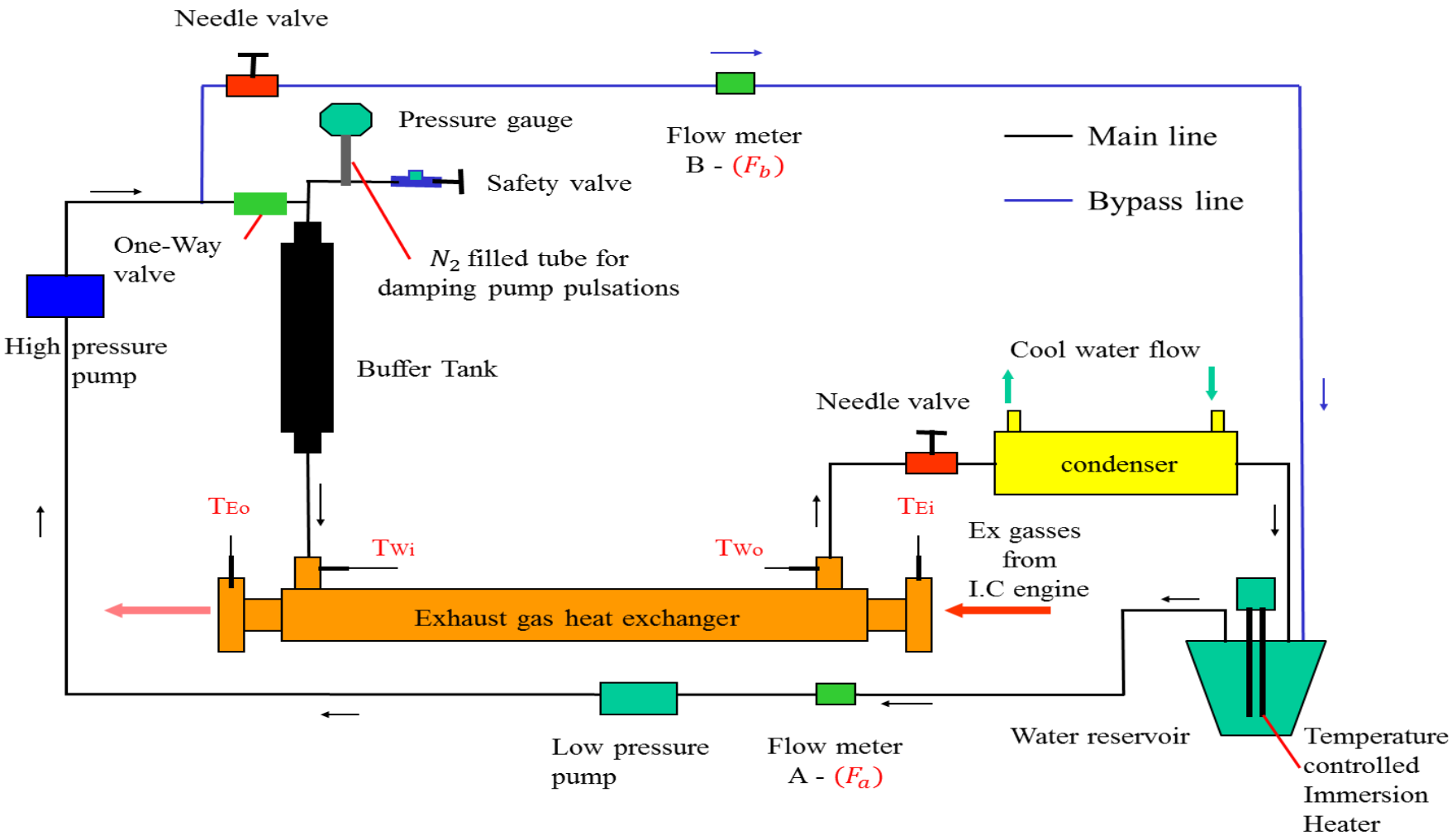

Figure 16. The experimental setup for testing the performance of the heat exchanger.

Table 4. Exhaust Heat Exchanger Performance Data at partial load.

IC Engine Operating Speed	1300RPM	
Exhaust in temp	°C	492
Exhaust out temp	°C	225
Water in Temp	°C	77
Water out Temp	°C	247
Mass flow rate of Exhaust gasses	kg/s	0.0102
Mass flow rate of water	kg/s	0.0035
Power Output	kW	2.502
Effectiveness (Average)		0.71
Pump Power consumption	kW	0.5
Net Power Output	kW	2.002

When the engine was operated at varied loads, the exhaust gas temperatures at the heat exchanger inlet and exit were seen to vary, dropping with reduced load and increasing with increasing load. The effectiveness of the heat exchanger was seen to reduce with increased engine speeds and exhaust temperatures. This relationship between exhaust temperatures and "Effectiveness" is shown in Figure 17. For the purpose of clarity, the effectiveness of a heat exchanger may be described by equation 7.

$$Effectiveness = \frac{actual\ \ heat\ \ transfer}{maximum\ \ possible\ \ heat\ \ transfer} \quad (7)$$

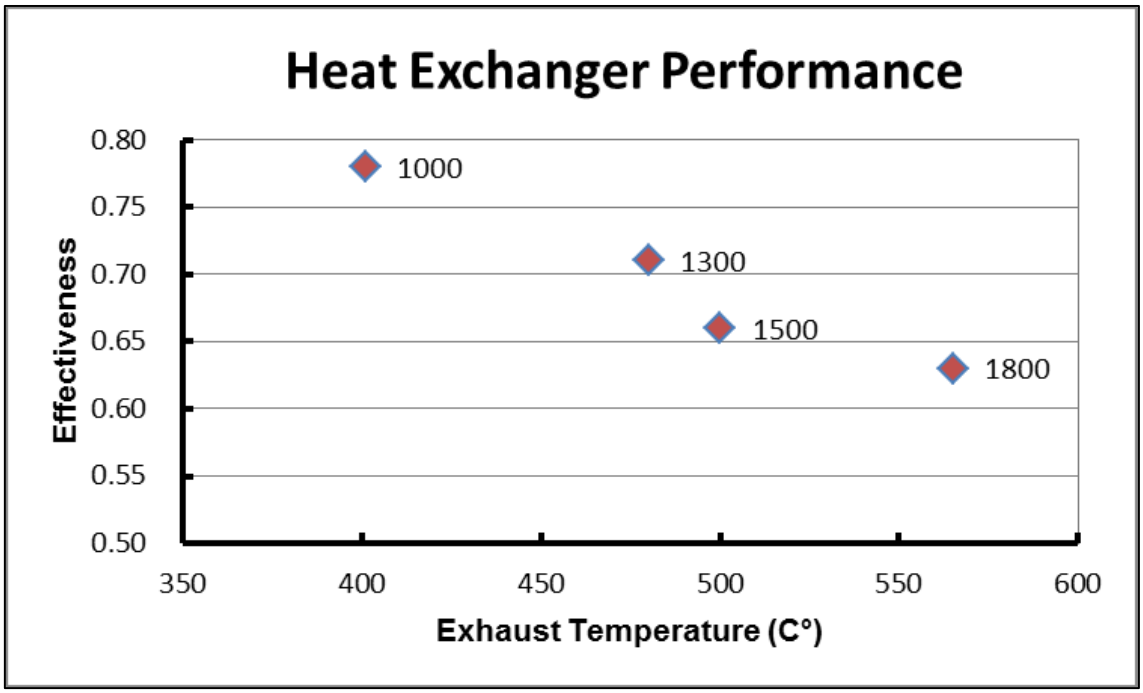

Figure 17. The performance of the exhaust heat exchanger with respect to exhaust temperature. The data labels indicate engine RPM.

The reduction in heat exchanger effectiveness at elevated engine speeds and exhaust temperatures is hypothesized as being due to the increase in exhaust gas velocity as it passes through the heat exchanger. This increase in velocity leads to a reduction in the effective time within which heat exchange can happen.

The current heat exchanger design places no more restriction on the exhaust flow than the standard exhaust pipes of the exhaust system the road going version of this engine would experience. This is due to the “straight-pipe” like design of the heat exchange surface, and the internal diameter of that virtual pipe being larger than the internal diameter of the standard exhaust pipes. Thus, in order to maintain the low exhaust restriction of the current design while improving its effectiveness, lengthening of the heat exchanger would be required. It is also worthy of note that the heat exchanger was attached over 2m downstream of the engine’s exhaust manifold, when performing these experiments.

At ~250°C (The output temperature of subcooled water from the heat exchanger), the temperature of the subcooled liquid is high and an SLFB engine

operating at appropriate engine speeds to maximize convective Boiling and Block Heat Transfer should deliver good efficiency. The current FB1 engine which has not been designed with efficiency in mind but solely for the investigation of the SLFB phenomenon has shown itself to be able to operate at E_{sw} efficiencies of up to 21% in single event experiments when the boiling plate temperature is below the Leidenfrost point. The low efficiencies observed in cyclic operation have been due to the significant influence of residual mass buildup in the Boiling Plate and the Dissipation that results. By effective removal of the residual mass during the exhaust stroke, Dissipation can be eliminated and appropriately controlling engine speed should work to improve the overall efficiency of the engine. Further improvements such as increasing the stroke length and adding boiling enhancements to the interior of the boiling plate should improve efficiency even further. It is also worthy of note that in order to achieve high power outputs, the injection system will also have to be improved upon to deliver larger injection masses in shorter injection durations. As has been proven in the authors' earlier work [1], the SLFB Cycle if optimized can be superior to both the TLC and the ORC as a waste heat recovery option.

4.6 CONCLUSIONS

At low temperatures of subcooled water of ~150°C, single injections of smaller masses resulting from 20ms injection durations are able to achieve higher levels of efficiency in converting the total enthalpy of injected subcooled water to work, than single larger injection masses at the same temperature which result from 30ms injection durations. However at higher temperatures, subcooled water of (~180°C) smaller injection masses lead to a reduction in efficiency, whereas larger masses increase engine thermal efficiency. In cyclic operation, the efficiency of converting the enthalpy of subcooled water to work falls off significantly due to the effects of "Residual Mass and Dissipation" effects hypothesised in an earlier study [1]. Furthermore, multiple equal small injections of subcooled water at high temperatures are able to achieve higher levels of efficiency than single large injections at the same subcooled temperature. The effective removal of the Cyclic-Build up Residual Liquid mass during the exhaust stroke is vital to improving the overall efficiency of the engine.

REFERENCES

1. D. Hewavitarane, S. Yoshiyama, H. Wadahama, X. Li, “The Development of a Superheated Liquid Flash, Boiling (S.L.F.B) Engine for Waste Heat Recovery from Reciprocating Internal Combustion Engines”, SAE Int. J. Engines 7(4):2014, doi:10.4271/2014-01-2592
2. Michael Steffen, Michael Löffler, Karlheinz Schaber, “Efficiency of a new Triangle Cycle with flash evaporation in a piston engine”, Energy, Volume 57, 1 August 2013, Pages 295-307, ISSN 0360-5442, doi:10.1016/j.energy.2012.11.054.
3. Ngoc Anh Lai, Johann Fischer, “Efficiencies of power flash cycles”, Energy, Volume 44, Issue 1, August 2012, Pages 1017-1027, ISSN 0360-5442, doi:10.1016/j.energy.2012.04.046.
4. Johann Fischer, “Comparison of trilateral cycles and organic Rankine cycles”, Energy, Volume 36, Issue 10, October 2011, Pages 6208-6219, ISSN 0360-5442, doi:10.1016/j.energy.2011.07.041.
5. Henrik Öhman, Per Lundqvist, “Theory and method for analysis of low temperature driven power cycles”, Applied Thermal Engineering, Volume 37, May 2012, Pages 44-50, ISSN 1359-4311, doi:10.1016/j.applthermaleng.2011.12.046.
6. Sipeng Zhu, Kangyao Deng, Shuan Qu, “Energy and exergy analyses of a bottoming Rankine cycle for engine exhaust heat recovery”, Energy, Volume 58, 1 September 2013, Pages 448-457, ISSN 0360-5442, doi:10.1016/j.energy.2013.06.031.
7. Alberto Boretti, “Recovery of exhaust and coolant heat with R245fa organic Rankine cycles in a hybrid passenger car with a naturally aspirated gasoline engine”, Applied Thermal Engineering, Volume 36, April 2012, Pages 73-77, ISSN 1359-4311, doi:10.1016/j.applthermaleng.2011.11.060

DEFINITIONS, ACRONYMS, ABBREVIATIONS

H_s	Enthalpy of subcooled water
h_{CB}	Constant of heat transfer
h_{fvp}	Specific enthalpy of liquid at final vapour pressure
h_{isl}	Initial specific enthalpy of subcooled liquid
A_{cl}	Area covered by liquid
B_s	Convective boiling speed
E_{sw}	Efficiency of converting the enthalpy of subcooled water to Indicated Work
H_{fs}	Enthalpy of flash steam
L_{fvp}	Latent heat of vaporization at final vapour pressure
P_{cyl}	In-cylinder pressure
P_{ei}	In-cylinder pressure at end of injection
P_{max}	Maximum pressure of working fluid
P_{min}	Minimum pressure of working fluid
P_{peak}	Peak in-cylinder pressure
Q_{cb}	Heat from convective boiling
T_{blo}	Temperature of block
T_{bp}	Temperature of boiling plate
T_{gi}	Temperature of heating gasses at inlet
T_{go}	Temperature of heating gasses at outlet
T_{inj}	Temperature of injector
T_l	Temperature of liquid striking surface
T_{max}	Maximum temperature of working fluid
T_{min}	Minimum temperature of working fluid
T_{pv}	Temperature of pressure vessel
T_s	Temperature of surface
W_i	Indicated work
m_i	Injection mass
p_i	Indicated power
t_{cyc}	Time taken for one cycle of rotation
v_f	Final volume
v_i	Initial volume
LFP	Leidenfrost Point
$ATDC$	After top dead center
$AWHR$	Automotive waste heat recovery
$BBDC$	Before bottom dead center
L	Latent heat of vaporization of liquid striking the surface
TDC	Top dead center
TLC	Trilateral cycle
WHR	Waste heat recycling
x	Quality of vapour

Chapter 5: Optimisation of the SLFB Cycle Powered System for Automotive Waste Heat Recovery

5.1 INTRODUCTION

The SLFB Cycle is hitherto unprecedented and the mechanical systems needed for its application in a reciprocating piston engine have required the designing and manufacturing of unique components. In this process, many new insights have been made and these discoveries have required the redesigning of key components and the re-thinking of system outlines for improving the efficiency of the WHR system. Their application to the experimental engine will lead to the improvement of its experimental capabilities. This chapter deals with these design improvements and some alternative applications of the SLFB cycle for automotive WHR.

5.2 THE NEW SYSTEM OUTLINE

The WHR system for automotive applications is illustrated by Figure 1. This set up employs a single heat exchanger to generate both the subcooled working fluid and the heating fluid for the convective boiling process and engine block heating. It also includes a storage system for the heating oil and the subcooled working fluid to allow a certain degree of energy storage and on-demand delivery of power from the system at a later stage.

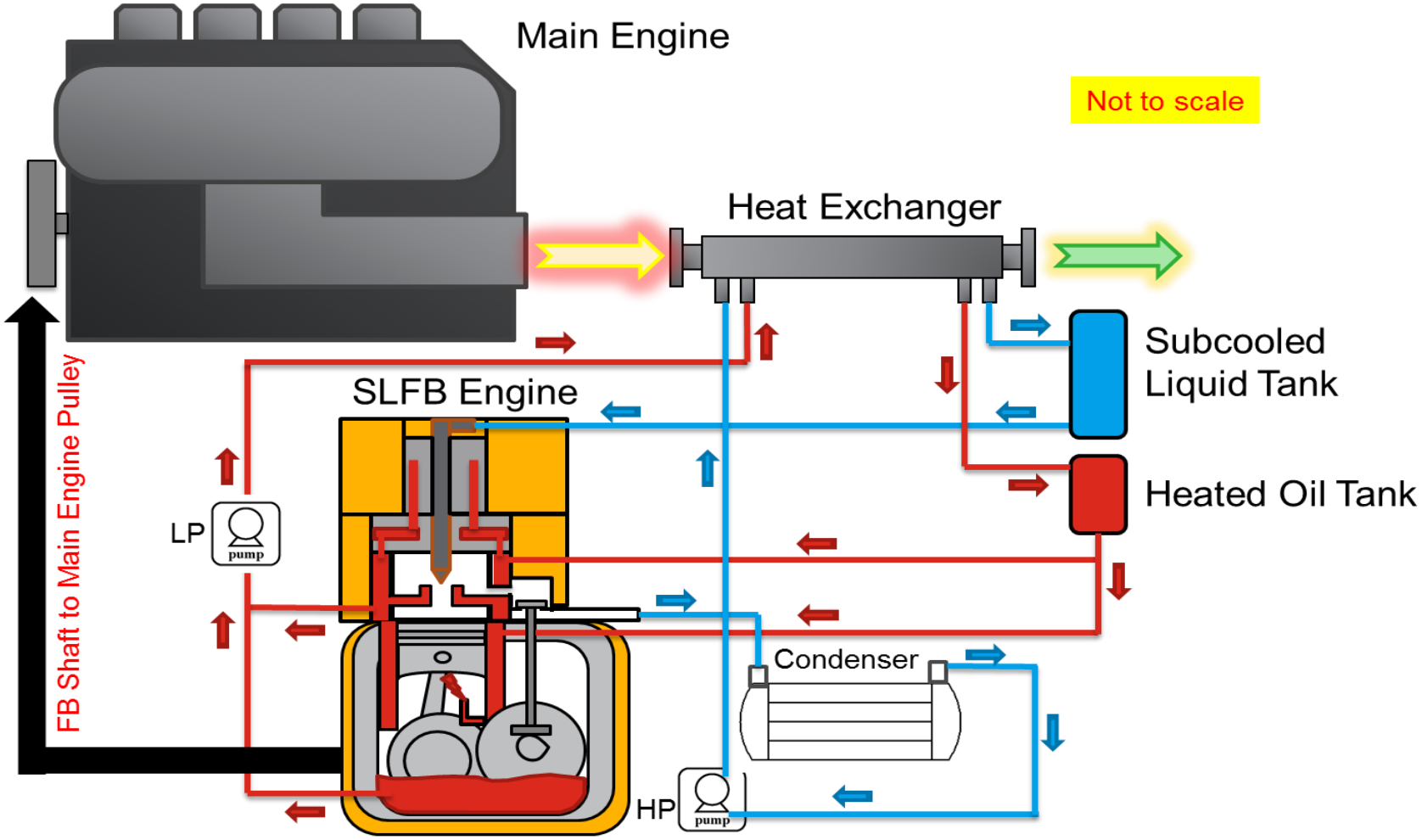

Figure 1. The SLFB WHR System for Automotive Applications

5.2.1 The FB2: The Second Generation Experimental Engine

Lessons learned with experimentation on the first generation FB1 engine demanded the re-designing of it to optimise several of its systems. These included the mitigation of the cyclic built-up residual mass effect, a revised heating system for the engine block and convective boiling surface, a robust lubricating system that would allow continuous engine operation and a re-designed piston and an injection system that eliminated injector back leakage and subsequent efficiency losses related to this back leakage. These changes and improvements have given birth to the second generation experimental SLFB cycle engine, the FB2.

5.2.1.1 Mitigating the cyclic build-up residual mass effect

The discovery of the cyclic build-up residual mass effect has led to a redesigning of components of the engine where the convective boiling takes place. The new design has the injector, boiling surface and the exhaust valve in a unit assembly known as the boiling unit. In this unit, the injection of the subcooled liquid is done directly onto a heated surface. The liquid portion strikes the surface and undergoes convective boiling as it flows down the surface due to the effects of gravity. The steam generated from the flashing and convective boiling processes flows out the top of the boiling unit into the piston expansion unit. At the bottom of the heated surface is the exhaust poppet valve which opens during the exhaust stroke. Exhaust steam is pushed out the expansion unit, back into the boiling unit and out the exhaust valve. This flow of steam will ensure that any unvaporised liquid flowing down the boiling surface is flushed out eliminating the cyclic build-up of residual mass. Figure 2a shows this new design and Figure 2b shows the comparison between the FB1 and FB2 experimental engines.

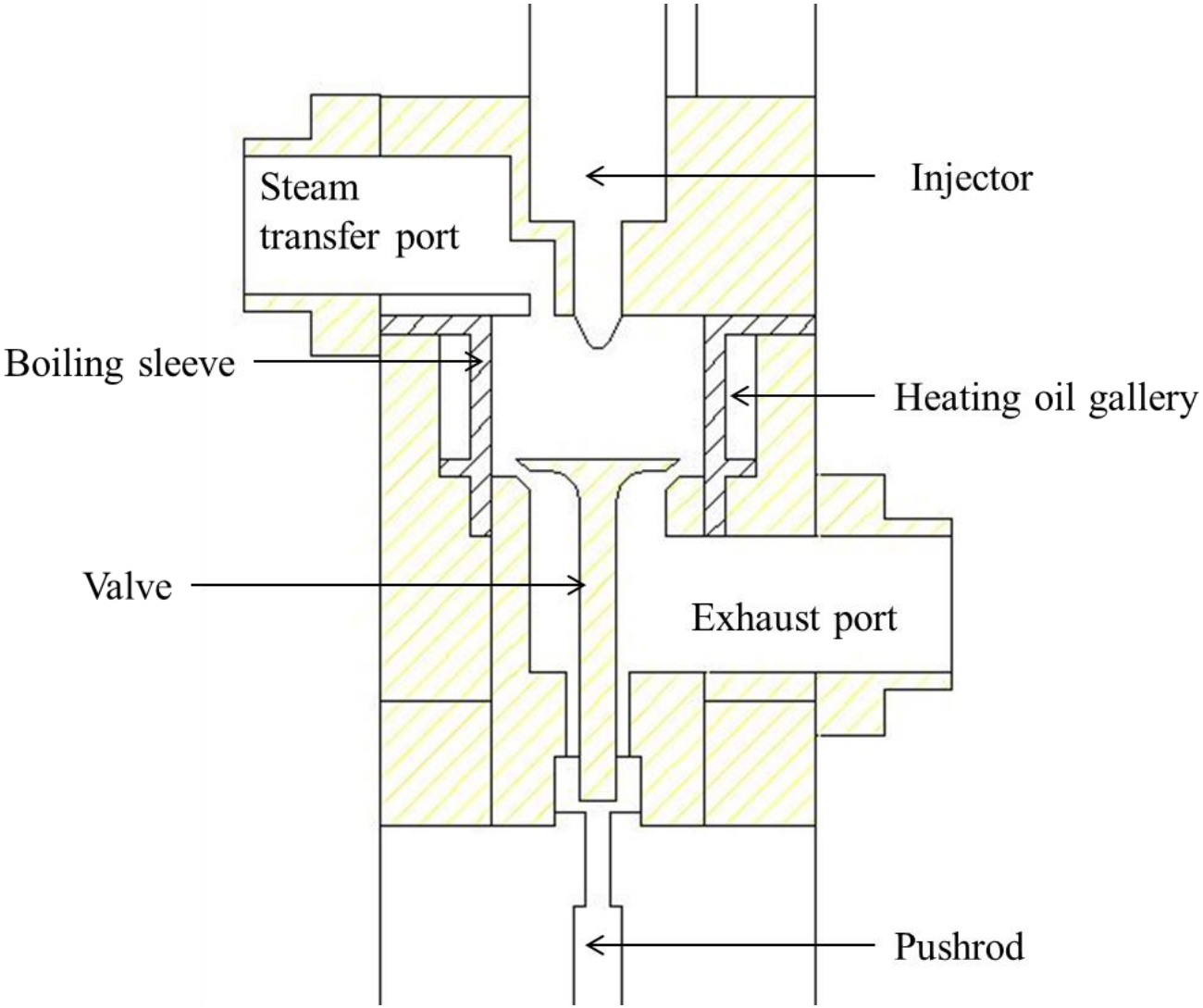

Figure 2a. Design alterations to eliminate the cyclic build-up residual mass effect

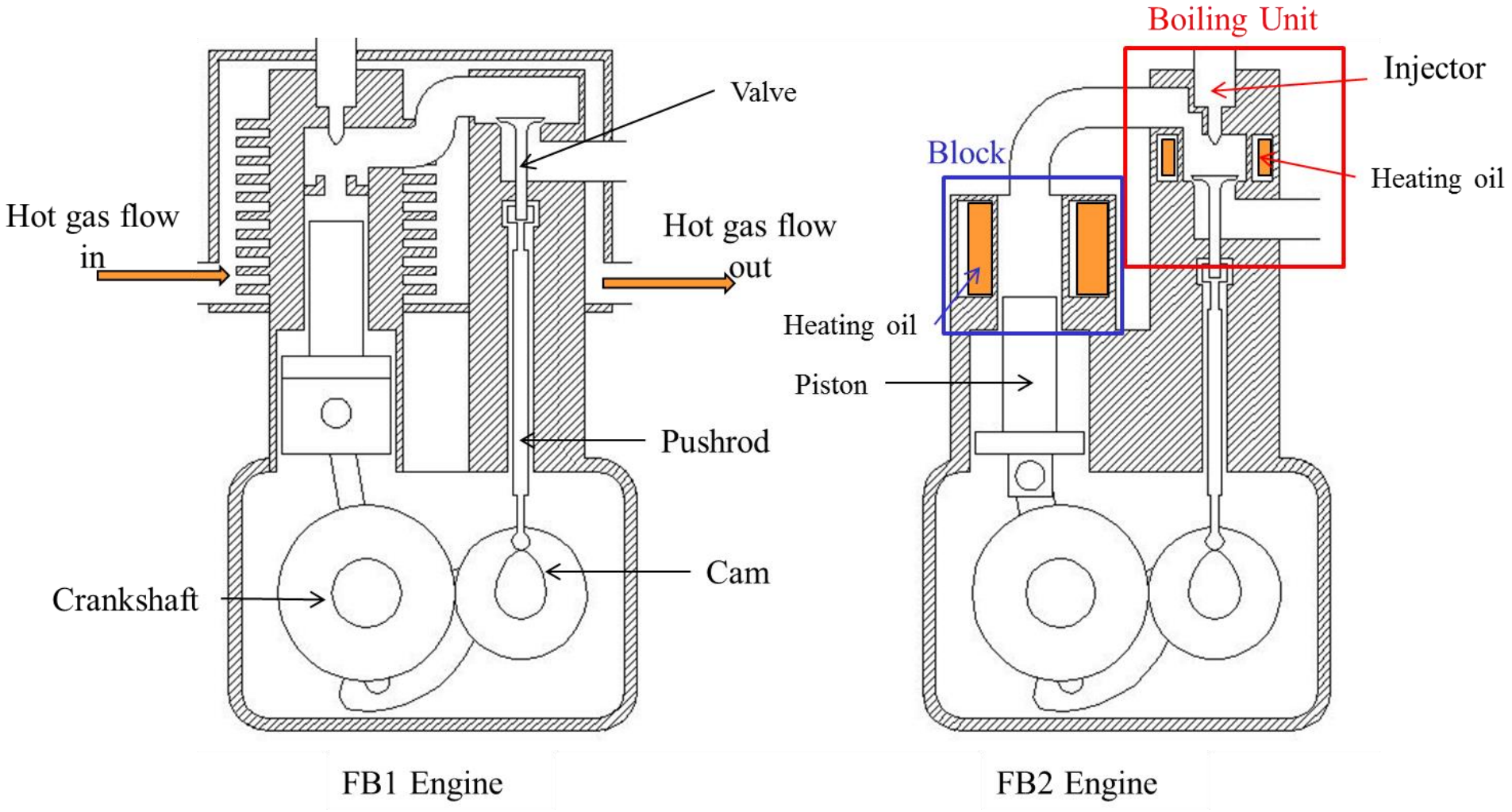

Figure 2b. Comparison between the FB1 and FB2 engines.

It is clear from Figure 2b that the design of the FB1 engine leads to the build-up of residual mass due to the exhaust valve being at a higher elevation than the surface where convective boiling occurs. The FB2 engine overcomes this problem with its new boiling unit design.

5.2.1.2 Quantification of convective boiling and block transferred heat input

The first generation experimental engine, the FB1 had experimental limitations due to its design. Of these, the one that required immediate attention was a boiling unit and block heating system that allowed accurate measurement of the heat flow. The previous system in the FB1 engine employed a heated gas system but high temperature gas mass flow rates proved difficult to measure accurately. However, this issue has been resolved through a heat transfer fluid based heating system. In fact this heat transfer fluid based system is envisioned as the heating system the revised road going version of the WHR system will employ. Figures 3a and 3b show the new experimental engine setup with the heat transfer fluid heating system. The FB2 engine employs the same bottom end from the original FB1 engine, i.e. the Yamaha 7CN, and maintains the bore and stroke dimensions of the FB1 engine.

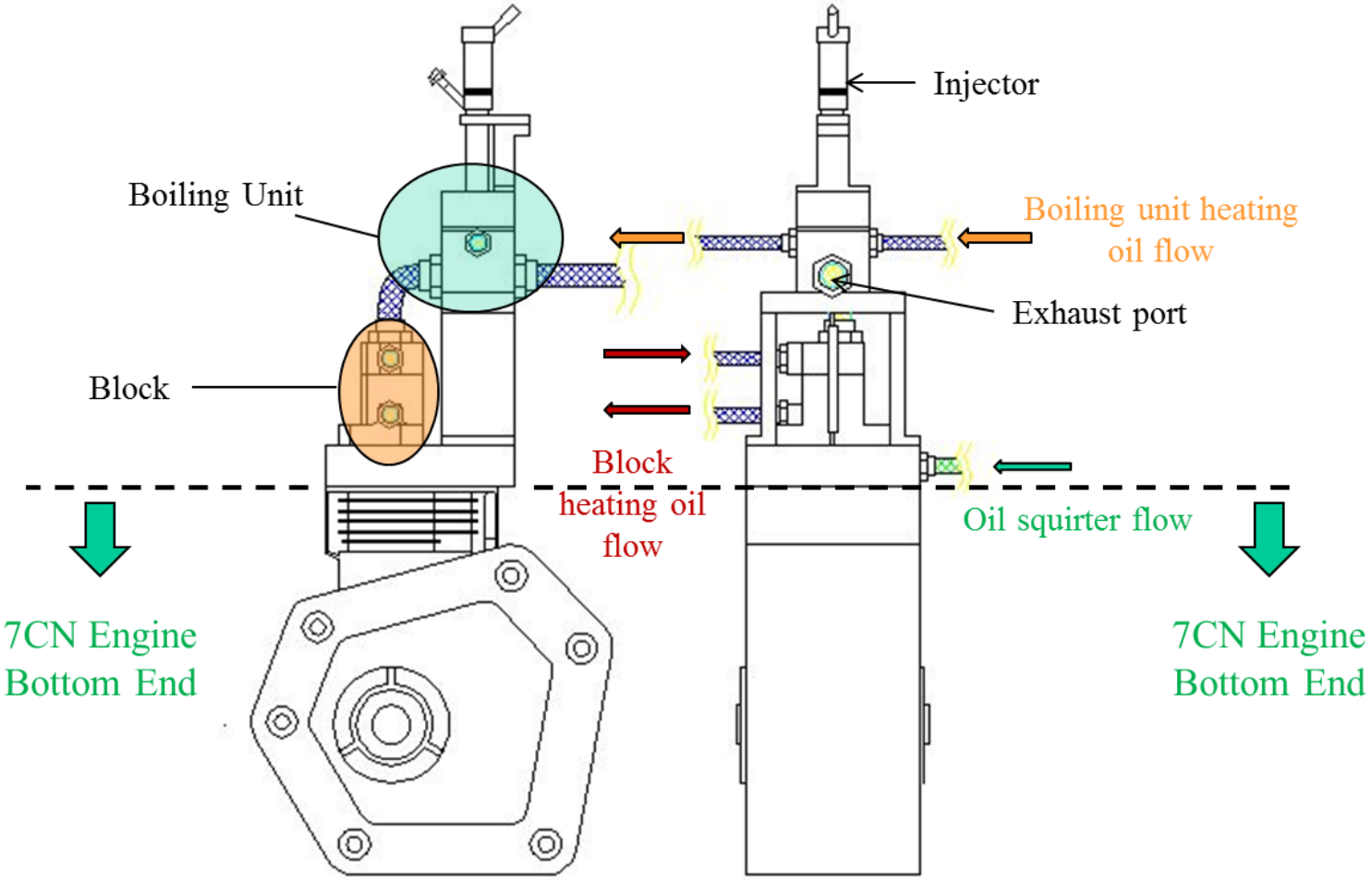

Figure 3a. The FB2 experimental engine.

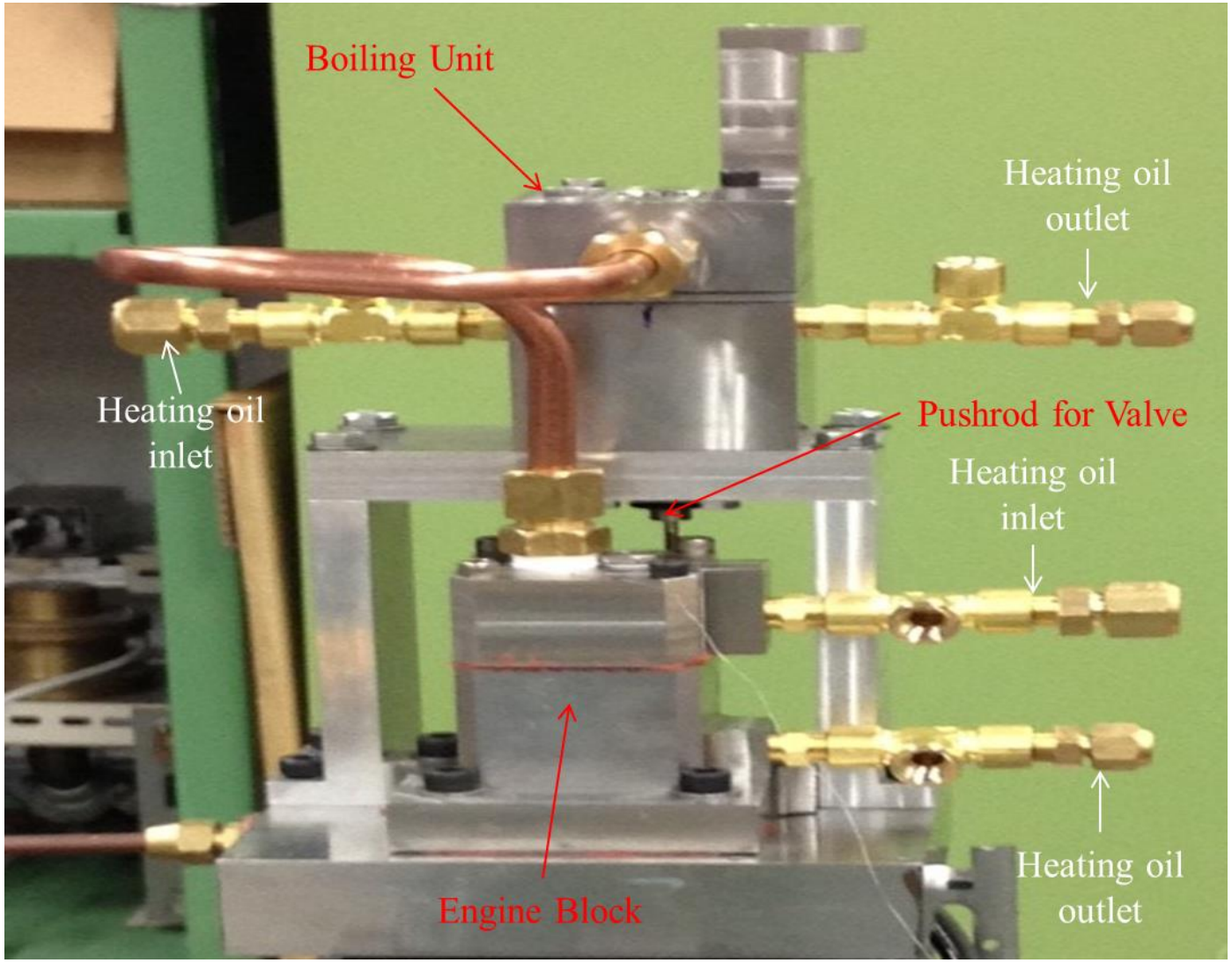

Figure 3b. The FB2 experimental engine with the heat transfer fluid based heating system.

5.2.1.3 Piston and lubrication

The FB1 engine used the 7CN engine's piston with a piston extension mounted on this piston to form the piston of the SLFB expansion unit. This design led to ineffective lubrication and didn't allow engine operation for more than 100 cycles. The stable continuous operation demanded a more robust lubrication system and with it a re-designed piston. Figures 4a show the FB1 extension piston setup. Due to this extension piston setup, the lubricating oil couldn't return to the crankcase directly and required a scavenging system. The inability to scavenge effectively led to oil pooling in the 7CN engine bore and the engine stalling when the system was run for extended durations of time. Figure 4b shows the unit piston setup employed by the FB2 engine.

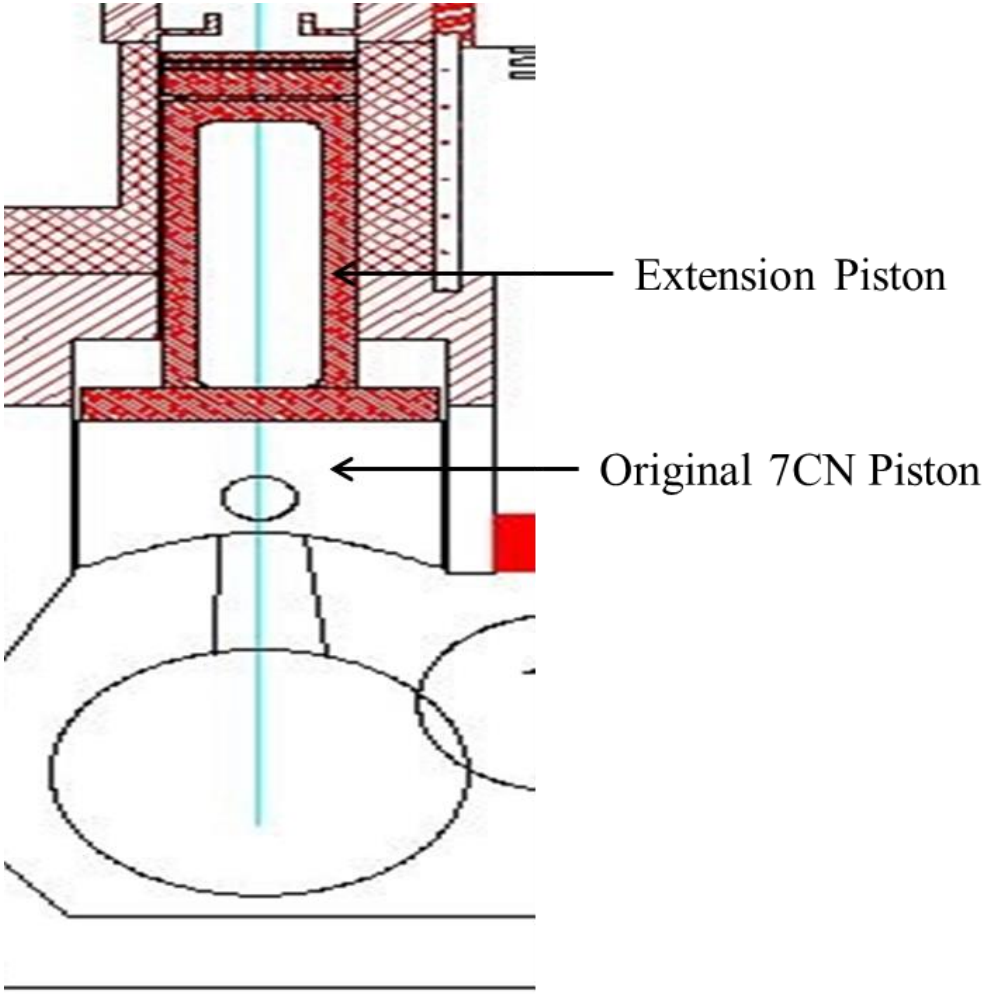

Figure 4a. The FB1 extension piston setup

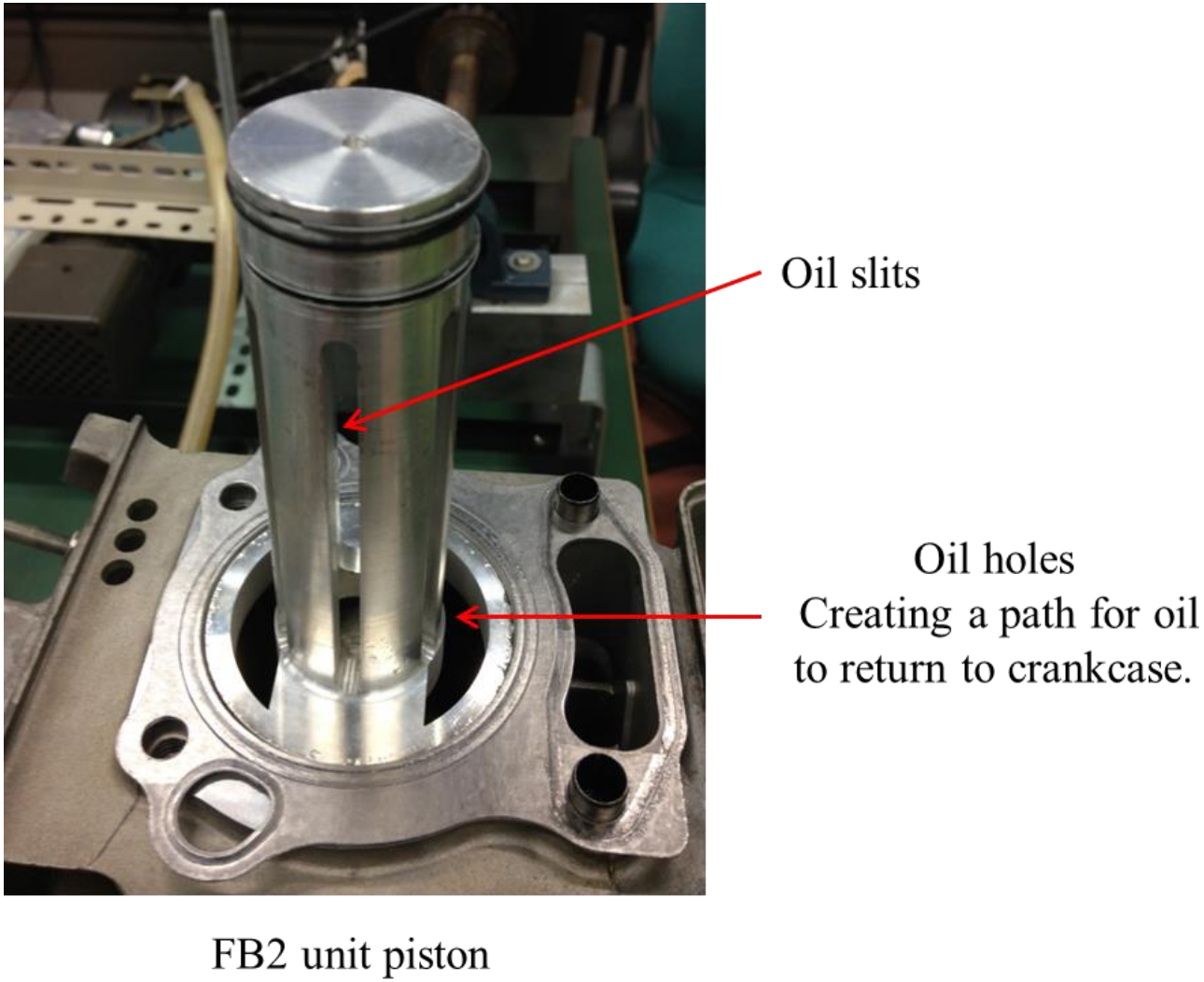

Figure 4b. The FB2 piston

This design with oil return holes cut into the base of the piston allowed lubrication oil to flow down into the crankcase eliminating the need for an oil scavenging system, and solved the problem of oil pooling and consequent engine stalling. This design had the added advantage of reducing the total weight of the reciprocating parts, namely the piston by almost 35% as the 7CN piston was eliminated. Furthermore, it helped better center the piston in the bore of the SLFB expansion unit, which could not be achieved in the FB1 engine. Figures 4c show the detailed design of the FB2 unit piston.
The lubrication system for the piston included an oil squirter which was inserted at the center of the moving piston through an enlarged slit in the piston skirt as can be seen in the C-C cross-section of Figure 4c. The oil that leaves the squirter does so through 6 strategically placed orifices which ensures that the oil travels out through the oil slits in the skirt of the piston onto the bore assuring a good supply of oil for lubrication. Excess oil runs down the bore, through oil return holes in the base of the piston back into the crankcase. The oil supply for the squirter comes from the crankcase through a pump. Figures 4d show the comparison between the FB1 extension piston and FB2 unit piston.

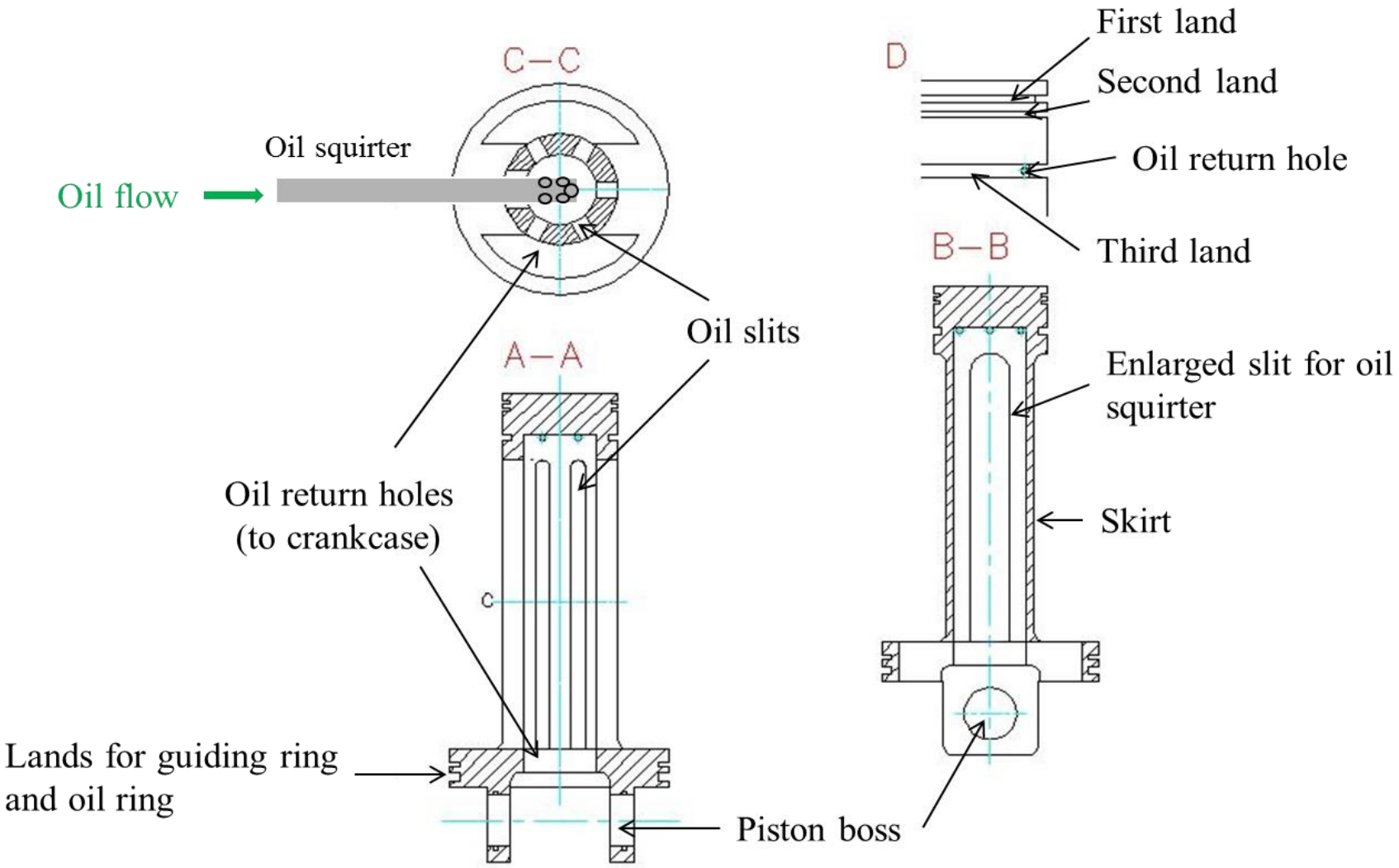

Figure 4c. Details of the FB2 unit piston with its lubrication system.

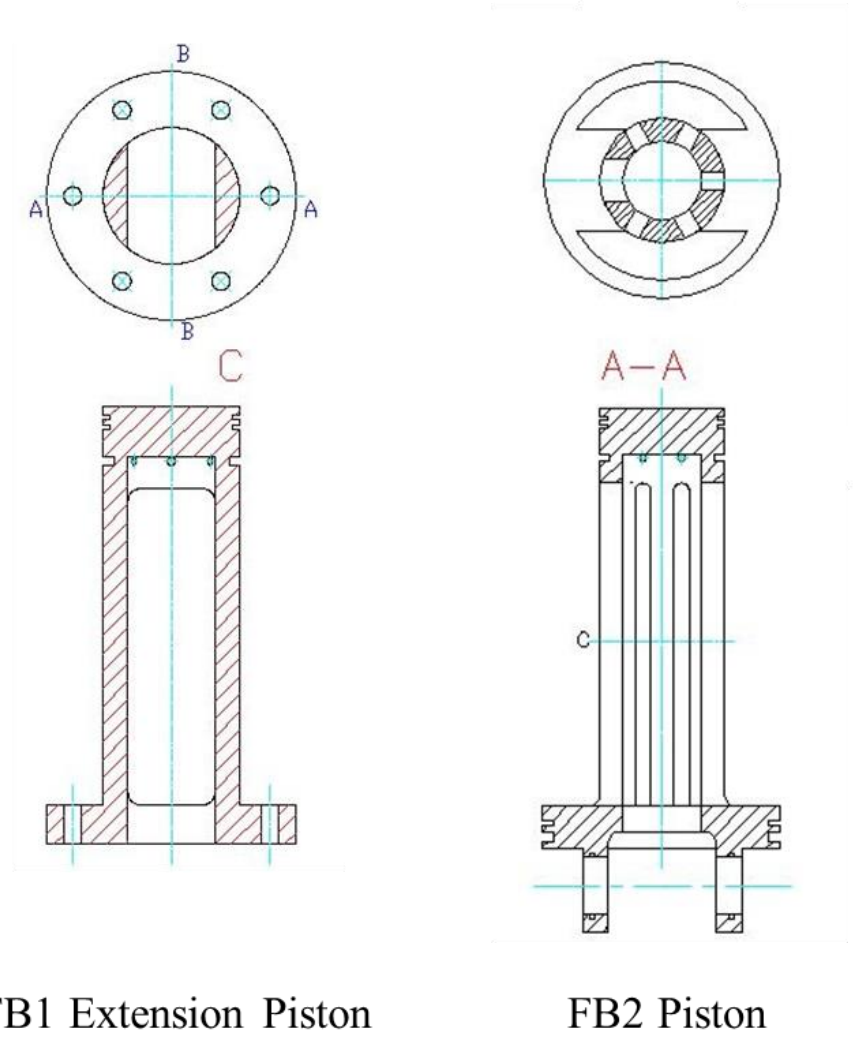

FB1 Extension Piston FB2 Piston

Figure 4d. The FB1 and FB2 pistons compared.

This oil squirting system has its applications in the road going version of the SLFB engine as heated lubrication oil is to be used to heat up the piston head.

5.2.2 The Injection System

The current injection system employs a modified common rail diesel injector. As the original injector was designed to operate at fuel pressures of 160MPa, it uses a hydraulic servo-system to achieve extremely short duration injection at these high pressures. The hydraulic servo-system operates by using a solenoid to actuate a control valve that allows small amounts of high-pressure liquid to leak out of the top of the injector which in turn controls the “nozzle needle lift” and injection events through a pressure difference in the hydraulic circuit within the injector body. Figure 5 (www.car-engineer.com) illustrates the principle involved in the hydraulic servo.

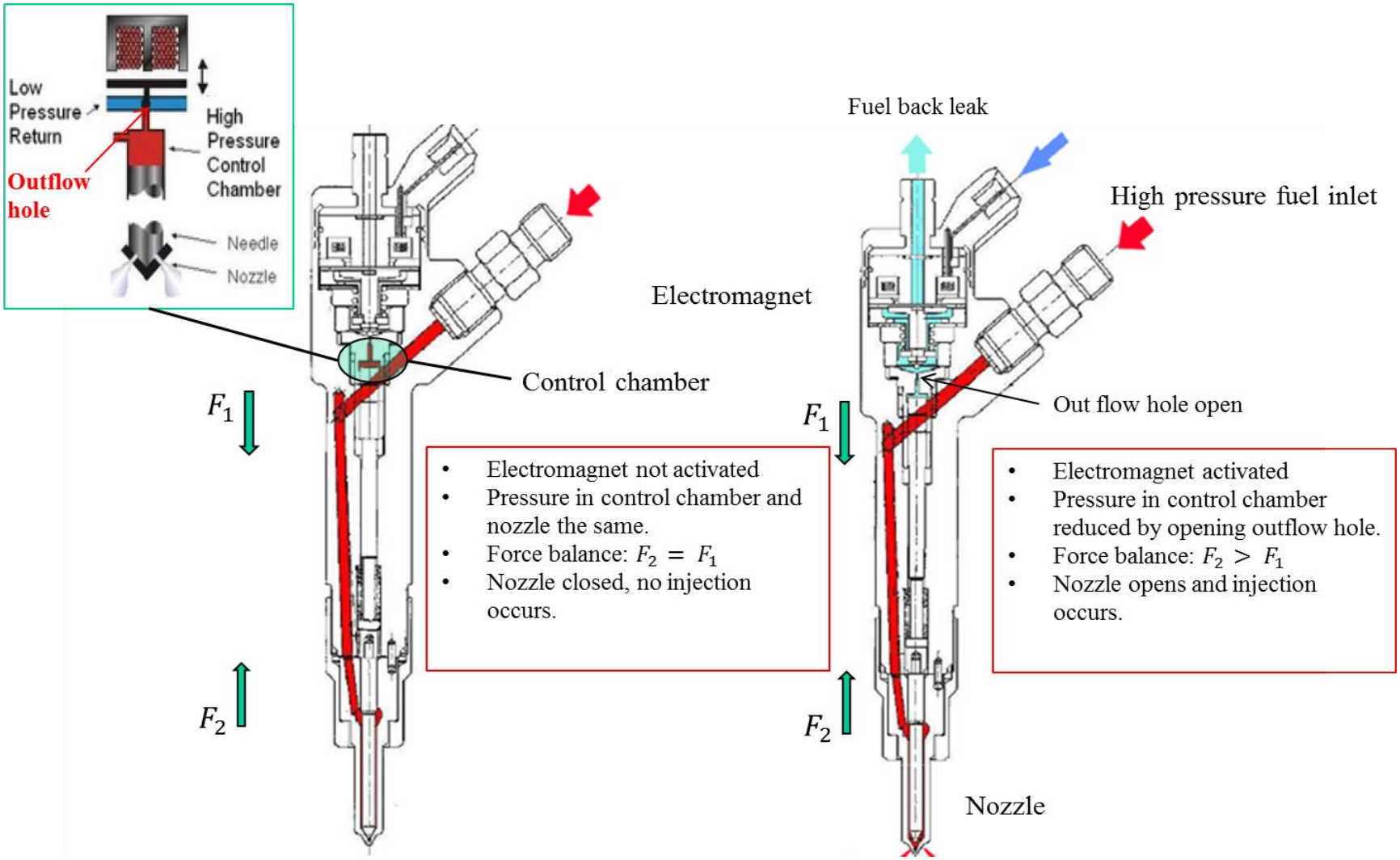

Figure 5. The operational principle of a hydraulic servo injector (Source: www.car-engineer.com)

Thus, every time an injection is performed, a portion of the higher pressure fuel leaks out of the control chamber. As the injector used in current SLFB system operates on the same principle, the back leak phenomenon leads to loss of subcooled liquid. This subcooled liquid flashes in the low pressure return channel and loses its energy resulting in a net loss of energy from the system and a decrease in the SLFB WHR system efficiency. Furthermore flashing of subcooled liquid in the return channel generates low temperature liquid which in turn has a cooling effect on the injector. This leads to further heat losses.

It thus becomes necessary to prevent back leak from the injector. The revised injection system is to use a much simpler injector. This injector is completely mechanical with no heat sensitive components and has no back leakage. These injectors are the injector nozzle holders used in diesel engines prior to common rail technology. Figure 6 shows the operating principle of these injectors.

A nozzle holder of similar design to Figure 6 is to be used with the subcooled water generation system that includes the heat exchanger, a high pressure pump and a high-speed solenoid actuated valve. Figure 7 describes the revised injection system.

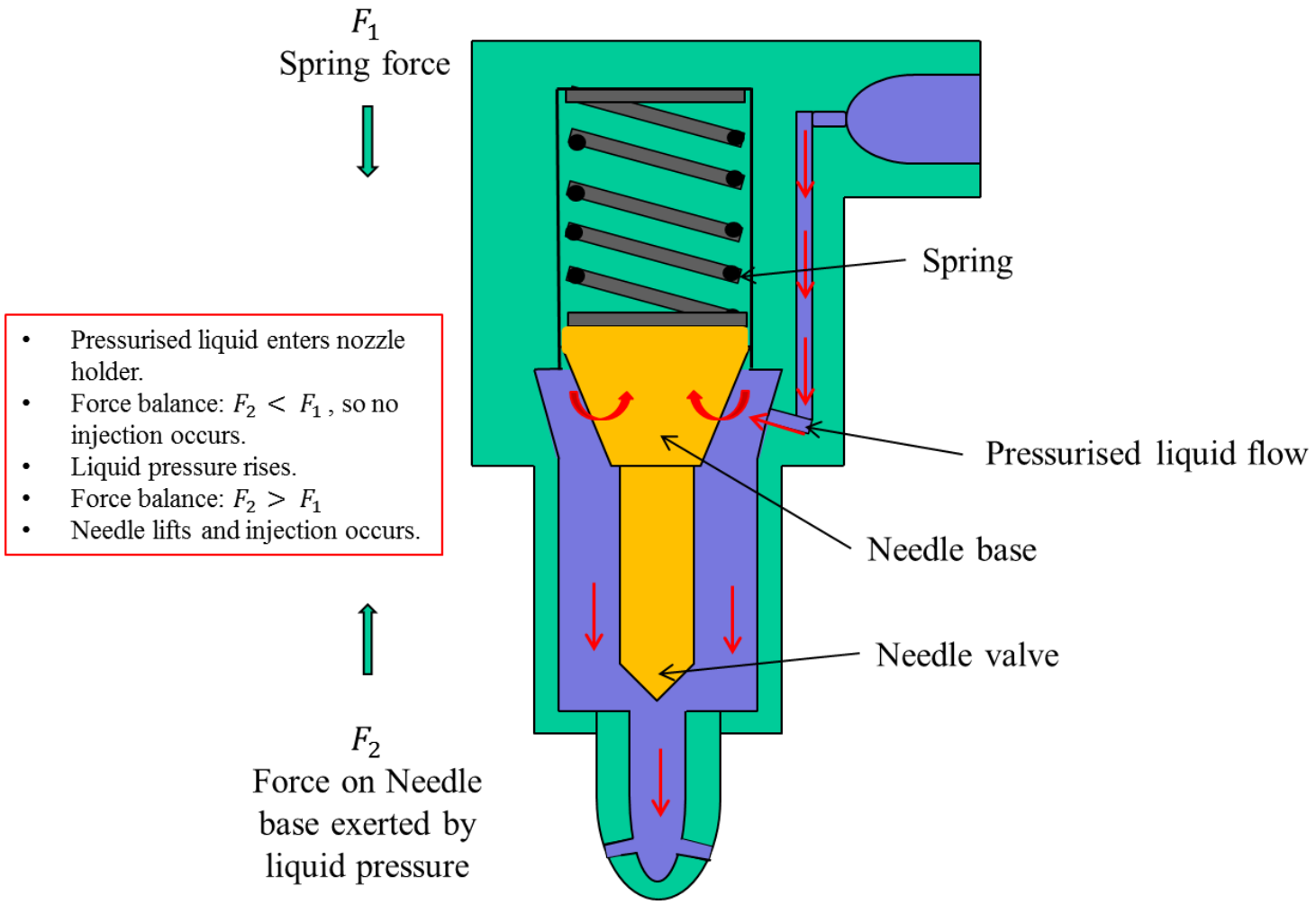

Figure 6. The standard diesel nozzle holder with no back leakage.

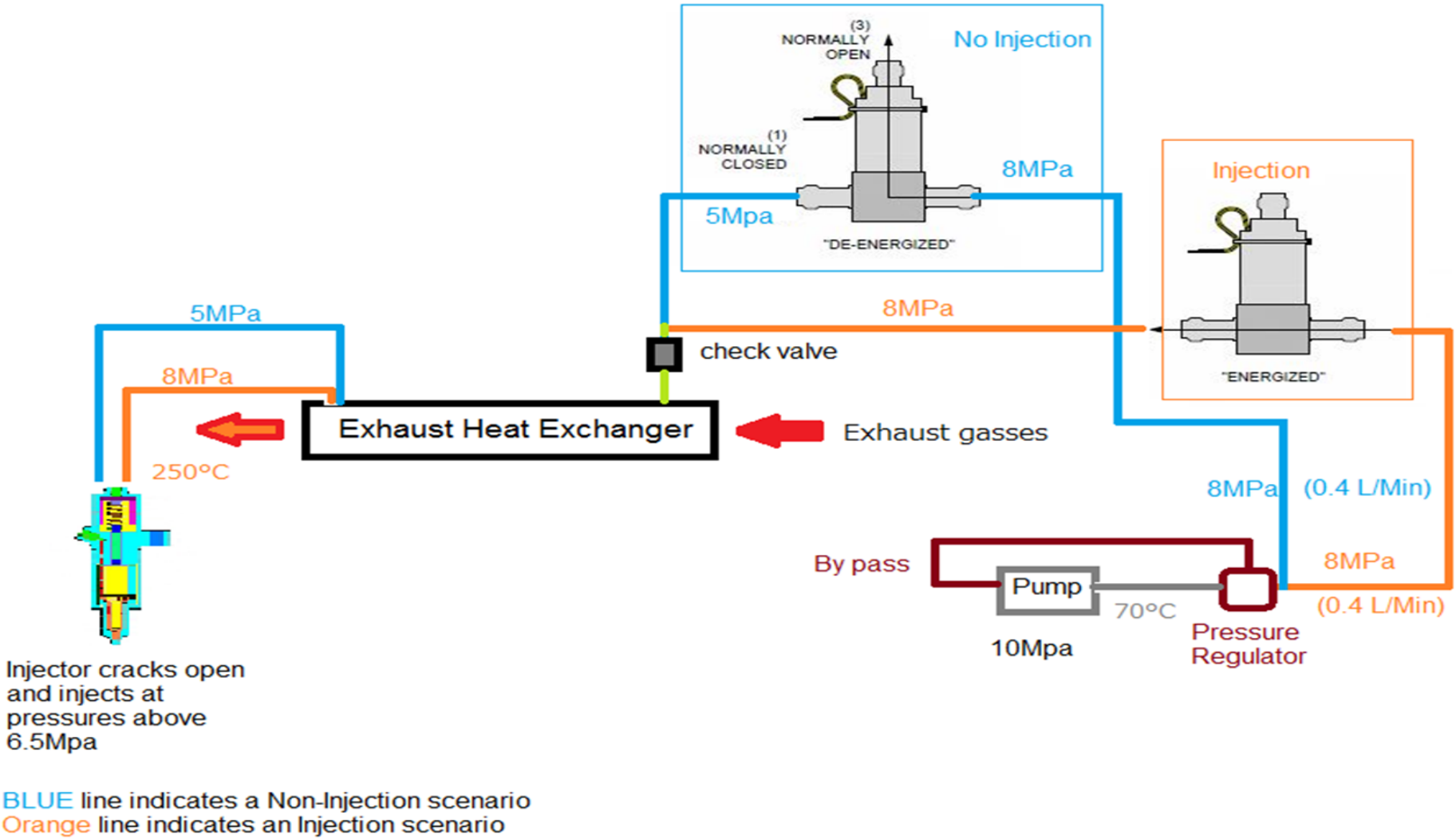

Figure 7. The revised injection system

The revised injection system will have the following benefits:

1. No back leakage so no heat losses related to this.
2. The elimination of back leakage reduces the mass-flow rate of working fluid thorough the system and reduces the pump work.
3. As the injection control electronics are not within the injector holder, no cooling of the injector in required, further eliminating heat loss.
4. Currently available injector holders of the design envisioned for the system are 1/5 the cost of common rail injectors reducing system cost.

One drawback with the above injection system is the inability to perform multiple injections with the accuracy and speed possible with a solenoid based injector. However, the SLFB cycle based reciprocating engine is envisioned operating at relatively low revolutions speeds. The response of an injection system described in figure 7 needs to be research and optimized for the entire SLFB WHR system.

5.3 ALTERNATIVE MODES OF APPLICATION OF THE S.L.F.B CYCLE FOR AUTOMOTIVE W.H.R

The SLFB WHR system investigated thus far is of a design that would allow it to be attached as a sub-system to the IC engine powertrain of any currently mass produced road going vehicle. In other words as a “bolt-on “option. Other variations of bolt-on systems and IC engine integrated systems have been envisioned and are described below.

5.3.1 The SLFB Cycle in a Wankel Rotary Expander

The Wankel rotary engine is of a simpler and cheaper design than conventional piston reciprocating engines due to its fewer components. However, the Wankel IC engine has lower thermal efficiencies than it piston counterparts due to the larger surface areas the combustion gasses come into contact with. This causes larger amounts of heat to be transferred out of the combustion gasses reducing their work potential. The SLFB cycle on the other hand, transfers heat from the engine surroundings (block and piston) to the working medium and so the issue of heat losses in IC Wankel engines becomes a mode of improved heat addition in the SLFB Wankel engine. In addition, the Wankel engine allows separation of the in-cylinder lubrication from the eccentric shaft lubrication system and prevents lubrication oil contamination by the working medium. This provides it with a further advantage over the piston engine. These advantages of the Wankel rotary expander combined with it being a positive displacement expander

like the piston expander makes it ideal for application with the SLFB cycle. This system would involve an induction stroke where hot gasses or even low pressure steam is drawn into the engine before it is compressed and highly subcooled liquid injected into it. It is expected that the existence of vapour prior to injection would improve heat transfer and overall efficiency.

5.3.2 The Open Cycle S.L.F.B Engine

Another option involves the SLFB cycle running in an open cycle. A certain portion of the exhaust gasses from the main IC engine are to be ingested as the intake charge of a suitable expansion engine such as a two-stroke piston engine. These exhaust gasses are then compressed in the compression stroke. Subcooled water which is generated from the major portion of the IC engine's exhaust gasses is then injected just after TDC into the now even hotter (due to compression) exhaust gasses. Provided the saturation pressure inside the piston is lower than the saturation pressure of the subcooled water, flashing will occur. The advantage of this system is that better heat transfer can be expected between the saturated flash steam and the hot exhaust gasses which contain a large concentration of high temperature water vapour from combustion. Exhaust from the SLFB engine is cooled by the use of an appropriate exhaust cooler/condenser, and a large portion of this exhaust steam should be recoverable for re-use. The remaining exhaust gasses from the SLFB cycle are re-mixed with the main exhaust stream and leave the tail pipe. Figure 9 shows the concept of the open cycle SLFB engine.

5.3.3 The Six Cycle Engine

Another variation involves the use of the SLFB cycle in a six stroke engine. This engine is to operate on either the Otto cycle or the Diesel cycle for the first 4 strokes. The 5^{th} stroke is a partial exhaust stroke. At the end of the exhaust stroke a new power stroke is generated by the injection of subcooled water. This power stroke is then followed by a steam exhaust stroke, which completes the engine cycle. This system can be applied to a single cylinder of a multi cylinder engine and activated only when necessary. Integrating the SLFB cycle expansion unit into the IC engine should help reduce cost, package weight and size. Figure 10 shows the concept of the six-cycle engine.

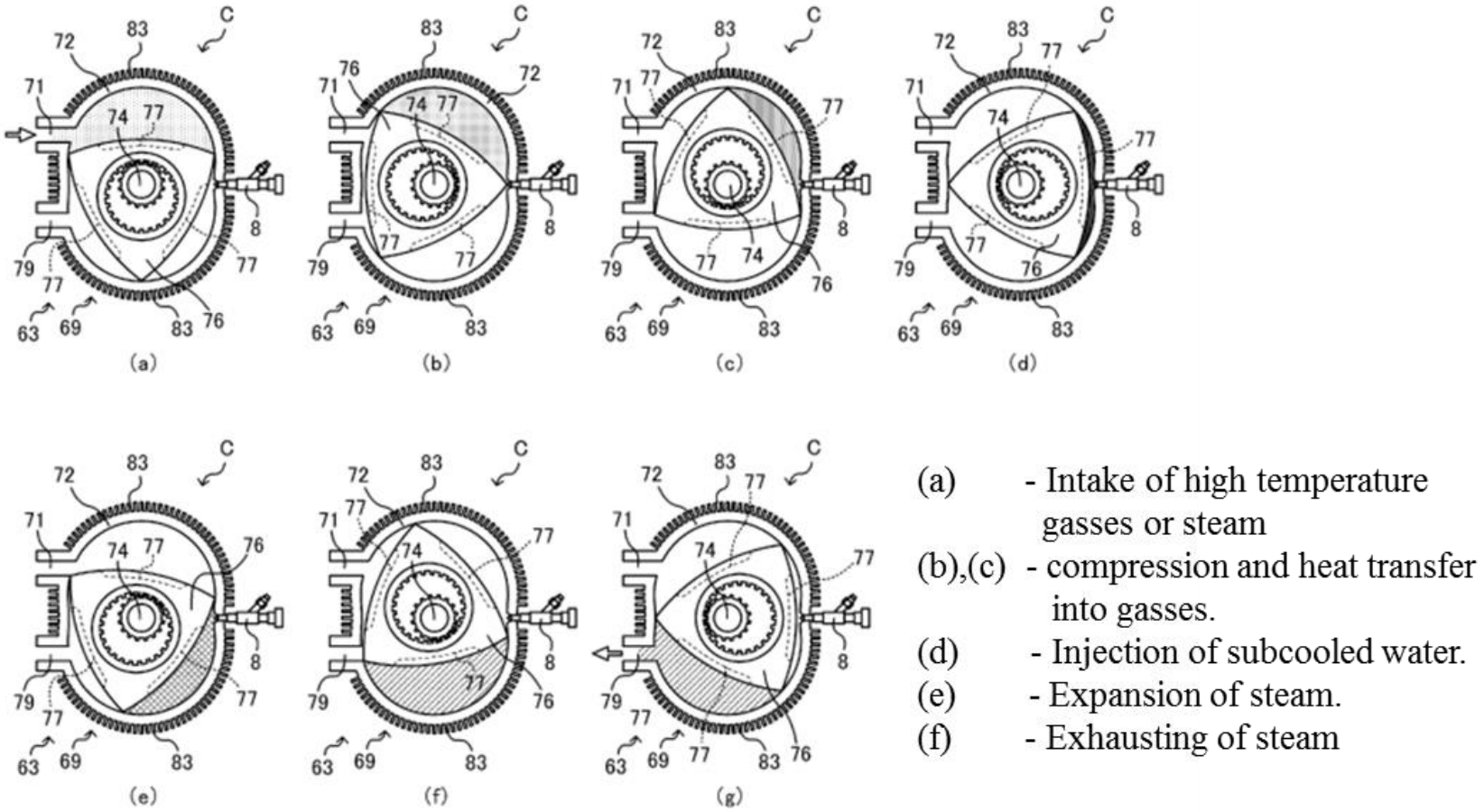

Figure 8. The application of the SLFB Cycle in a Wankel Rotary Expander (Source: Japan Patent No 5804555 (2015))

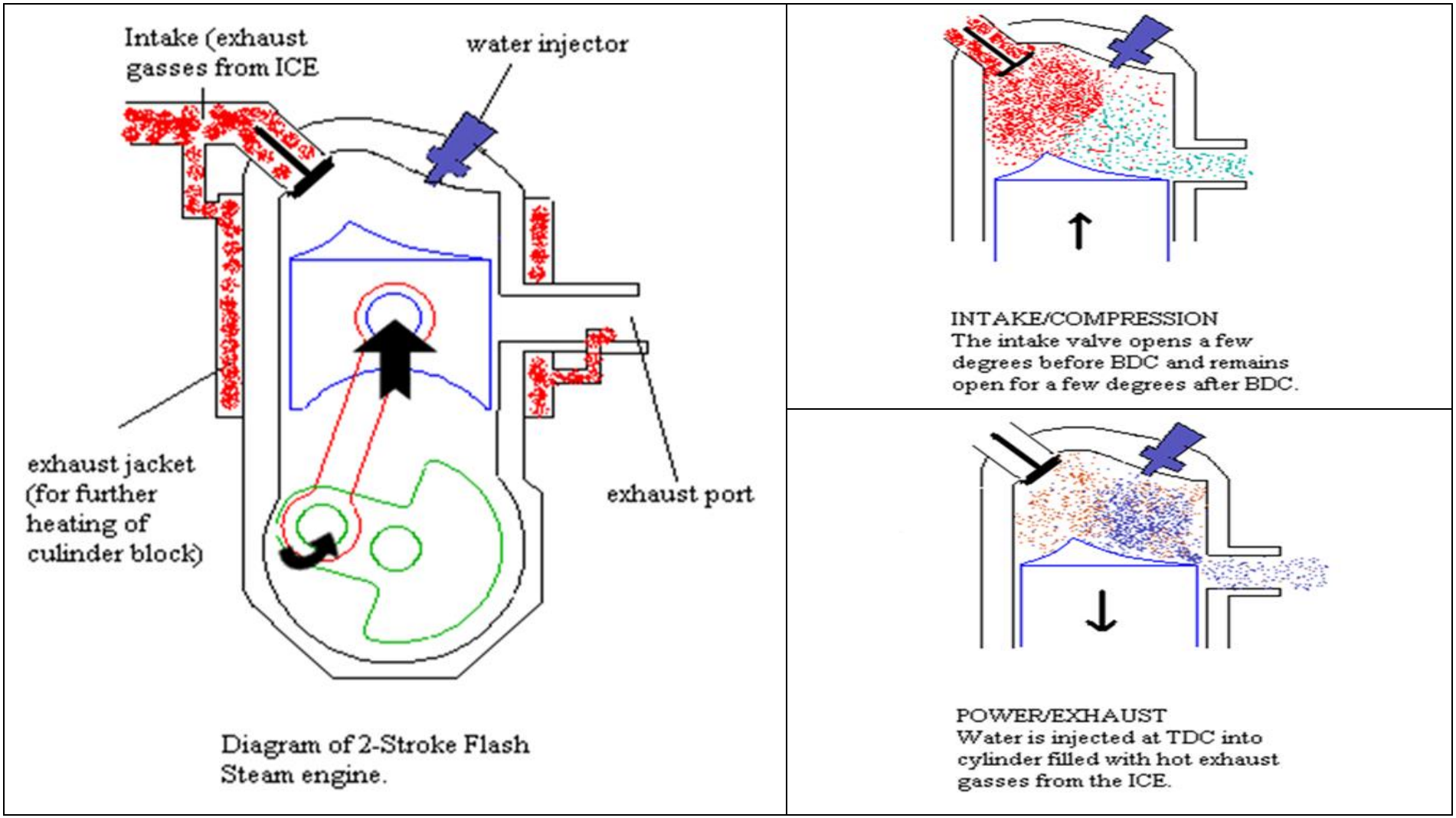

Figure 9. The Open cycle SLFB engine.

(a) - Induction
(b) - Compression
(c) - Ignition (combustion power)
(d) - Exhaust
(e) - Flashing (Flash power)
(f) - Exhaust

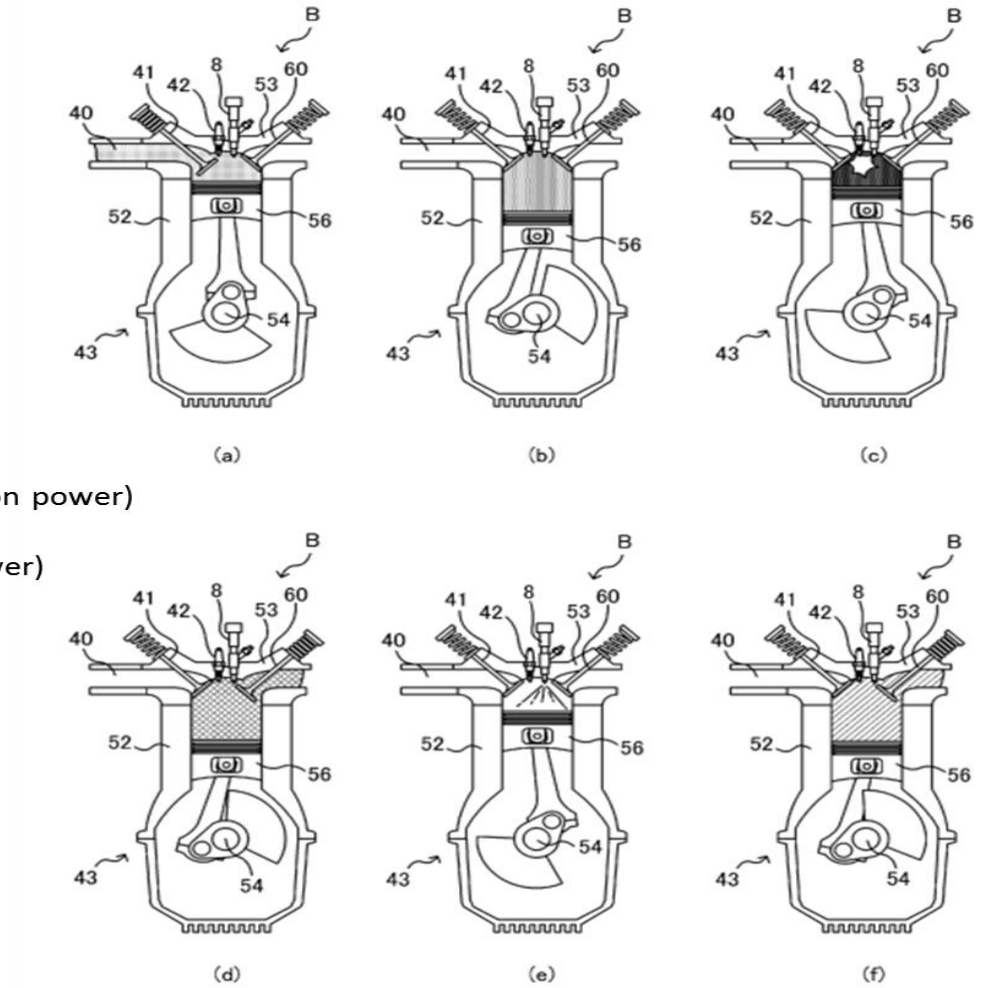

Figure 10. The six stroke engine incorporating the SLFB Cycle (Source: Japan Patent No 5804555 (2015))

5.4 SUMMARY

Certain areas of the FB1 experimental engine require improvement. New phenomena that affect the efficiency of a SLFB cycle powered reciprocating engine have also come to light. In order for the system to be viable in road going vehicle applications, it requires compactness. One way of achieving this is to use a heat transfer liquid to heat the boiling unit, block and piston of the SLFB engine. This in turn would require a heat exchanger that could generate both the subcooled working fluid and the high temperature heat transfer fluid. This system would also provide a means of energy storage from high waste heat outputs situations for later use. The FB2 experimental engine has been designed to work with such a heating system. This engine also incorporates an improved lubrication system and piston design.

A phenomenon that affects the efficiency of the SLFB cycle powered engine is the Cyclic Build-up Residual mass effect. This is a result of liquid that doesn't boil off from one cycle prior to the beginning of the next cycle. This leads to heat loss through dissipation and a subsequent loss of efficiency. This phenomenon can be mitigated by the flushing of any un-boiled liquid in the exhaust stroke with the exhaust gasses.

The injection system for the SLFB cycle powered engine requires an injector that is more robust and capable of operating without back leakage as back leakage results in the loss of efficiency of the SLFB WHR system. This can be achieved by the use of a simple injector design similar to that of pre-common rail diesel injectors. Alternative applications of the SLFB cycle include a Wankel rotary engine powered by the cycle which could provide better heat transfer to the working fluid within the expander and minimize lubrication issues. Another alternative is the Open Cycle SLFB engine that would involve injecting subcooled water into an expander which has ingested hot exhaust gasses. The improved heat exchange between the water vapour rich hot exhaust gasses and the flash steam would result in improved engine efficiency. The third and most ambitious application is a six cycle engine that has the 4 cycles of a conventional Otto or Diesel cycles, followed by a SLFB power cycle and exhaust. This system could be run on just one cylinder of a multi-cylinder engine and called into action when necessary to increase engine output.

REFERENCES

1. www.car-engineer.com, The operational principle of a hydraulic servo injector, digital image, Diesel-injector, viewed 11 September, 2015. <http://www.car-engineer.com/introduction-to-engine-fuelling-systems/>

2. D.N.Hewavitarane and S.Yoshiyama, Japan Patent No: 5804555 (11 September, 2015)

Chapter 6: Conclusions

From the literature study of the state of IC engines and their future prospects, the following conclusions can be drawn of the SLFB cycle and its applicability to automotive waste heat recovery;

6.1 AUTOMOTIVE WASTE HEAT RECOVERY

It has been shown in chapter 1 that the internal combustion engine will continue to dominate the transportation sector as the means of power generation. This is due to its reliability, higher power to weight ratio than battery powered electrical vehicles, ready availability of liquid fuels and relative low cost. In a world striving to cut down on CO_2 emissions, electrical cars of both, battery powered and fuel cell design currently produce as much or even more CO_2 emissions over their lifetimes than IC engine cars do because the electricity and hydrogen they require come either directly from fossil fuels and/or from the burning of them.

The IC engine is relatively inefficient in its conversion of combustion energy to mechanical work and typically up to 60% of combustion energy is wasted. The recovery of this waste heat is an obvious and effective means of improving the IC engine's overall efficiency. With current IC powered car being equal to or less polluting than its electrical rivals in terms of CO_2 emissions, improving the IC engine's overall efficiency will help them become even less polluting and this is vitally important as the IC engine will continue to dominate the market for many years to come. Various WHR systems exist but their cost, poor efficiency or the difficulty of application to automotive situations have resulted in no mass produced commercial application to date. The SLFB cycle offers an attractive alternative.

6.2 THE S.L.F.B CYCLE

In chapter 2, it was seen that the Subcooled Liquid Flash, Boiling Cycle (SLFB) is a heat cycle that belongs to the family of Power Flash Cycles. It is however different to hitherto well known Power Flash Cycles such as the Trilateral Cycle (TLC), in that it makes use of the unflashed portion of the working fluid by inducing convective boiling

on this through a second heat transfer process. The vapour thus generated contributes to the expansion stage of the cycle. Figure 1 illustrates this.

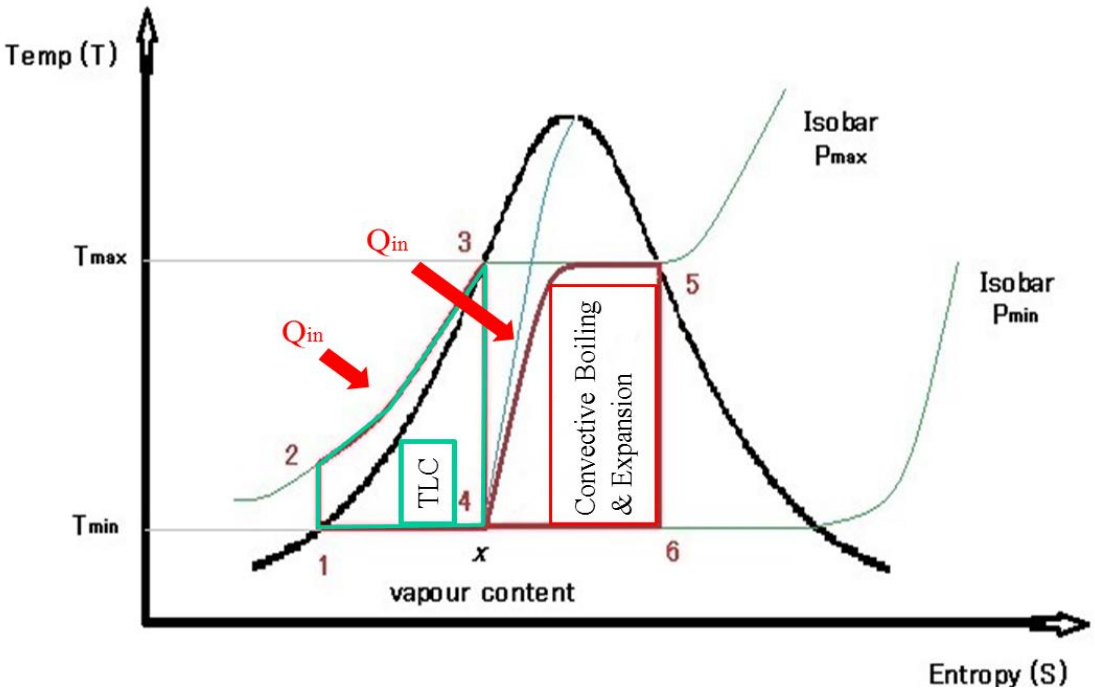

Figure 1. The SLFB Cycle

The TLC has been shown to have higher power production efficiency than the RC due to the improved efficiency with which heat transfer occurs in the heat exchanger that generates the subcooled working fluid of the cycle. The SLFB Cycle shares this advantage with the TLC over the RC. While the TLC discards the energy rich unflashed portion of the working fluid, the SLFB Cycle makes use of this energy and as a result, is more efficient than the TLC. This makes the SLFB Cycle more efficient in power production than both the RC and the TLC.

6.3 THE S.L.F.B CYCLE POWERED RECIPROCATING ENGINE SYSTEM

The development of the FB1 experimental engine and experimentation done with it has led to the following conclusions:

6.3.1 The Expansion Unit

Chapter 3 demonstrated the proof of concept of the SLFB Cycle and showed that it is best suited for application in a positive displacement volumetric expander such as a reciprocating piston. This is due to the working fluid being in a two-phase state in the expansion stage of the cycle. The reciprocating piston provides a more durable cost-effective solution than rotodynamic turbomachinery. The ideal piston engine would have a long stroke to maximize the expansion of the working fluid and have its components; the block and piston heated to prevent heat transfer from the working fluid to these components. In addition the engine would be operated at high load as this would ensure that the working fluid would begin its expansion process at a high temperature, improving it Carnot efficiency. In order for the engine to operate at high loads the level of subcooling of the working medium would have to be proportionately high.

6.3.2 The Boiling Unit

It was also seen in chapter 3 that the boiling unit where the atomized unflashed liquid undergoes convective boiling needs to have the largest possible surface area to maximize boiling but the smallest possible dead volume as the expansion of the vapour in the dead volume doesn't generate any work and reduces efficiency. Furthermore, the temperature of the boiling surface should be just below the Leidenfrost point as temperatures at or above the Leidenfrost point reduces boiling efficiency and leads to a phenomenon known as the "residual mass effect".

6.3.3 The Residual Mass Effect

The residual mass effect was discovered in the first stages of experimentation done on the FB1 engine seen in chapter 3. This effect is due to the relatively low temperature liquid that remains in the boiling unit when flashing occurs, and leads to efficiency losses through heat dissipation from the flash vapour to this liquid. The residual mass effect can be divided into two categories. The first termed the "Leidenfrost Residual Mass" arises from the Leidenfrost effect and affects efficiency from the very first cycle of engine operation. This was observed in the single cycle injection experiments carried out in the experiments of the third chapter. The fourth chapter involved running the

engine in multiple cycle operation and led to the discovery of a similar phenomenon which is termed the “Cycle Built-Up Residual Mass”. This was seen to result from unvapourised liquid which builds up from cycle to cycle. This phenomenon was also seen to drastically reduce engine efficiency. The residual mass effect can be mitigated by maintaining the boiling surface just below the Leidenfrost point and by designing the boiling unit so that any unvapourised liquid is flushed out with the exhaust steam.

6.3.4 Injection Pattern

The effects of injection pattern on engine efficiency were investigated in the experiments of chapter four. Injection pattern was seen to have an effect on the efficiency of the engine. Split injections of equal masses undergo more efficient convective boiling and are better able to contribute to the expansion phase. However the ability to inject the required mass of subcooled liquid in the shortest possible time is also important in order to maximize the duration of expansion available. In addition, higher temperatures of subcooled liquid and higher engine loads reduce the efficiency of the convective boiling process but increasing the boiling surface temperature can counteract this provided the temperature stays bellow the Leidenfrost point.

The SLFB reciprocating engine has many factors that affect its efficiency and power production. Power generation is achieved thorough a fast process and a slow process. The Flash Steam generation and expansion is the fast process and the convective boiling process is the slow process. It has also been experimentally observed that heat transfer occurs from the engine block to the working medium but whether this is able to effectively contribute to power production needs to be further investigated. Figure 2 illustrates the above mentioned fundamentals that govern the operation of the SLFB reciprocating engine.

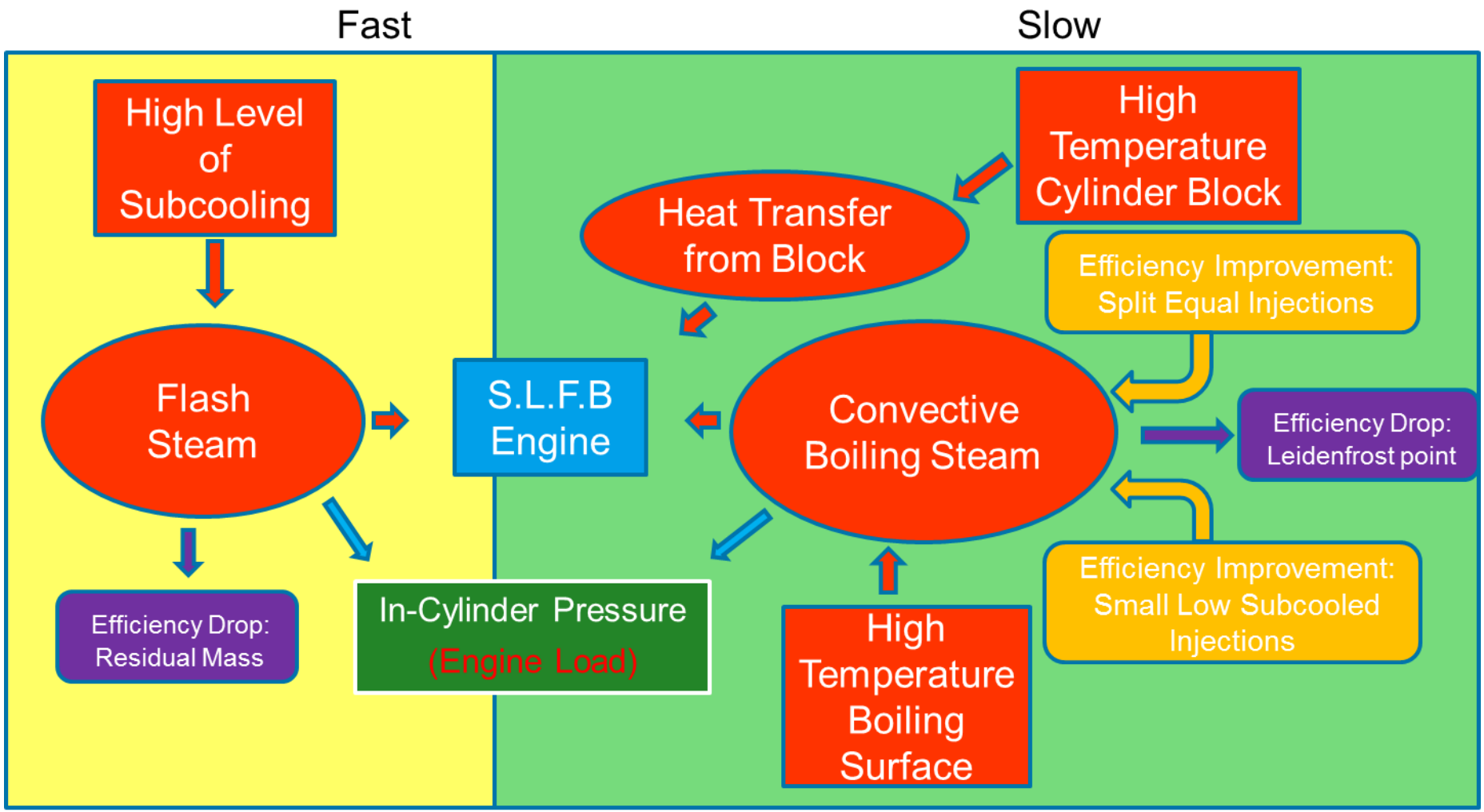

Figure 2. A Summary of the Fundamentals of the SLFB reciprocating engine

6.4 THE FUTURE OF THE S.L.F.B WASTE HEAT RECOVERY SYSTEM

While automotive WHR systems have taken the back burner to other IC engine developments, the significant amount of waste heat generated by IC engines cannot be ignored and their recovery will at some stage become cost effective through necessity. The SLFB cycle is a novel heat cycle and research into it is still in its infancy. The research to date has proven its viability to harness power from automotive waste heat and has come to understand, albeit not exhaustively, the fundamentals governing the cycle and its applications to a reciprocating piston engine. It is thus vital that the research on the SLFB cycle and the WHR system based on it continue so that it is optimized and ready to offer an efficient and effective alternative when car makers are finally ready to mass produce WHR systems for their vehicles. It has great potential if the various systems continue to be optimized and developed. It is also worthy of note that the SLFB cycle has applications outside the automotive sector particularly in power generation from low grade heat sources. This is achievable by the use of PFC, HFCs and HCs as its working fluid. This opens a new frontier for its application.

One may be led to believe that in a world of ever increasing electrification, heat engines would gradually be phased out. However, Heat is a fundamental form of energy and harnessing it to do work is and will always be an endeavor of engineering. The SLFB cycle is a cycle that allows the harnessing of heat to generate power. Automotive applications are just the beginning.